Innovative and Current Approaches for Streamlining the Design, Deployment, and Operation of Near-term and Emerging Reactors

Micromechanical models based on NTFA approach

(Visco)-Plastic strain heterogeneity in composite and polycrystalline materials and the Nonuniform Transformation Field Analysis (NTFA)

Dr. Rodrigue Largenton – Senior Expert
EDF R&D - Materials and Mechanics of Components Department
Civil and Fuel Engineering Group
CEA Cadarache Bât. 151 13108 St Paul lez Durance Cedex FRANCE
rodrigue.largenton@edf.fr

Outline

1. **Motivations - Two typical examples* at the microstructural scale: nonlinear behavior**
2. **Classical approach - Transformation Field Analysis**
3. **Reduced model - Nonuniform Transformation Field Analysis (NTFA)**
4. **NTFA-TSO applied to the two typical examples – Implementation & Results**
5. **NTFA: Conclusion - Outlook & Reflection**

**Appendix 2: other examples with linear and nonlinear behaviors at the microstructural and structural scales*

1. Motivations - Two typical examples at the microstructural scale: nonlinear behavior

1. **Composite material - MOX nuclear fuel** (Largenton et al., 2014).

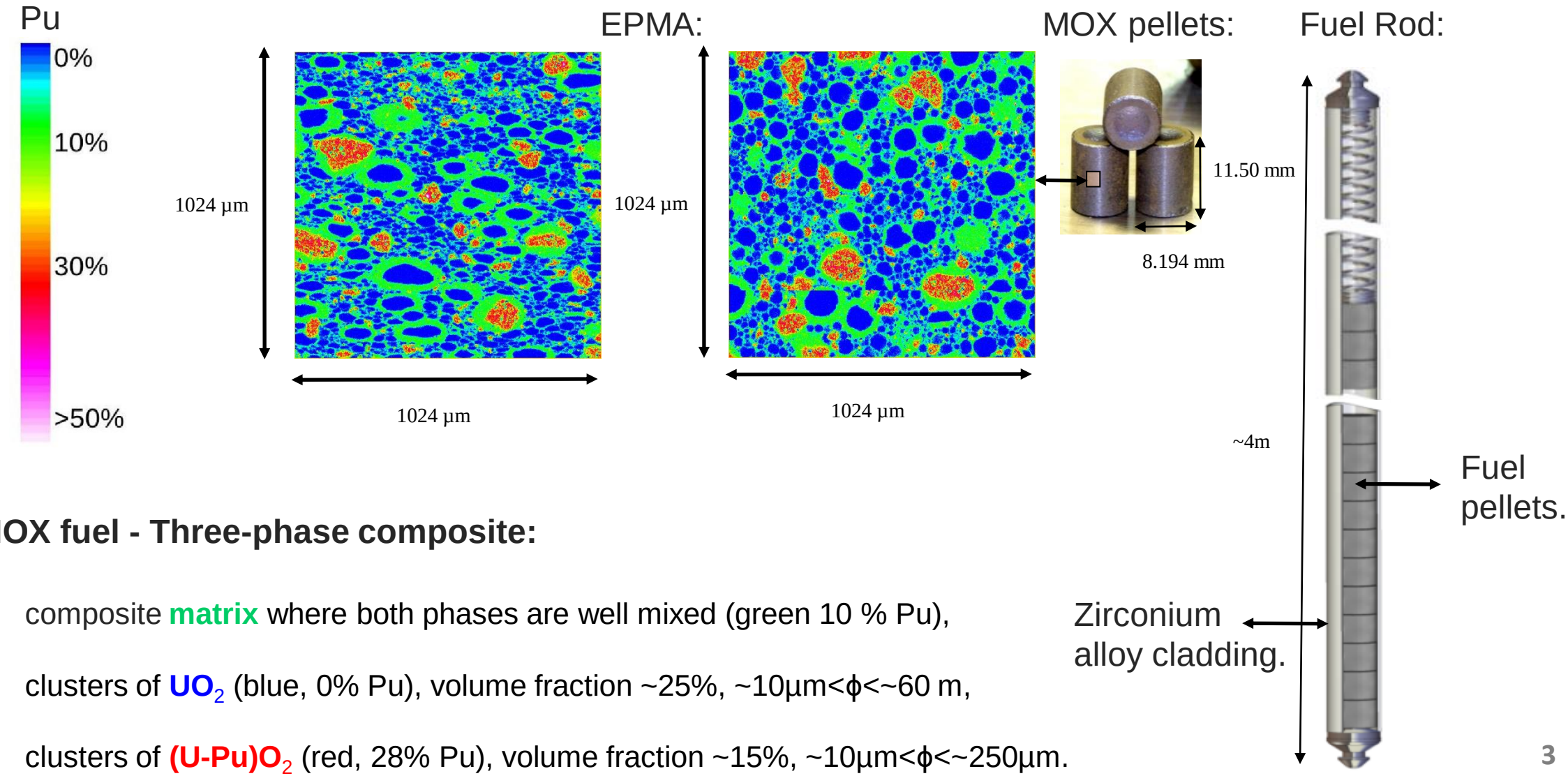

MOX fuel - Three-phase composite:

- composite **matrix** where both phases are well mixed (green 10 % Pu),
- clusters of **UO_2** (blue, 0% Pu), volume fraction ~25%, ~10µm<ϕ<~60 m,
- clusters of **$(U\text{-}Pu)O_2$** (red, 28% Pu), volume fraction ~15%, ~10µm<ϕ<~250µm.

1. Motivations - Two typical examples at the microstructural scale: nonlinear behavior

1. <u>Composite material</u> - MOX nuclear fuel under irradiation (Largenton et al., 2019).

Constitutive relations for the individual phases (r):

$$\boldsymbol{\varepsilon}(\boldsymbol{x},t) = \boldsymbol{\varepsilon}_{\mathsf{e}}(\boldsymbol{x},t) + \boldsymbol{\varepsilon}_{\mathsf{v}}(\boldsymbol{x},t) + \boldsymbol{\varepsilon}_{\mathsf{s}}(\boldsymbol{x},t) \quad \text{, with}$$

$$\boldsymbol{\varepsilon}_{\mathsf{e}}(\boldsymbol{x},t) = \boldsymbol{M}^{(r)} : \boldsymbol{\sigma}(\boldsymbol{x},t)\,,$$

$$\dot{\boldsymbol{\varepsilon}}_{\mathsf{v}}(\boldsymbol{x},t) = \frac{\partial \psi^{(r)}}{\partial \boldsymbol{\sigma}}(\boldsymbol{\sigma}(\boldsymbol{x},t))\,,$$

$$\boldsymbol{\varepsilon}_{\mathsf{s}}(\boldsymbol{x},t) = \varepsilon_{\mathsf{s}}^{(r)}(t)\,\boldsymbol{i}\ .$$

$$\begin{cases} \psi^{(r)}(\boldsymbol{\sigma}) = \psi_1^{(r)}(\sigma_{\mathsf{m}}, \sigma_{\mathsf{eq}}) + \psi_n^{(r)}(\sigma_{\mathsf{eq}}), \\ \psi_n^{(r)}(\sigma_{\mathsf{eq}})(\boldsymbol{x},t) = \dfrac{\sigma_{\mathsf{eq}}^{n+1}(\boldsymbol{x},t)}{3(n+1)G_{\mathsf{v}_n}^{(r)}}\,, \\ \psi_1^{(r)}(\sigma_{\mathsf{m}}, \sigma_{\mathsf{eq}})(\boldsymbol{x},t) = \dfrac{\sigma_{\mathsf{m}}^2(\boldsymbol{x},t)}{2k_{\mathsf{v}_1}^{(r)}} + \dfrac{\sigma_{\mathsf{eq}}^2(\boldsymbol{x},t)}{6G_{\mathsf{v}_1}^{(r)}(t)}. \end{cases}$$

MOX pellets:

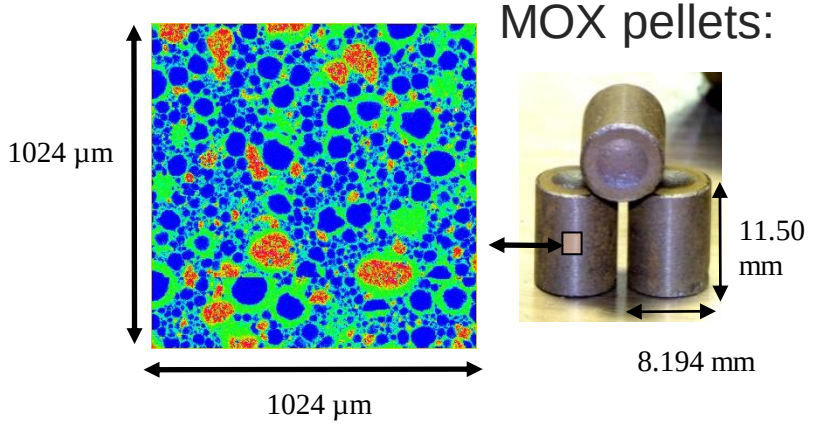

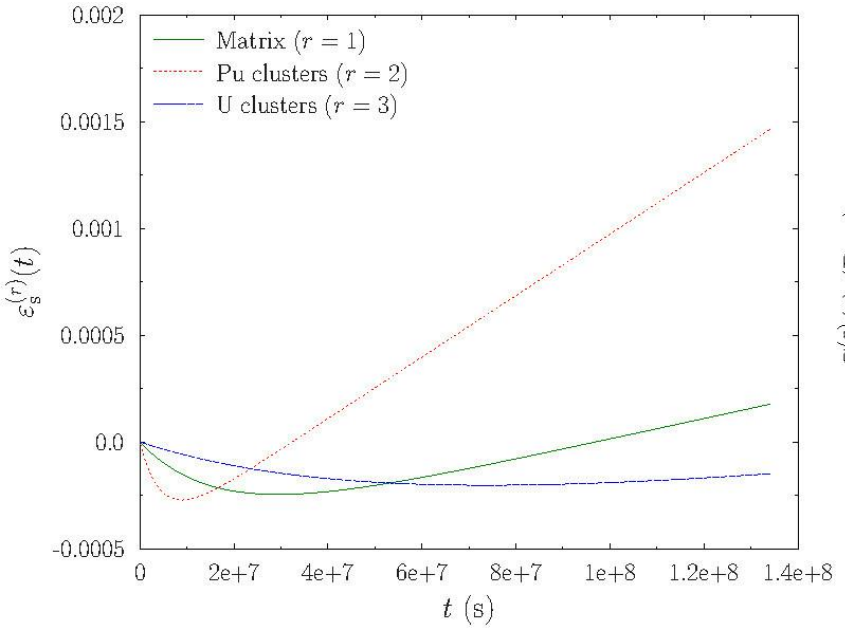

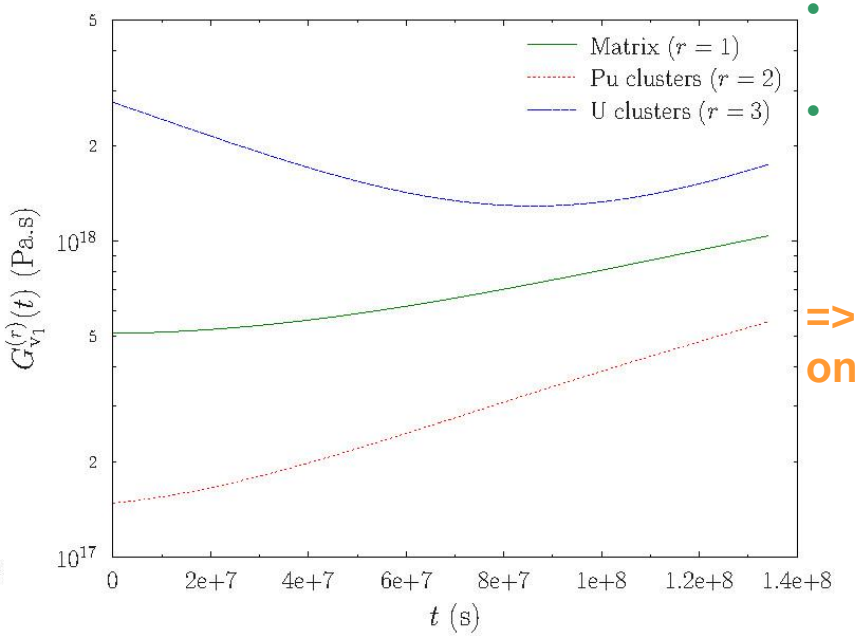

- **Shrinkage-Swelling:** effects of fission products.
- **Creep:** effects of fission rate and temperature.
- **Aging:** time-dependent material properties (function of irradiation which is a function of time).

=> Pellet-Cladding-Interaction => Impact on the first safety barrier ("cladding")?

PREDICT: effective and local behavior of this composite material?

1. Motivations - Two typical examples at the microstructural scale: nonlinear behavior

2. **Polycrystalline material - UO_2 nuclear fuel** (Labat et al., 2023).

Fuel Rod:

UO_2 fuel after irradiation:

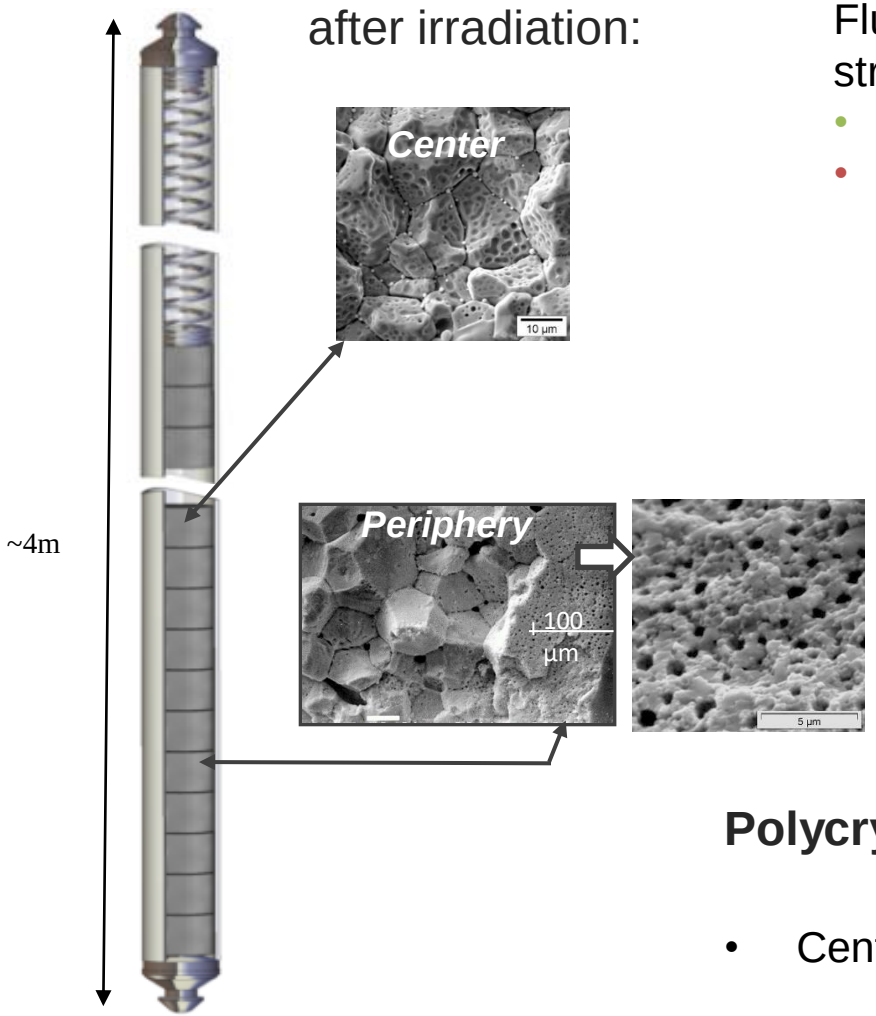

Fluorite crystallographic structure:

- oxygen atoms in green,
- uranium atoms in red.

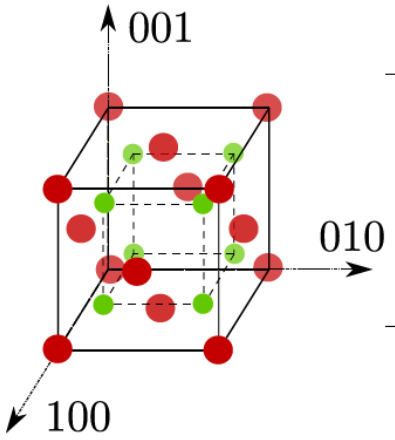

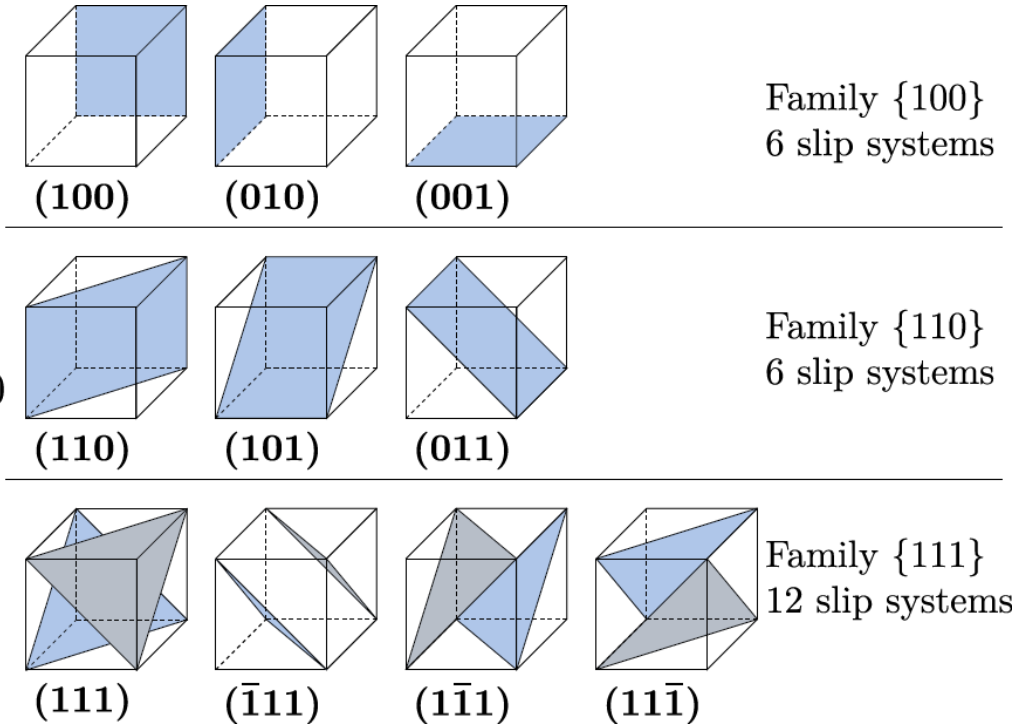

Polycrystalline material:

- Center: Φ_{grain} ~10µm.
- Periphery: Φ_{grain} ~0.3µm.

1. Motivations - Two typical examples at the microstructural scale: nonlinear behavior

2. <u>Polycrystalline material</u> - UO_2 nuclear fuel (Labat et al., 2023)].

Constitutive relations for the slip systems (s):

$$\dot{\gamma}_s^{vp} = \dot{\gamma}_i^0 \times \left(\frac{|\tau_s|}{r_i} \right)^{n_i} \times sgn(\tau_s),$$

$$r_i(\boldsymbol{x}, t) = \tau_i^0(T, \dot{\bar{\varepsilon}}) + h_i(T, \dot{\bar{\varepsilon}}) \times p_i(\boldsymbol{x}, t),$$

$$\dot{p}_i = \sum_{s \in S_i} \dot{\gamma}_s^p, \; \dot{\gamma}_s^p = |\dot{\gamma}_s^{vp}|,$$

$\dot{\gamma}_s^{vp}$ evolution law inspired by [**Knezevic et al.**, *IJP* (2013)] .

- **Thermal creep:** effects of temperature and macroscopic strain rate.
- **High temperature gradient and strain rate** → heterogeneous strain, damage and cracking.

=> Pellet-Cladding-Interaction => Impact on the first safety barrier ("cladding")?

Variation of T°C – $\dot{\bar{\varepsilon}}$ = 10^{-1} $[s]^{-1}$:

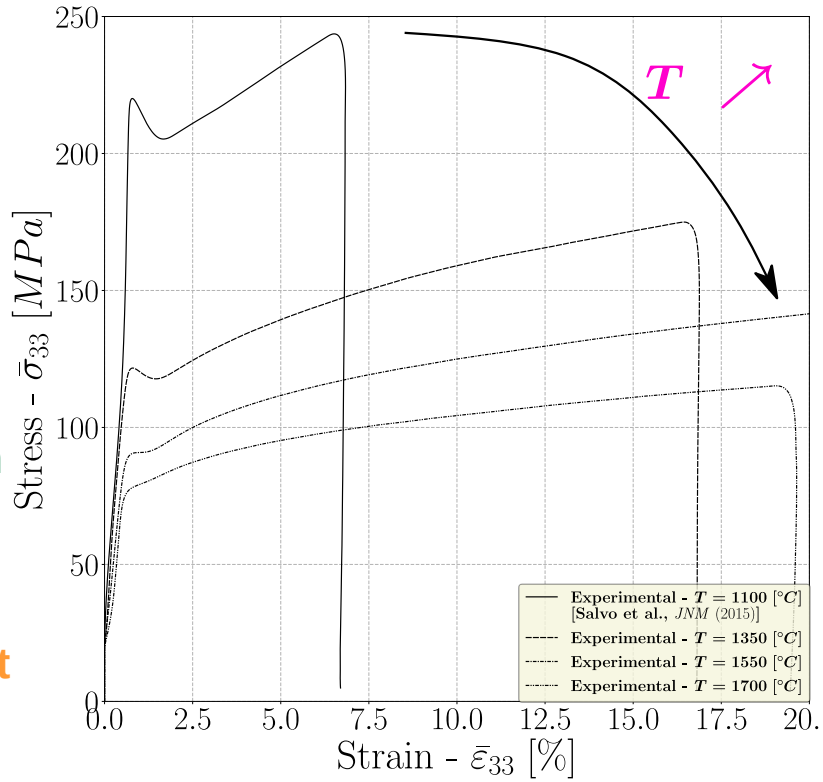

Variation of $\dot{\bar{\varepsilon}}$ – T°C = 1500°C:

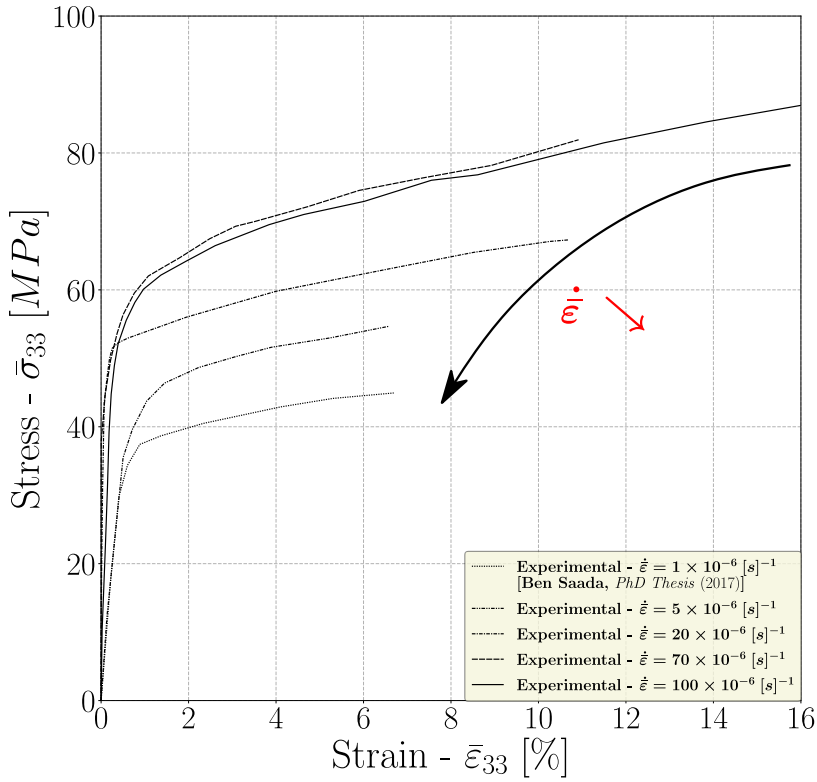

T°C = 1550°C
– $\dot{\bar{\varepsilon}}$ = 10^{-1} $[s]^{-1}$:

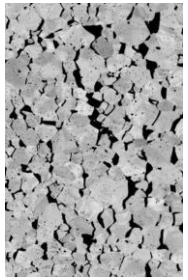

T°C = 1700°C
– $\dot{\bar{\varepsilon}}$ = 10^{-1} $[s]^{-1}$:

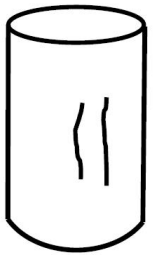

T°C = 1100°C
– $\dot{\bar{\varepsilon}}$ = 10^{-1} $[s]^{-1}$

PREDICT: effective and local behavior of this polycrystalline material?

1. Homogenization of these composite and polycrystalline materials

- **Homogenization of highly heterogeneous materials with nonlinear dissipative constituents entering the class of Generalized Standard Materials** (GSM) (Halphen & Nguyen, 1975) **governed by two convex potentials.**

At each point x of the microstructure:

State of the system (state variables) : $\varepsilon, \alpha = \boldsymbol{\varepsilon^p}\ (\boldsymbol{\varepsilon_v}, \boldsymbol{\varepsilon_s}, \boldsymbol{\varepsilon_{vp}}, \boldsymbol{p}\ \ldots),$

Energy available in the system : $w(\varepsilon, \alpha),$

$\Rightarrow$ **Driving forces** : $\boldsymbol{\sigma} = \dfrac{\partial w}{\partial \boldsymbol{\varepsilon}}(\varepsilon, \alpha), \quad \boldsymbol{\mathcal{A}} = -\dfrac{\partial w}{\partial \boldsymbol{\alpha}}(\varepsilon, \alpha),$

Evolution of the internal variables : $\dot{\alpha} = \dfrac{\partial \psi}{\partial \boldsymbol{\mathcal{A}}}(\boldsymbol{\mathcal{A}}) \quad \Leftrightarrow \quad \boldsymbol{\mathcal{A}} = \dfrac{\partial \varphi}{\partial \dot{\boldsymbol{\alpha}}}(\dot{\alpha}).$

Where ψ *and* φ are dual potentials.

1. Homogenization of these composite and polycrystalline materials

- **EXACT separation of scales in nonlinear problems is seldomly met : an infinite number of internal variables is required** (Mandel, 1968 – Rice, 1971 – Suquet, 1982 1987).

State variables	:	$\overline{\varepsilon}, \quad \widetilde{\alpha} = \{\varepsilon^{\mathrm{p}}(x)\}_{x \in V},$
Potentials	:	$\widetilde{w}\,(\overline{\varepsilon}, \widetilde{\alpha}) = \left\langle w(\varepsilon, \varepsilon^{\mathrm{p}}) \right\rangle, \quad \widetilde{\varphi}(\dot{\widetilde{\alpha}}) = \left\langle \varphi(\dot{\varepsilon}^{\mathrm{p}}) \right\rangle,$
Driving forces	:	$\overline{\sigma} = \frac{\partial \widetilde{w}}{\partial \overline{\varepsilon}}(\overline{\varepsilon}, \widetilde{\alpha}), \quad \widetilde{\mathcal{A}} = -\frac{\partial \widetilde{w}}{\partial \widetilde{\alpha}}(\overline{\varepsilon}, \widetilde{\alpha}),$
Evolution of internal variables	:	$\widetilde{\mathcal{A}} = \frac{\partial \widetilde{\varphi}}{\partial \dot{\widetilde{\alpha}}}(\dot{\widetilde{\alpha}}).$

=> No scale decoupling : both scales have to be resolved simultaneously

Differential Equation in a space of infinite dimension:

$$\dot{\widetilde{\alpha}} = \frac{\partial \widetilde{\psi}}{\partial \widetilde{\mathcal{A}}} \left(-\frac{\partial \widetilde{w}}{\partial \widetilde{\alpha}}(\overline{\varepsilon}, \widetilde{\alpha}) \right).$$

$$\langle * \rangle = \frac{1}{|V|} \int * \, dx$$

Aim of this work: **derive a reduced model.**

2. Classical approach - Transformation Field Analysis (TFA)

- **Objective :** approximate homogenized model for the r.v.e. *V*. Internal variables =>

$$\tilde{\boldsymbol{\alpha}} = \boldsymbol{\varepsilon}^{\mathrm{p}}(\boldsymbol{x})|_{\boldsymbol{x}\in V},$$

where *V* = r.v.e. (representative volume element).

Reduction (Dvorak, 1992) **of the plastic strain field on the r.v.e to** $6 \times N$ **internal variables,** N**= number of phases in the composite or polycrystalline material:**

- **H1. Plastic strain uniform / phase:**

$$\boldsymbol{\varepsilon}^{\mathrm{p}}(\boldsymbol{x}) = \sum_{r=1}^{N} \boldsymbol{\varepsilon}_r^{\mathrm{p}} \chi^{(r)}(\boldsymbol{x}), \quad \boldsymbol{x} \in V.$$

Internal variables : $\boldsymbol{\varepsilon}_r^{\mathrm{p}} | r = 1, \ldots N.$

- **H2. Evolution of ε_r^p governed by the average stress in phase *r*:**

$$\boldsymbol{\varepsilon}_r = \boldsymbol{M}^{(r)} : \boldsymbol{\sigma}_r + \boldsymbol{\varepsilon}_r^{\mathrm{p}}, \quad \boldsymbol{\sigma}_r = \langle \boldsymbol{\sigma} \rangle_r,$$

$$\dot{\boldsymbol{\varepsilon}}_r^{\mathrm{p}} = \frac{\partial \psi^{(r)}}{\partial \boldsymbol{\sigma}} (\overline{\boldsymbol{\sigma}}_r).$$

2. Classical approach - Transformation Field Analysis (TFA)

- **Very stiff predictions...**

Simulations
(Michel & Suquet, 2003)

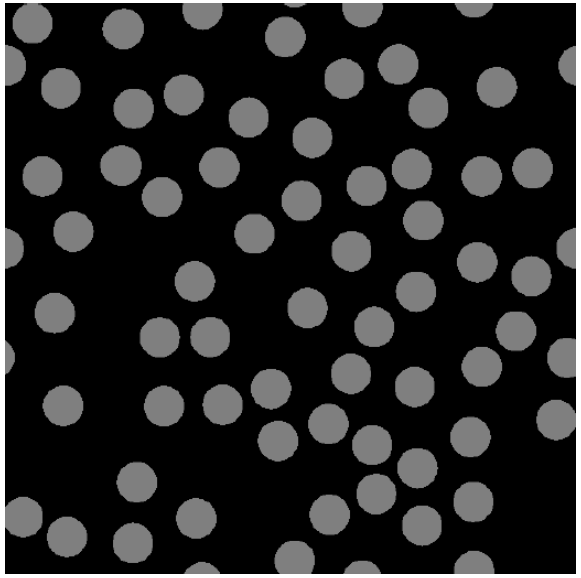

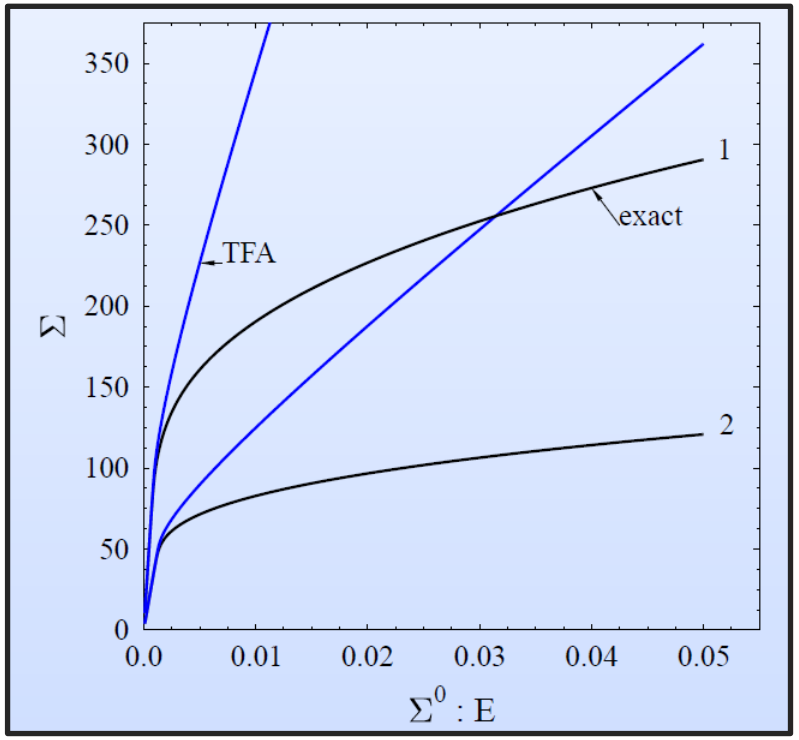

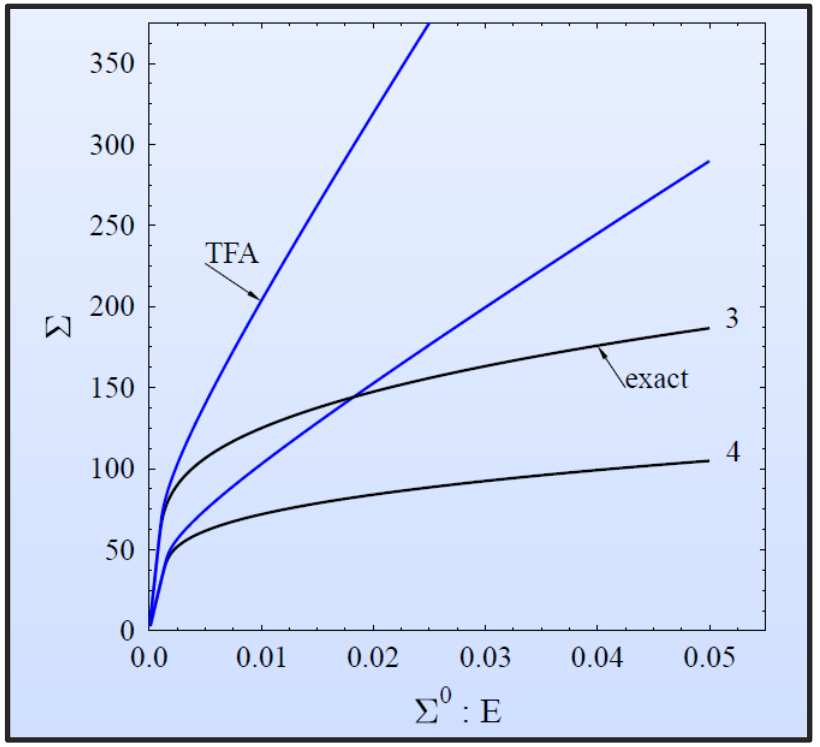

4 loading conditions:

$$\overline{\boldsymbol{\sigma}} = \overline{\sigma}(t)\boldsymbol{\Sigma}^0.$$

$$\boldsymbol{\Sigma}^{(1)} = \boldsymbol{e}_1 \otimes \boldsymbol{e}_1,\ \boldsymbol{\Sigma}^{(2)} = \boldsymbol{e}_1 \otimes \boldsymbol{e}_2 + \boldsymbol{e}_2 \otimes \boldsymbol{e}_1,\ \boldsymbol{\Sigma}^{(3)} = \boldsymbol{\Sigma}^{(1)} + \frac{1}{2}\boldsymbol{\Sigma}^{(2)},\ \boldsymbol{\Sigma}^{(4)} = \boldsymbol{\Sigma}^{(1)} + \boldsymbol{\Sigma}^{(2)}.$$

2. Classical approach - Transformation Field Analysis (TFA)

- **What's wrong?**

Simulations
(Michel & Suquet, 2003)

Experiments
(Doumalin & al, 2003)

Nonlinear composite (two−phase):

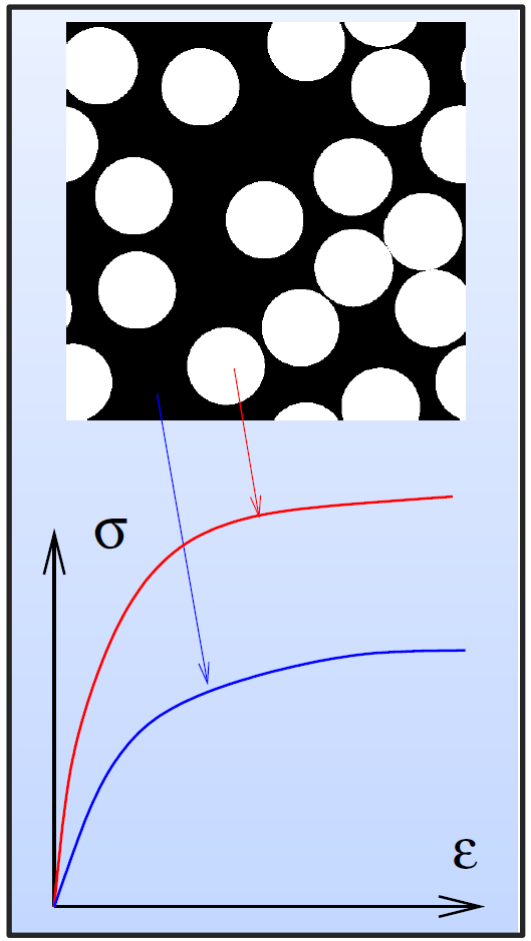

Actual nonuniform plastic strain field:

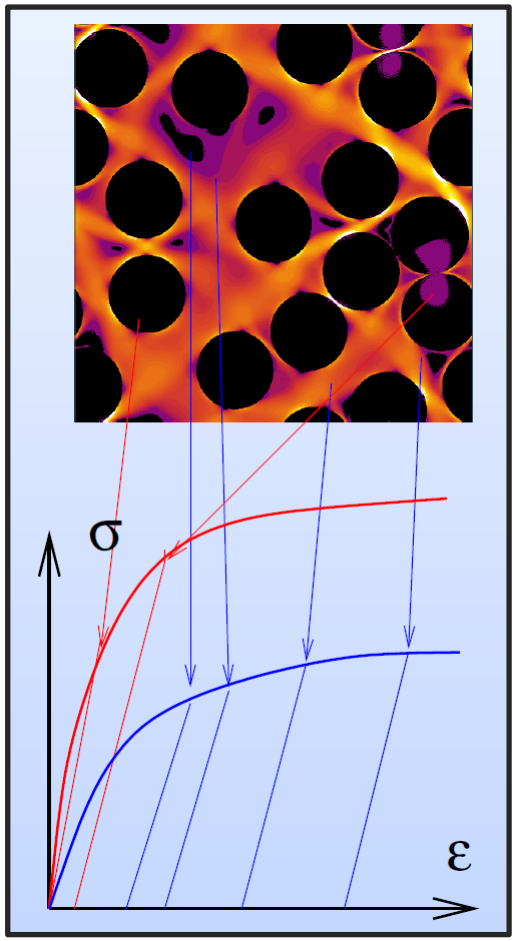

Uniform plastic strain field (TFA):

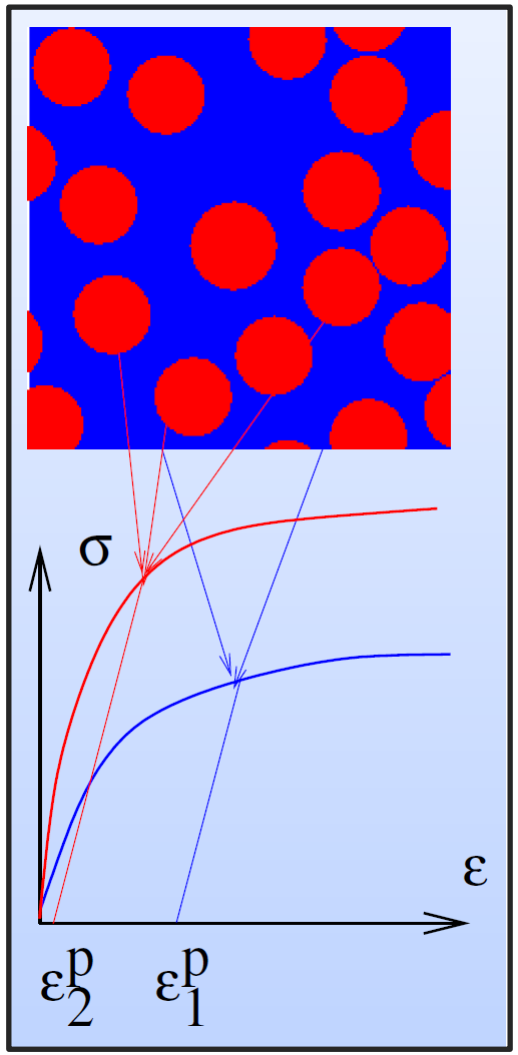

Polycrystalline Zirconium:

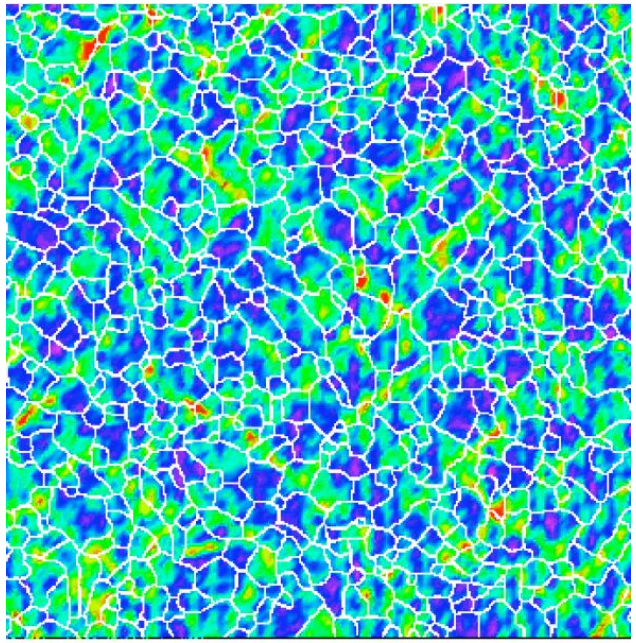

Field fluctuations do exist !

The TFA assumes that the plastic strain field is uniform per phase.

3. Reduced model - Nonuniform Transformation Field Analysis (NTFA)

- **Reduction** (Michel & Suquet, 2003)**:** reproduce the “dynamics” (evolution) and the observed "patterns" with **just a few variables, but physically motivated.**

1st ingredient: Re-formulation of assumptions H1 TFA => internal variables $\alpha = \varepsilon^p, \varepsilon_v, \varepsilon_s, \varepsilon_{vp}, p$ **... decomposed on nonuniform “(visco)plastic modes”, “hardening modes” …**

Example for ε^p **:**

$$\varepsilon^{\mathrm{p}}(x,t) = \sum_{k=1}^{M} \varepsilon_k^{\mathrm{p}}(t)\, \boldsymbol{\mu}^{(k)}(x), \quad x = \text{microscopic variable} \in \text{volume element } V.$$

$\boldsymbol{\mu}^{(k)}$ **tensorial field** defined on *V* only, capturing the pattern of the plastic deformation, ε_k^p is a **scalar**. The ε_k^p’s are the **internal variables of the model.** Other possible notations for ε_k^p depending on the studied behavior: $\xi^{(k)}, \xi_{vp}^{(k)}, \xi_p^{(k)} \dots$

- $\boldsymbol{\mu}^{(k)}$ has its support in a single phase in *V* or “on” *V*: mode identification “on” *V* reduces the number of modes (Largenton et al., 2014).
- $\boldsymbol{\mu}^{(k)}$ are mutually orthogonal: $\langle \boldsymbol{\mu}^{(k)} : \boldsymbol{\mu}^{(l)} \rangle = 0$ when $k \neq l$.

$$\text{State variables} \quad : \quad \bar{\varepsilon},\ (\varepsilon_k^{\mathrm{p}})_{k=1,M}.$$

3. Reduced model - Nonuniform Transformation Field Analysis (NTFA)

- **What do these modes look like?**

Composite material
[**Michel and Suquet**, *JMPS* (2016)]

(a) *Micrograph.*

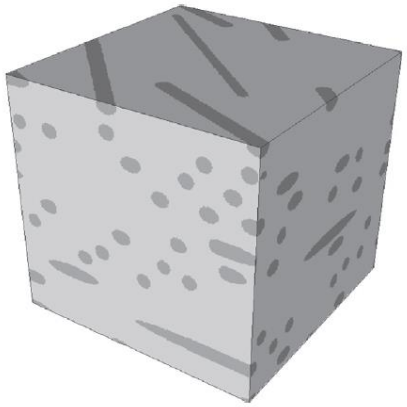

(b) *r.v.e. V.*

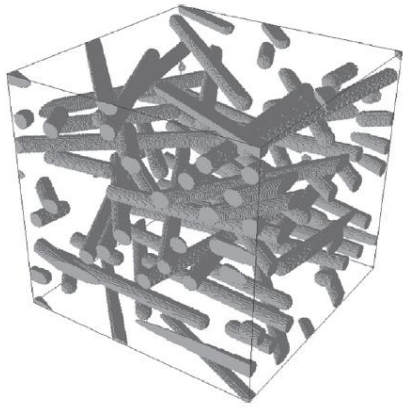

(c) *r.v.e. V – Only fibers.*

- Elastic fibers.
- Elasto-viscoplastic matrix with nonlinear kinematic hardening.
- Fiber volume fraction: 0.1.

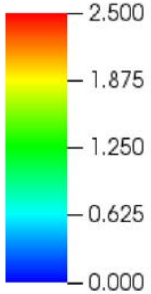

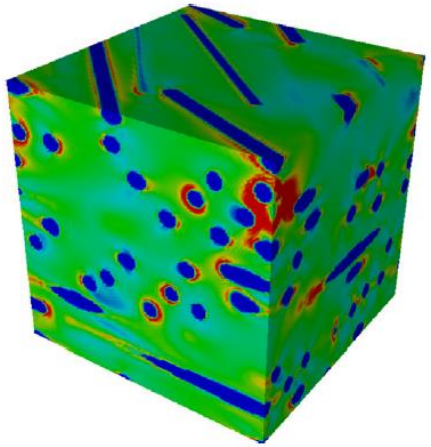

(a) Mode 1.

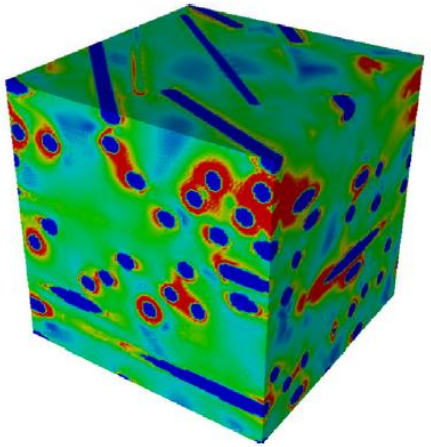

(b) Mode 2.

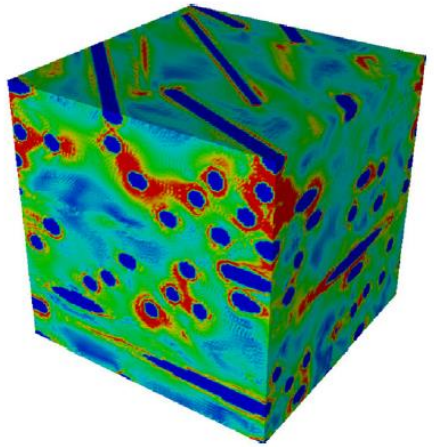

(c) Mode 3.

Snapshot of the modes (the equivalent strain μ_{eq}):

3. Reduced model - Nonuniform Transformation Field Analysis (NTFA)

- **What do these modes look like?**

Polycrystalline material
[**Michel and Suquet**, *CM* (2016)]

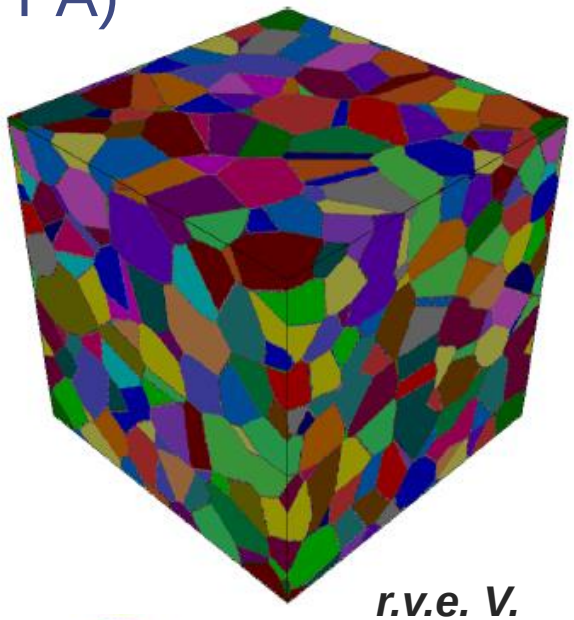

r.v.e. V.

- 500 grains.
- The crystal plasticity model for ice proposed by [**Castelnau et al.**, 2008] and modified in [**Suquet et al.**, 2012]: similar to the model of Méric-Cailletaud [**Méric and Cailletaud**, 1991].

Snapshot of the modes
(the equivalent strain μ_{eq}):

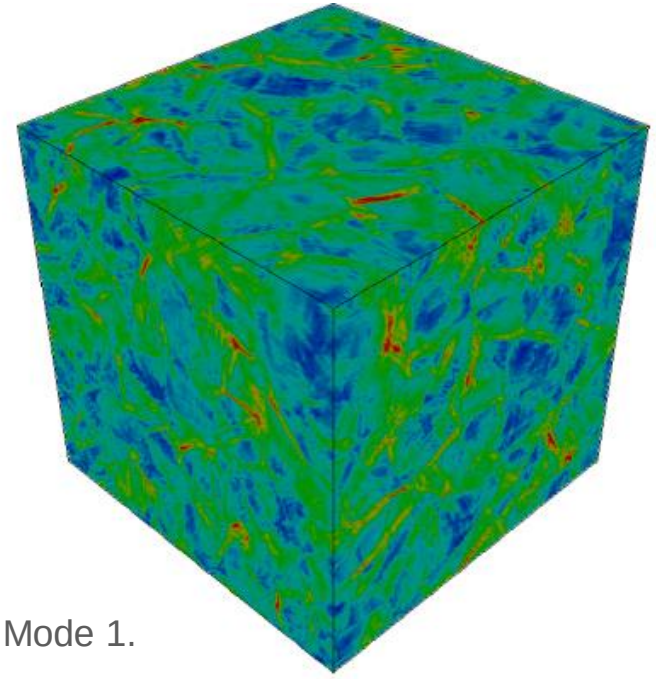

Mode 1.

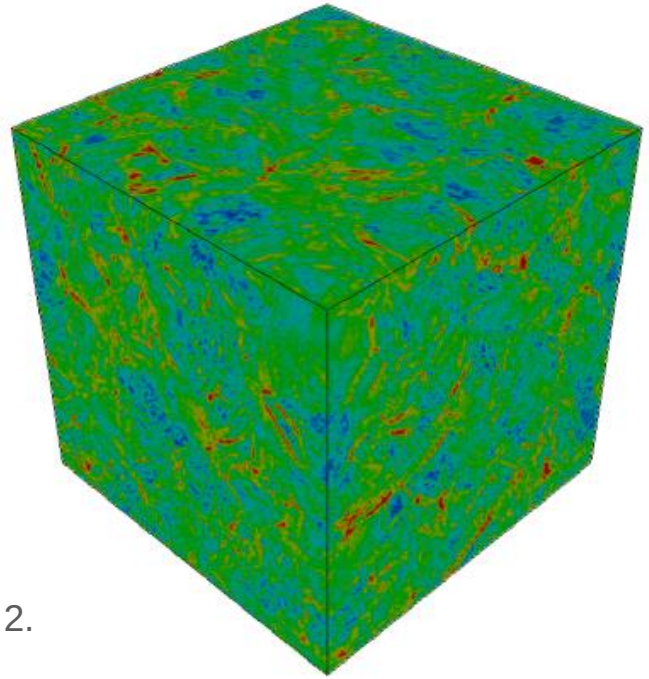

Mode 2.

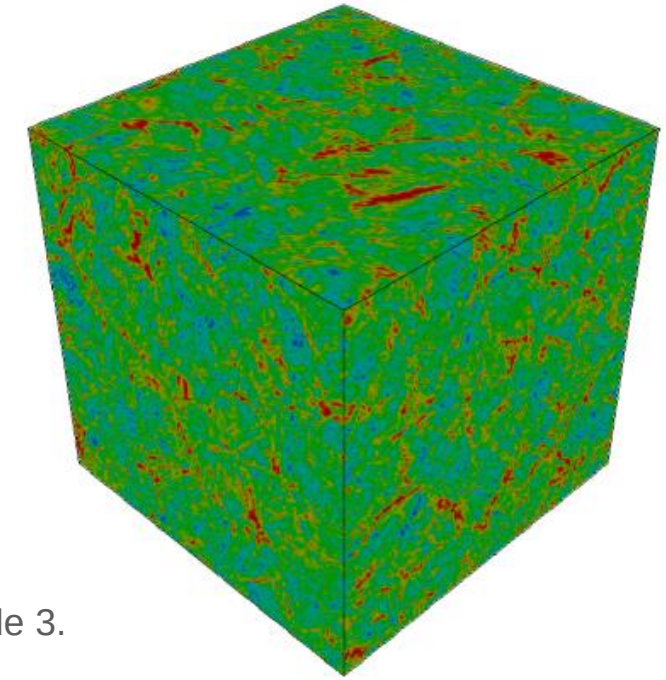

Mode 3.

Requires an accurate evolution law for the amplitudes ε_k^p on the modes.

3. Reduced model - Nonuniform Transformation Field Analysis (NTFA)

- **2nd ingredient : evolution law for the reduced variables.**

1. Local fields : Prescribe the macroscopic state variables $\bar{\varepsilon}, (\varepsilon_k^p)_{k=1,M}$.

$$\boldsymbol{\sigma}(x) = \boldsymbol{L}(x) : (\varepsilon(x) - \varepsilon^{\mathrm{p}}(x)), \quad \varepsilon^{\mathrm{p}}(x) = \sum_{k=1}^{M} \varepsilon_k^{\mathrm{p}} \boldsymbol{\mu}^{(k)}(x),$$
$$\operatorname{div}(\boldsymbol{\sigma}(x)) = 0, \quad \langle \varepsilon \rangle = \bar{\varepsilon}, \quad + \text{B.C. (periodicity)}.$$

Linear (thermoelastic) problem => superposition:

$$\varepsilon(x,t) = \boldsymbol{A}(x) : \bar{\varepsilon}(t) + \sum_{k=1}^{M} \boldsymbol{D} * \boldsymbol{\mu}^{(k)}(x) \varepsilon_k^{\mathrm{p}}$$
$$\boldsymbol{\sigma}(x,t) = \boldsymbol{L}(x) : \boldsymbol{A}(x) : \bar{\varepsilon}(t) + \sum_{k=1}^{M} \boldsymbol{\rho}^{(k)}(x) \varepsilon_k^{\mathrm{p}}(t),$$

To simplify notation $\boldsymbol{\varepsilon_l^p} = \xi^{(l)}$:

$$\boldsymbol{\varepsilon}(\boldsymbol{x}) = \boldsymbol{A}(\boldsymbol{x}) : \bar{\varepsilon} + \sum_{\ell=1}^{M} (\boldsymbol{D} * \boldsymbol{\mu}^{(\ell)})(\boldsymbol{x}) \xi^{(\ell)},$$

$$\boldsymbol{\sigma}(\boldsymbol{x}) = \boldsymbol{L}(\boldsymbol{x}) : \boldsymbol{A}(\boldsymbol{x}) : \bar{\varepsilon} + \sum_{\ell=1}^{M} \boldsymbol{\rho}^{(\ell)}(\boldsymbol{x}) \xi^{(\ell)}.$$

- $\boldsymbol{A}(x)$ **elastic strain-localization tensor.**
- $\boldsymbol{D}$ Green's operator, $\boldsymbol{D} * \boldsymbol{\mu}^{(k)}(x)$ **influence tensors.**
- $\boldsymbol{\rho}^{(k)}(x) = \boldsymbol{L}(x) : \left(\boldsymbol{D} * \boldsymbol{\mu}^{(k)}(x) - \boldsymbol{\mu}^{(k)}(x)\right)$.

3. Reduced model - Nonuniform Transformation Field Analysis (NTFA)

- **2nd ingredient : evolution law for the reduced variables.**

2. Knowing that the effective free energy $\widetilde{w}$ is the average in V of the local free energy w, the reduced thermodynamic forces associated with the macroscopic state variables are $a^{(k)}$:

$$\widetilde{W}(\bar{\varepsilon}, \boldsymbol{\xi}) = \frac{1}{2}\bar{\varepsilon}: \widetilde{\boldsymbol{L}}: \bar{\varepsilon} - \bar{\varepsilon}: \sum_{k=1}^{M} \boldsymbol{a}^{(k)}\xi^{(k)} + \frac{1}{2}\sum_{k,\ell=1}^{M} (\mathcal{L}^{(k\ell)} - \mathcal{D}^{(k\ell)})\xi^{(k)}\xi^{(\ell)}.$$

$$\mathfrak{a}^{(k)} = -\frac{\partial \widetilde{W}}{\partial \xi^{(k)}}(\bar{\varepsilon}, \boldsymbol{\xi}) = \bar{\varepsilon}: \boldsymbol{a}^{(k)} + \sum_{\ell=1}^{M} (\mathcal{D}^{(k\ell)} - \mathcal{L}^{(k\ell)})\xi^{(\ell)}, \text{ with}$$

$$\left.\begin{aligned} \widetilde{\boldsymbol{L}} &= \langle \boldsymbol{A}^{\mathrm{T}}: \boldsymbol{L}: \boldsymbol{A}\rangle, & \boldsymbol{a}^{(k)} &= \langle \boldsymbol{\mu}^{(k)}: \boldsymbol{L}: \boldsymbol{A}\rangle, \\ \mathcal{D}^{(k\ell)} &= \langle \boldsymbol{\mu}^{(k)}: \boldsymbol{L}: (\boldsymbol{D}^{*}\boldsymbol{\mu}^{(\ell)})\rangle, & \mathcal{L}^{(k\ell)} &= \langle \boldsymbol{\mu}^{(k)}: \boldsymbol{L}: \boldsymbol{\mu}^{(\ell)}\rangle. \end{aligned}\right\}$$

Reminder – At each point x of the microstructure:

State of the system (state variables)	:	$\varepsilon, \alpha = \varepsilon^{p}\,(\varepsilon_v, \varepsilon_s, \varepsilon_{vp}, p \ldots)$,
Energy available in the system	:	$w(\varepsilon, \alpha), w(\varepsilon, \alpha) = \frac{1}{2}(\varepsilon - \alpha): \boldsymbol{L}: (\varepsilon - \alpha)$,
$\Rightarrow$ **Driving forces**	:	$\sigma = \frac{\partial w}{\partial \varepsilon}(\varepsilon, \alpha), \quad \mathcal{A} = -\frac{\partial w}{\partial \alpha}(\varepsilon, \alpha)$,
Evolution of the internal variables	:	$\dot{\alpha} = \frac{\partial \psi}{\partial \mathcal{A}}(\mathcal{A}) \quad \Leftrightarrow \quad \mathcal{A} = \frac{\partial \varphi}{\partial \dot{\alpha}}(\dot{\alpha})$.

Where ψ *and* φ are dual potentials.

3. Reduced model - Nonuniform Transformation Field Analysis (NTFA)

- **2nd ingredient : evolution law for the reduced variables.**

3. Reduced kinetics: the hard problem!

$$\alpha^{(k)} = -\frac{\partial \widetilde{w}}{\partial \xi^{(k)}}(\bar{\varepsilon}, \boldsymbol{\xi}) = \bar{\varepsilon} : \boldsymbol{a}^{(k)} + \sum_{\ell=1}^{M} (\mathcal{D}^{(k\ell)} - \mathcal{L}^{(k\ell)})\xi^{(\ell)}$$

, with

$$\left.\begin{aligned} \boldsymbol{a}^{(k)} &= \langle \boldsymbol{\mu}^{(k)} : \boldsymbol{L} : \boldsymbol{A} \rangle, \\ \mathcal{D}^{(k\ell)} &= \langle \boldsymbol{\mu}^{(k)} : \boldsymbol{L} : (\boldsymbol{D} * \boldsymbol{\mu}^{(\ell)}) \rangle, \quad \mathcal{L}^{(k\ell)} = \langle \boldsymbol{\mu}^{(k)} : \boldsymbol{L} : \boldsymbol{\mu}^{(\ell)} \rangle. \end{aligned}\right\}$$

Evolution of the reduced thermodynamic forces:

$$\dot{\xi}^{(k)} = \frac{\partial \widetilde{\psi}}{\partial \alpha^{(k)}}(\bar{\varepsilon}, \boldsymbol{\alpha})$$

$$\dot{\alpha}^{(k)} = \frac{\partial \alpha^{(k)}}{\partial \bar{\varepsilon}} : \dot{\bar{\varepsilon}} + \sum_{\ell=1}^{M} \frac{\partial \alpha^{(k)}}{\partial \xi^{(\ell)}} \dot{\xi}^{(\ell)} = \frac{\partial \alpha^{(k)}}{\partial \bar{\varepsilon}} : \dot{\bar{\varepsilon}} + \frac{\partial \widetilde{\psi}}{\partial \xi^{(k)}}(\bar{\varepsilon}, \boldsymbol{\xi}(\bar{\varepsilon}, \boldsymbol{\alpha})).$$

$\widetilde{\psi}$ **unknown?**

3. Reduced model - Nonuniform Transformation Field Analysis (NTFA)

- **2nd ingredient : evolution law for the reduced variables.**

4. The effective dissipation potential: two proposals!

- **1st proposal: A hybrid formulation - Approximation of the effective dissipation potential [Fritzen and Leuschner,** *CMAME* (2013)]

$$\widetilde{\psi} = < \psi >$$

- [**Michel and Suquet**, *JMPS* (2016)] has shown that the definition of the effective dissipation potential chosen here by [**Fritzen and Leuschner**, *CMAME* (2013)] is not rigorously equivalent to the exact definition by duality.
  - Nevertheless, it is a good approximation when the number of modes chosen is sufficiently large!
- The derivative of the effective dissipation potential must be known at each integration time step.
- When the dissipation potential of the phases is not quadratic, knowledge of these derivatives requires calculation of local quantities before performing averaging operations.
  - We therefore lose the interest of a reduced model based on the NTFA approach, especially for our two typical examples!

3. Reduced model - Nonuniform Transformation Field Analysis (NTFA)

- **2nd ingredient : evolution law for the reduced variables.**

4. The effective dissipation potential: two proposals!

- **2nd proposal: Tangent Second-Order linearization (TSO)** [**Castañeda**, *JMPS* (1996)], [**Michel and Suquet**, *JMPS* (2016)] – In each individual phase *r the potential* $\psi^{(r)}$ is expanded to second-order in the stress as:

$$\psi^{(r)}(\mathcal{A}) \simeq \psi^{(r)}_{TSO}(\mathcal{A}),$$

$$\psi^{(r)}_{TSO}(\mathcal{A}) = \psi^{(r)}(\check{\mathcal{A}}^{(r)}) + \frac{\partial \psi^{(r)}}{\partial \mathcal{A}}(\check{\mathcal{A}}^{(r)}) : \left(\mathcal{A} - \check{\mathcal{A}}^{(r)}\right) + \frac{1}{2}\left(\mathcal{A} - \check{\mathcal{A}}^{(r)}\right) : \boldsymbol{M}_0^{(r)} : \left(\mathcal{A} - \check{\mathcal{A}}^{(r)}\right) \text{ , with } \quad \check{\mathcal{A}}^{(r)} = \langle \mathcal{A} \rangle^{(r)}, \quad \boldsymbol{M}_0^{(r)} = \frac{\partial^2 \psi^{(r)}}{\partial \mathcal{A}^2}(\check{\mathcal{A}}^{(r)}).$$

$$\widetilde{\psi}_{TSO}(\bar{\varepsilon}, \boldsymbol{\xi}) = \sum_{r=1}^{P} c^{(r)} \left[\psi^{(r)}(\langle \mathcal{A} \rangle^{(r)}) + \frac{1}{2} \frac{\partial^2 \psi^{(r)}}{\partial \mathcal{A}^2}(\langle \mathcal{A} \rangle^{(r)}) :: \boldsymbol{C}^{(r)}(\mathcal{A}) \right],$$

with

$$\boldsymbol{C}^{(r)}(\mathcal{A}) = \langle \left(\mathcal{A} - \langle \mathcal{A} \rangle^{(r)}\right) \otimes \left(\mathcal{A} - \langle \mathcal{A} \rangle^{(r)}\right) \rangle^{(r)} = \langle \mathcal{A} \otimes \mathcal{A} \rangle^{(r)} - \langle \mathcal{A} \rangle^{(r)} \otimes \langle \mathcal{A} \rangle^{(r)}.$$

NTFA-TSO - The differential equation of the reduced thermodynamic forces (reduced variables):

$$\dot{\alpha}^{(k)} = \frac{\partial \alpha^{(k)}}{\partial \bar{\varepsilon}} : \dot{\bar{\varepsilon}} + \sum_{r=1}^{P} c^{(r)} \left[\frac{\partial \psi^{(r)}}{\partial \mathcal{A}}(\langle \mathcal{A} \rangle^{(r)}) : \frac{\partial \langle \mathcal{A} \rangle^{(r)}}{\partial \xi^{(k)}} + \frac{1}{2} \frac{\partial^2 \psi^{(r)}}{\partial \mathcal{A}^2}(\langle \mathcal{A} \rangle^{(r)}) :: \frac{\partial \boldsymbol{C}^{(r)}(\mathcal{A})}{\partial \xi^{(k)}} + \frac{1}{2} \frac{\partial^3 \psi^{(r)}}{\partial \mathcal{A}^3}(\langle \mathcal{A} \rangle^{(r)}) ::: \boldsymbol{C}^{(r)}(\mathcal{A}) \otimes \frac{\partial \langle \mathcal{A} \rangle^{(r)}}{\partial \xi^{(k)}} \right].$$

4. NTFA-TSO applied to the 1st typical example - Implementation & results

- **Exact local problem** (Largenton et al., 2019).

***Equation System** (1) **Coupled with Evolution Law** (2):*

$$\left.\begin{aligned} \boldsymbol{\sigma}(\boldsymbol{x},t) &= \boldsymbol{L}(\boldsymbol{x}) : (\boldsymbol{\varepsilon}(\boldsymbol{x},t) - \boldsymbol{\varepsilon}_{\mathsf{v}}(\boldsymbol{x},t) - \boldsymbol{\varepsilon}_{\mathsf{s}}(\boldsymbol{x},t)), \\ \operatorname{div} \boldsymbol{\sigma}(\boldsymbol{x},t) &= 0, \quad \boldsymbol{\sigma}(\boldsymbol{x},t)\cdot\boldsymbol{n}(\boldsymbol{x}) \text{ antiperiodic on } \partial V, \\ \boldsymbol{\varepsilon}(\boldsymbol{x},t) &= \overline{\boldsymbol{\varepsilon}}(t) + \tfrac{1}{2}(\boldsymbol{\nabla}\boldsymbol{u}^*(\boldsymbol{x},t) + \boldsymbol{\nabla}\boldsymbol{u}^{*T}(\boldsymbol{x},t)), \quad \boldsymbol{u}^*(\boldsymbol{x},t) \text{ periodic on } \partial V, \end{aligned}\right\} \quad (1)$$

$$\boldsymbol{\varepsilon}(\boldsymbol{x},t) = \boldsymbol{\varepsilon}_{\mathsf{e}}(\boldsymbol{x},t) + \boldsymbol{\varepsilon}_{\mathsf{v}}(\boldsymbol{x},t) + \boldsymbol{\varepsilon}_{\mathsf{s}}(\boldsymbol{x},t) \text{ , with}$$

$$\boldsymbol{\varepsilon}_{\mathsf{e}}(\boldsymbol{x},t) = \boldsymbol{M}^{(r)} : \boldsymbol{\sigma}(\boldsymbol{x},t),$$

$$\dot{\boldsymbol{\varepsilon}}_{\mathsf{v}}(\boldsymbol{x},t) = \frac{\partial \psi^{(r)}}{\partial \boldsymbol{\sigma}}(\boldsymbol{\sigma}(\boldsymbol{x},t)),$$

$$\boldsymbol{\varepsilon}_{\mathsf{s}}(\boldsymbol{x},t) = \varepsilon_{\mathsf{s}}^{(r)}(t)\,\boldsymbol{i}\,.$$

$$\left.\begin{aligned} \psi^{(r)}(\boldsymbol{\sigma}) &= \psi_1^{(r)}(\sigma_{\mathsf{m}},\sigma_{\mathsf{eq}}) + \psi_n^{(r)}(\sigma_{\mathsf{eq}}), \\ \psi_n^{(r)}(\sigma_{\mathsf{eq}})(\boldsymbol{x},t) &= \frac{\sigma_{\mathsf{eq}}^{n+1}(\boldsymbol{x},t)}{3(n+1)G_{\mathsf{V}_n}^{(r)}}, \\ \psi_1^{(r)}(\sigma_{\mathsf{m}},\sigma_{\mathsf{eq}})(\boldsymbol{x},t) &= \frac{\sigma_{\mathsf{m}}^2(\boldsymbol{x},t)}{2k_{\mathsf{V}_1}^{(r)}} + \frac{\sigma_{\mathsf{eq}}^2(\boldsymbol{x},t)}{6G_{\mathsf{V}_1}^{(r)}(t)}. \end{aligned}\right\} \quad (2)$$

Evolution of $G_{v1}^{(r)}$ and ε_s: given in part 1 (Motivations).

Phase	E (Pa)	ν (-)	$k_{\mathsf{V}_1}^{(r)}$ (Pa.s)	$G_{\mathsf{V}_n}^{(r)}$ (Pa^n.s)	n (-)
Matrix (r=1)	2.e+11	0.3	1.67e+18	1.e+39	3.67
Pu clusters (r=2)	2.e+11	0.3	5.01e+17	1.e+39	3.67
U clusters (r=3)	2.e+11	0.3	1.04e+19	1.e+39	3.67

RVE *V*
(3 phases & 147³ Voxels).

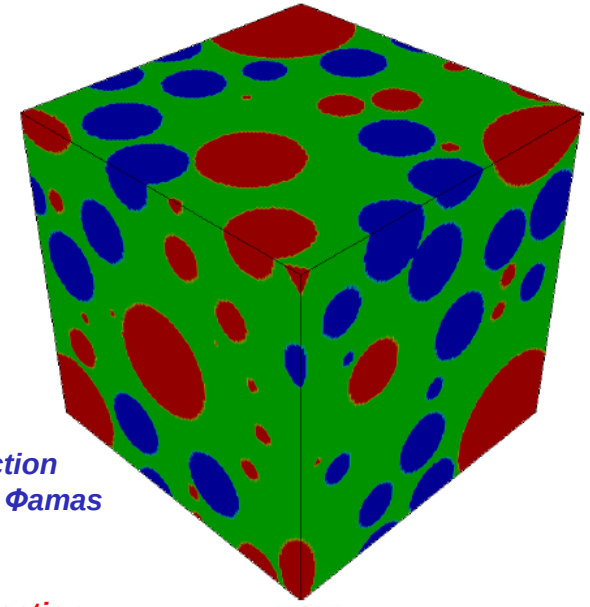

57 Amas U : fraction volumique 25%, Φamas 30µm.

121 Amas Pu : fraction volumique 15%, Φamas [10µm,70µm].

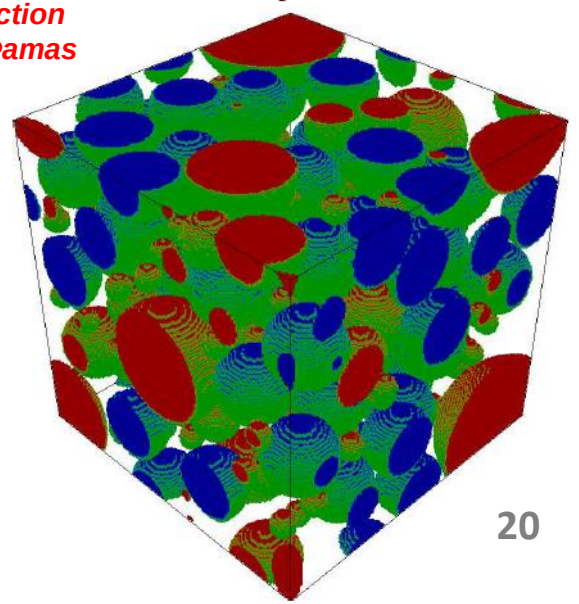

4. NTFA-TSO applied to the 1st typical example - Implementation & results

- **Implementation** (Largenton et al., 2019).

NTFA Decomposition of Internal Variables:

$$\varepsilon_{\mathsf{v}}(\boldsymbol{x},t) = \sum_{k=1}^{M} \xi^{(k)}(t)\, \boldsymbol{\mu}^{(k)}(\boldsymbol{x}).$$

Local Fields Expressed with Mode Decomposition:

$$\boldsymbol{\varepsilon}(\boldsymbol{x},t) = \boldsymbol{A}(\boldsymbol{x}) : \overline{\boldsymbol{\varepsilon}}(t) + \sum_{k=1}^{M} (\boldsymbol{D} * \boldsymbol{\mu}^{(k)})(\boldsymbol{x}) \xi^{(k)}(t) + \sum_{r=1}^{N} (\boldsymbol{D} * \chi^{(r)}\boldsymbol{i})(\boldsymbol{x}) \varepsilon_{\mathsf{s}}^{(r)}(t), \text{ with}$$

$$\boldsymbol{\sigma}(\boldsymbol{x},t) = \boldsymbol{L}(\boldsymbol{x}) : \boldsymbol{A}(\boldsymbol{x}) : \overline{\boldsymbol{\varepsilon}}(t) + \sum_{k=1}^{M} \boldsymbol{\rho}^{(k)}(\boldsymbol{x}) \xi^{(k)}(t) + \sum_{r=1}^{N} \boldsymbol{\eta}^{(r)}(\boldsymbol{x}) \varepsilon_{\mathsf{s}}^{(r)}(t),$$

$$\boldsymbol{\rho}^{(k)}(\boldsymbol{x}) = \boldsymbol{L}(\boldsymbol{x}) : \left((\boldsymbol{D} * \boldsymbol{\mu}^{(k)})(\boldsymbol{x}) - \boldsymbol{\mu}^{(k)}(\boldsymbol{x}) \right), \quad \boldsymbol{\eta}^{(r)}(\boldsymbol{x}) = \boldsymbol{L}(\boldsymbol{x}) : \left((\boldsymbol{D} * \chi^{(r)}\boldsymbol{i})(\boldsymbol{x}) - \chi^{(r)}(\boldsymbol{x})\boldsymbol{i} \right).$$

Macroscopic State Law:

$$\frac{\partial \widetilde{w}}{\partial \overline{\boldsymbol{\varepsilon}}}(\overline{\boldsymbol{\varepsilon}}, \boldsymbol{\xi}, \boldsymbol{\varepsilon}_{\mathsf{s}}) = \overline{\boldsymbol{\sigma}} = \widetilde{\boldsymbol{L}} : \overline{\boldsymbol{\varepsilon}} + \sum_{k=1}^{M} \langle \boldsymbol{\rho}^{(k)} \rangle \xi_{\mathsf{v}}^{(k)} + \sum_{r=1}^{N} \langle \boldsymbol{\eta}^{(r)} \rangle \varepsilon_{\mathsf{s}}^{(r)}.$$

$$\widetilde{\boldsymbol{L}} = \langle \boldsymbol{L} : \boldsymbol{A} \rangle.$$

$$-\frac{\partial \widetilde{w}}{\partial \xi^{(k)}}(\overline{\boldsymbol{\varepsilon}}, \boldsymbol{\xi}, \boldsymbol{\varepsilon}_{\mathsf{s}}) \stackrel{\text{def}}{=} \tau^{(k)} = \langle \boldsymbol{\mu}^{(k)} : \boldsymbol{\sigma} \rangle.$$

$$\tau^{(k)}(t) = \boldsymbol{a}^{(k)} : \overline{\boldsymbol{\varepsilon}}(t) + \sum_{\ell=1}^{M} D^{(k\ell)} \xi^{(\ell)}(t) + \sum_{r=1}^{N} H^{(kr)} \varepsilon_{\mathsf{s}}^{(r)}(t),$$

$$\boldsymbol{a}^{(k)} = \langle \boldsymbol{\mu}^{(k)} : (\boldsymbol{L} : \boldsymbol{A}) \rangle, \quad D^{(k\ell)} = \langle \boldsymbol{\mu}^{(k)} : \boldsymbol{\rho}^{(\ell)} \rangle, \quad H^{(kr)} = \langle \boldsymbol{\mu}^{(k)} : \boldsymbol{\eta}^{(r)} \rangle.$$

4. NTFA-TSO applied to the 1st typical example - Implementation & results

- **Implementation** (Largenton et al., 2019).

Evolution of the Reduced Thermodynamic Variables:

$$\tau^{(k)}(t) = \boldsymbol{a}^{(k)} : \overline{\boldsymbol{\varepsilon}}(t) + \sum_{\ell=1}^{M} D^{(k\ell)} \xi^{(\ell)}(t) + \sum_{r=1}^{N} H^{(kr)} \varepsilon_{\mathsf{s}}^{(r)}(t) \quad \text{, with} \quad \dot{\xi}^{(k)} = \frac{\partial \widetilde{\psi}}{\partial \tau^{(k)}} \text{. =>} \quad \dot{\tau}^{(k)} = \boldsymbol{a}^{(k)} : \dot{\overline{\boldsymbol{\varepsilon}}} + \frac{\partial \widetilde{\psi}}{\partial \xi^{(k)}} + \sum_{r=1}^{N} H^{(kr)} \dot{\varepsilon}_{\mathsf{s}}^{(r)}.$$

$$\psi^{(r)}(\boldsymbol{\sigma}) \simeq \psi^{(r)}_{TSO}(\boldsymbol{\sigma}) = \psi^{(r)}(\overline{\boldsymbol{\sigma}}^{(r)}) + \frac{\partial \psi^{(r)}}{\partial \boldsymbol{\sigma}}(\overline{\boldsymbol{\sigma}}^{(r)}) : \left(\boldsymbol{\sigma} - \overline{\boldsymbol{\sigma}}^{(r)}\right) + \frac{1}{2}\left(\boldsymbol{\sigma} - \overline{\boldsymbol{\sigma}}^{(r)}\right) : \frac{\partial^2 \psi^{(r)}}{\partial \boldsymbol{\sigma}^2}(\overline{\boldsymbol{\sigma}}^{(r)}) : \left(\boldsymbol{\sigma} - \overline{\boldsymbol{\sigma}}^{(r)}\right),$$

where $\overline{\boldsymbol{\sigma}}^{(r)} = \langle \boldsymbol{\sigma} \rangle^{(r)}$, so that $\widetilde{\psi}$ is approximated by:

$$\widetilde{\psi} \simeq \widetilde{\psi}_{TSO} = \sum_{r=1}^{N} c^{(r)} \left[\psi^{(r)}(\overline{\boldsymbol{\sigma}}^{(r)}) + \frac{1}{2} \frac{\partial^2 \psi^{(r)}}{\partial \boldsymbol{\sigma}^2}(\overline{\boldsymbol{\sigma}}^{(r)}) :: \boldsymbol{C}^{(r)}(\boldsymbol{\sigma}) \right],$$

$$\boldsymbol{C}^{(r)}(\boldsymbol{\sigma}) = \langle \left(\boldsymbol{\sigma} - \overline{\boldsymbol{\sigma}}^{(r)}\right) \otimes \left(\boldsymbol{\sigma} - \overline{\boldsymbol{\sigma}}^{(r)}\right) \rangle^{(r)}.$$

$$\dot{\tau}^{(k)} = \boldsymbol{a}^{(k)} : \dot{\overline{\boldsymbol{\varepsilon}}} + \sum_{r=1}^{N} c^{(r)} \left[\frac{\partial \psi^{(r)}}{\partial \boldsymbol{\sigma}}(\overline{\boldsymbol{\sigma}}^{(r)}) : \frac{\partial \overline{\boldsymbol{\sigma}}^{(r)}}{\partial \xi^{(k)}} + \frac{1}{2} \frac{\partial^2 \psi^{(r)}}{\partial \boldsymbol{\sigma}^2}(\overline{\boldsymbol{\sigma}}^{(r)}) :: \frac{\partial \boldsymbol{C}^{(r)}(\boldsymbol{\sigma})}{\partial \xi^{(k)}} + \frac{1}{2} \frac{\partial^3 \psi^{(r)}}{\partial \boldsymbol{\sigma}^3}(\overline{\boldsymbol{\sigma}}^{(r)}) ::: \boldsymbol{C}^{(r)}(\boldsymbol{\sigma}) \otimes \frac{\partial \overline{\boldsymbol{\sigma}}^{(r)}}{\partial \xi^{(k)}} \right] + \sum_{r=1}^{N} H^{(kr)} \dot{\varepsilon}_{\mathsf{s}}^{(r)}.$$

4. NTFA-TSO applied to the 1st typical example - Implementation & results

- **Implementation** (Largenton et al., 2019).

Identification of the modal base – 1st Step:

- three uniaxial creep loadings with no shrinkage-swelling in the phases,

$$i = 1, 2 \text{ or } 3, \quad \overline{\boldsymbol{\sigma}}(t) = \sigma\, \boldsymbol{e}_i \otimes \boldsymbol{e}_i, \quad \sigma = 100 \text{ MPa}, \quad \varepsilon_{\mathrm{s}}^{(r)}(t) = 0 \text{ in each phase } r,$$

- one loading corresponding to a pure shrinkage-swelling of the phases with no macroscopic stress,

$$\overline{\boldsymbol{\sigma}}(t) = \mathbf{0}, \quad \varepsilon_{\mathrm{s}}^{(r)}(t)$$

For each of these four loading cases, 25 snapshots of the viscous strain field are stored every 5.36×10^6 seconds of the full-field simulation.

θ_{eq}

4. NTFA-TSO applied to the 1st typical example - Implementation & results

- **Implementation** (Largenton et al., 2019).

Reduction of the modal base – 2nd Step [Rousette et al., CST (2009)]:

$$\theta_{\mathrm{v}}^{(k)}(x) = \varepsilon_{\mathrm{v}}\ (x, t_{(k)}),$$

with: $\theta_{\mathrm{v}}^{(k)}$ tensor associated with the internal time variable t_k ,

$$g_{\mathrm{v}}^{ij} = < \theta_{\mathrm{v}}^{(i)} : \theta_{\mathrm{v}}^{(j)} >, \quad \textbf{Symmetric matrix.}$$

where: g_{v} , global viscoplastic correlation matrix.

POD:

$$g\ v^{(k)} = \lambda^{(k)}\ v^{(k)}, \quad \frac{\sum_{k}^{N} \lambda^{(k)}}{\sum_{k}^{N_T} \lambda^{(k)}} > 1 - \alpha,\ \alpha = 10^{-4}\,[-]\,.$$

$$\mu_{\mathrm{v}}^{(k)}(x) = \sum_{l}^{N_T} v_{l,\mathrm{v}}^{(k)}\ \theta_{\mathrm{v}}^{(l)}(x),$$

$$< \mu_{\mathrm{v}}^{(k)}(x) : \mu_{\mathrm{v}}^{(p)}(x) >= \begin{cases} \lambda^{(k)} & \text{if } k = p, \\ 0 & \text{otherwise.} \end{cases}$$ **Positive eigenvalues.**

Example Mode 1 μ_{eq}:

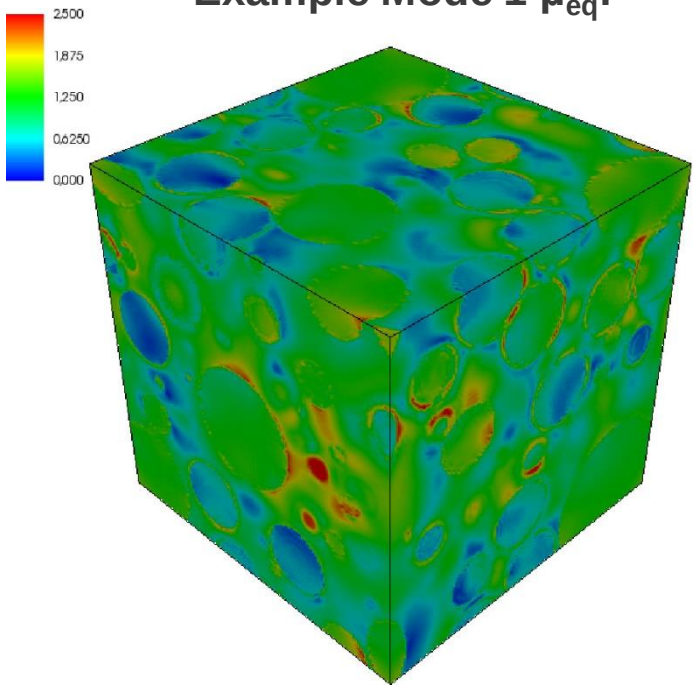

After application of this procedure, a total of 9 modes were selected (2 modes per uniaxial creep loading and 3 modes for the pure shrinkage-swelling test).

4. NTFA-TSO applied to the 1st typical example - Implementation & results

- **Results** (Largenton et al., 2019).

Macroscopic Comparison between Full-Field FFT and NTFA-TSO Model:

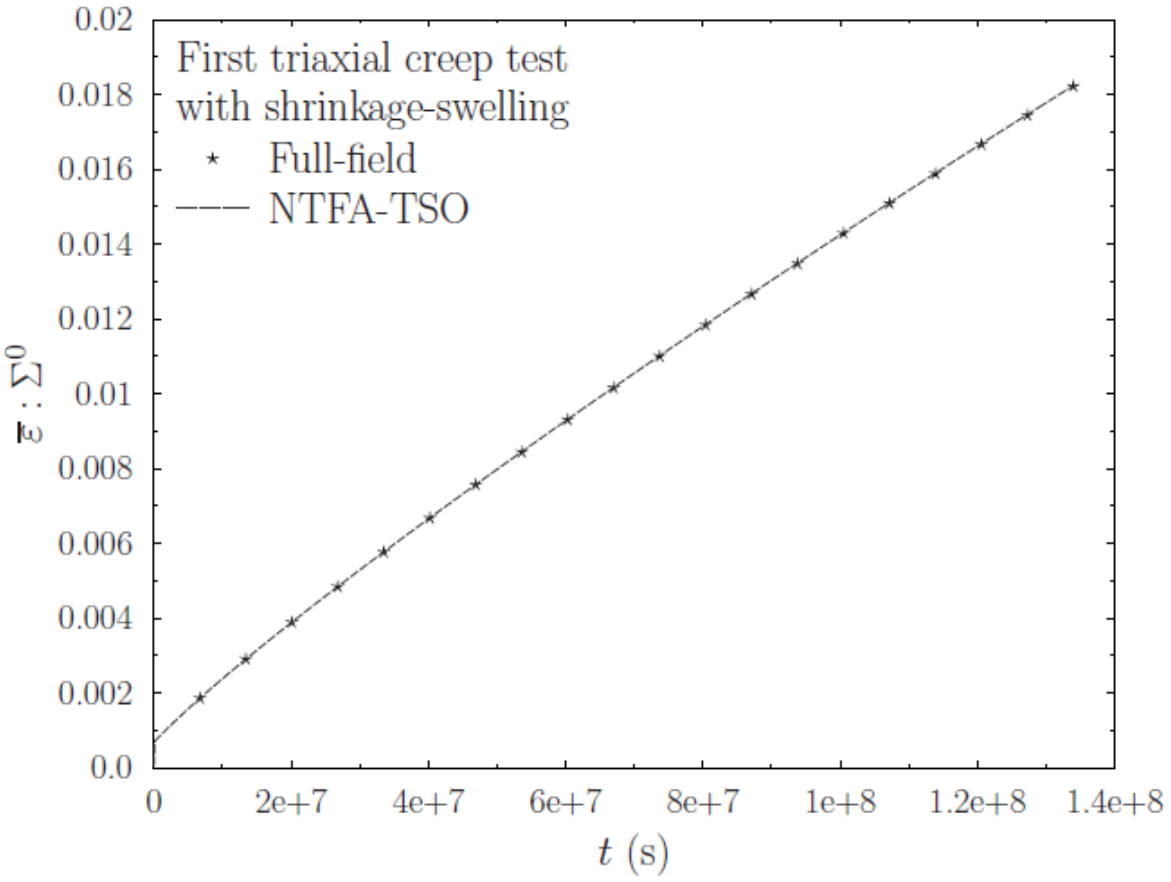

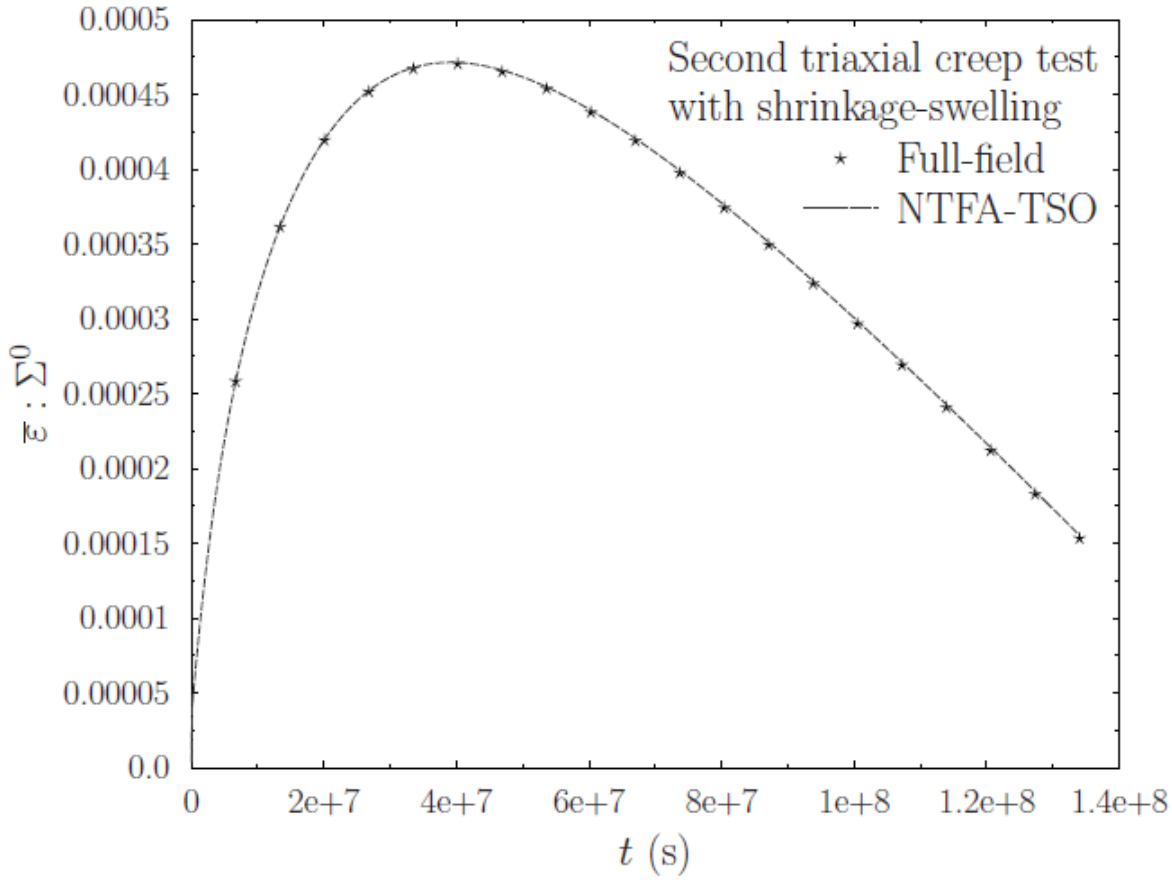

$$\overline{\boldsymbol{\sigma}}(t) = \sum_{i=1}^{3} \sigma_i \, \boldsymbol{e}_i \otimes \boldsymbol{e}_i, \qquad \varepsilon_{\mathbf{s}}^{(r)}(t)$$

1st triaxial creep test: $\sigma_1 = -115$ MPa, $\sigma_2 = -115$ MPa, $\sigma_3 = -230$ MPa

2nd triaxial creep test: $\sigma_1 = -10$ MPa, $\sigma_2 = -10$ MPa, $\sigma_3 = -6.66$ MPa

4. NTFA-TSO applied to the 1st typical example - Implementation & results

- **Results** (Largenton et al., 2019). ***Local Comparison between Full-Field FFT and NTFA-TSO Model:***

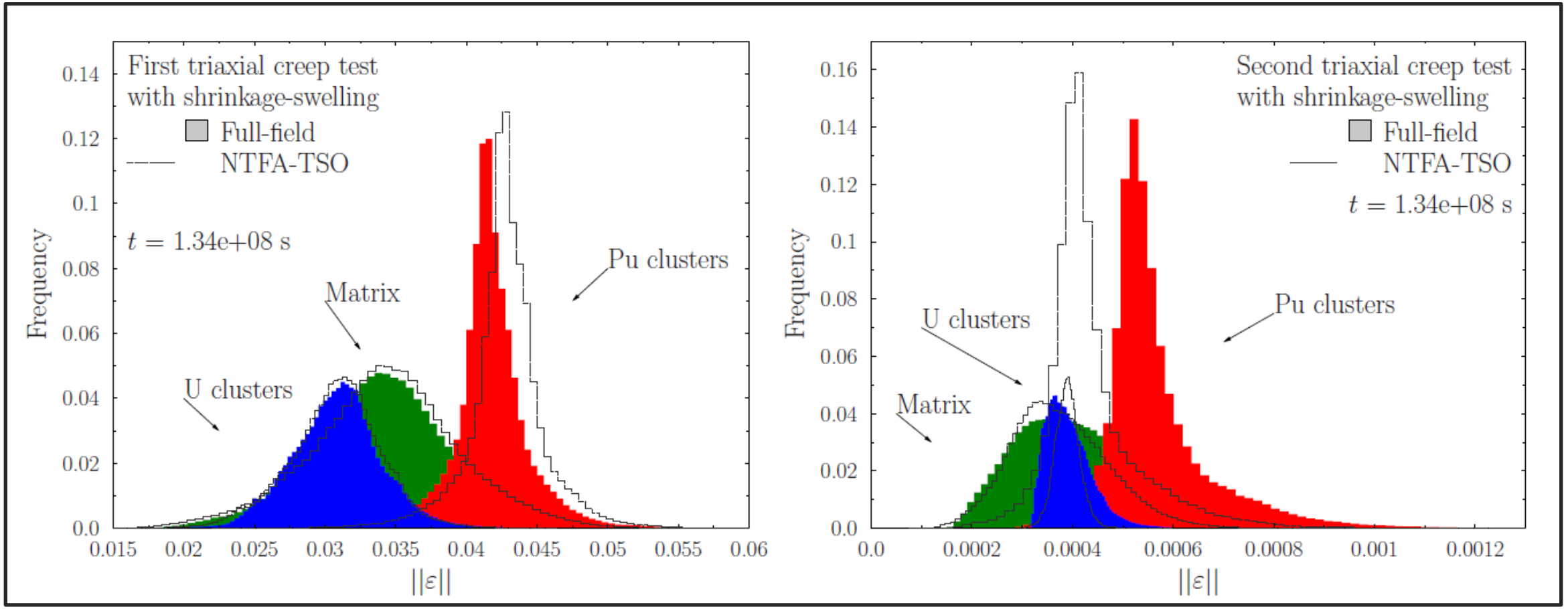

	Full-field simulation (FFT)	NTFA-TSO model (CPU ratio = FFT/TSO)
1st triaxial creep test	10 146 s	1.92 s (CPU ratio = 5 284)
2nd triaxial creep test	16 026 s	3.50 s (CPU ratio = 4 579)

CPU times. Processor Intel Xeon X5687 @ 3.6 GHz.

4. NTFA-TSO applied to the 2nd typical example - Implementation & results

- **Exact local problem** (Labat et al., 2023).

***Equation System** (1) **Coupled with Evolution Law** (2):*

$$\left.\begin{aligned}
&\boldsymbol{\sigma}(\boldsymbol{x},t) = \boldsymbol{L}(\boldsymbol{x}) : (\varepsilon(\boldsymbol{x},t) - \varepsilon_{\mathsf{vp}}(\boldsymbol{x},t)), \quad \varepsilon_{\mathsf{vp}}(\boldsymbol{x},t) = \sum_s \gamma_s^{\mathsf{vp}}(\boldsymbol{x},t)\, \boldsymbol{m_s}(\boldsymbol{x}),\\
&\operatorname{div} \boldsymbol{\sigma}(\boldsymbol{x},t) = 0, \quad \boldsymbol{\sigma}(\boldsymbol{x},t)\cdot\boldsymbol{n}(\boldsymbol{x}) \text{ antiperiodic on } \partial V,\\
&\varepsilon(\boldsymbol{x},t) = \overline{\varepsilon}(t) + \tfrac{1}{2}(\boldsymbol{\nabla} \boldsymbol{u}^*(\boldsymbol{x},t) + \boldsymbol{\nabla} \boldsymbol{u}^{*T}(\boldsymbol{x},t)),\ \boldsymbol{u}^*(\boldsymbol{x},t) \text{ periodic on } \partial V.
\end{aligned}\right\} \quad (1)$$

RVE *V*
(500 grains & 135³ Voxels):

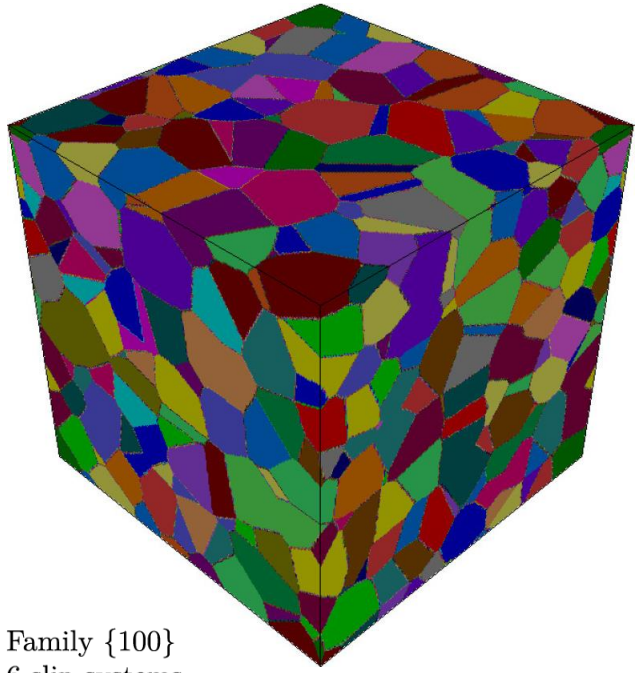

$$\dot{\gamma}_s^{\mathsf{vp}} = \dot{\gamma}_i^0 \times \left(\frac{|\tau_s|}{r_i}\right)^{n_i} \times sgn(\tau_s),$$

$$r_i(\boldsymbol{x},t) = \tau_i^0(T,\dot{\bar{\varepsilon}}) + h_i(T,\dot{\bar{\varepsilon}}) \times p_i(\boldsymbol{x},t),$$

$$\dot{p}_i = \sum_{s\in S_i} \dot{\gamma}_s^{\mathsf{p}},\ \dot{\gamma}_s^{\mathsf{p}} = |\dot{\gamma}_s^{\mathsf{vp}}|,$$

$\dot{\gamma}_s^{\mathsf{vp}}$ evolution law inspired by [**Knezevic et al.**, *IJP* (2013)] .

- Formalisms of h_i and τ_i^0 and parameter values in Appendix 1.
- For elastic coefficient values, see (Labat et al., 2023).

(2)

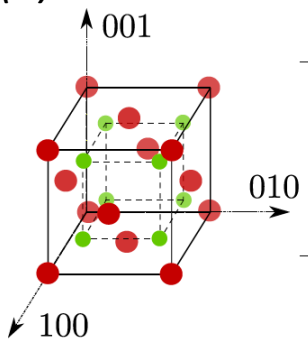

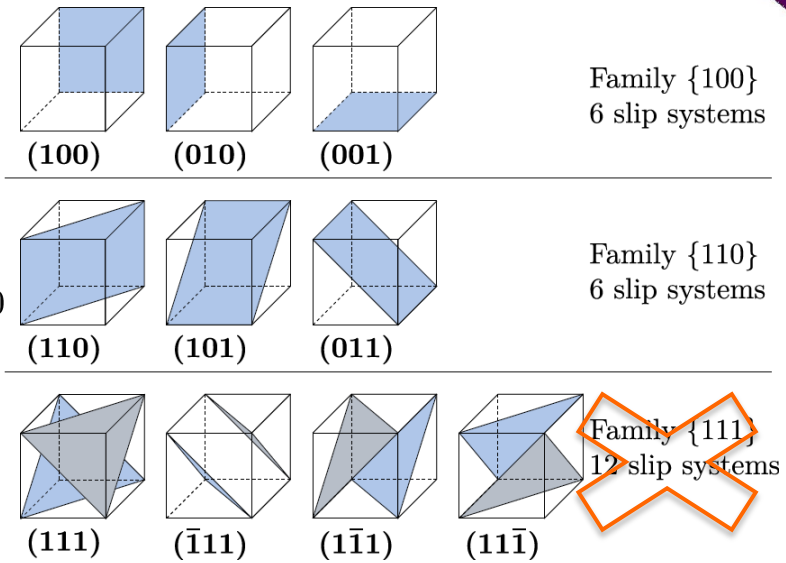

Observation but with activation of other families, so this family's CRSS cannot be measured

4. NTFA-TSO applied to the 2nd typical example - Implementation & results

- **Implementation** (Labat et al., 2023).

NTFA Decomposition of Internal Variables:

$$\boldsymbol{\varepsilon}_{\mathrm{vp}}(\boldsymbol{x},t) = \sum_{k}^{M_{\mathrm{vp}}} \xi_{\mathrm{vp}}^{(k)}(t)\ \boldsymbol{\mu}_{\mathrm{vp}}^{(k)}(\boldsymbol{x}),$$

|| **NTFA decompostion** [**Michel and Suquet**, *JMPS* (2016)],

$$p_i(\boldsymbol{x},t) = \left| \begin{array}{l} \displaystyle\sum_{l}^{M_{\mathrm{p},i}} \xi_{\mathrm{p},i}^{(l)}(t)\ \mu_{\mathrm{p},i}^{(l)}(\boldsymbol{x}) \text{ - [Decomposed]}, \\ \displaystyle\sum_{g} \xi_{\mathrm{p},i}^{(g)}(t)\ \chi^{(g)}(\boldsymbol{x}) \text{ - [Constant per grain]}. \end{array} \right.$$

|| **[Constant per grain] - decomposition** [**Michel and Suquet**, *CM* (2016)],
|| **[Decomposed] - tested decomposition**,

with:
- $\left(\boldsymbol{\mu}_{\mathrm{vp}}^{(k)}, \mu_{\mathrm{p},i}^{(l)}\right)$ modes used for the internal-variables decomposition,
- $\left(\xi_{\mathrm{vp}},\ \xi_{\mathrm{p},i}\right)$ reduced internal variables.

4. NTFA-TSO applied to the 2nd typical example - Implementation & results

- **Implementation** (Labat et al., 2023).

Local Fields Expressed with Mode Decomposition:

$$\blacktriangleright\ \boldsymbol{\varepsilon}(\boldsymbol{x},t) = \boldsymbol{A}(\boldsymbol{x}) : \bar{\boldsymbol{\varepsilon}}(t) + \sum_{l}^{M_{\text{vp}}} \boldsymbol{D} * \boldsymbol{\mu}_{\text{vp}}^{(l)}(\boldsymbol{x})\ \xi_{\text{vp}}^{(l)}(t),$$

$\|$ **induced by NTFA decompostion**,

with:

$\boldsymbol{\varepsilon}(\boldsymbol{x},t)$	using the superposition principle: solution to the linear thermoelastic problem **[Local problem (1)-(2)]**
$\bar{\boldsymbol{\varepsilon}}$	macroscopic strain tensor,
$\boldsymbol{A}(\boldsymbol{x})$	strain concentration tensor,
$\boldsymbol{D} * \boldsymbol{\mu}_{\text{vp}}^{(l)}(\boldsymbol{x})$	strain influence tensor,

$$\boldsymbol{D} * \boldsymbol{\mu}_{\text{vp}}^{(l)}(\boldsymbol{x}) = \frac{1}{|V|}\int_{V} \boldsymbol{D}(\boldsymbol{x},\boldsymbol{x'}) : \boldsymbol{\mu}_{\text{vp}}^{(l)}(\boldsymbol{x'})\,\mathrm{d}\boldsymbol{x'},\ \boldsymbol{D}(\boldsymbol{x},\boldsymbol{x'}) = \boldsymbol{\Gamma}(\boldsymbol{x},\boldsymbol{x'}) : \boldsymbol{L}(\boldsymbol{x'}),$$

with: $(\boldsymbol{D},\boldsymbol{\Gamma})$ nonlocal and nonlocal Green operators,

$$\blacktriangleright\ \boldsymbol{\sigma}(\boldsymbol{x},t) = \boldsymbol{L}(\boldsymbol{x}) : \boldsymbol{A}(\boldsymbol{x}) : \bar{\boldsymbol{\varepsilon}}(t) + \sum_{l}^{M_{\text{vp}}} \boldsymbol{\rho}_{\text{vp}}^{(l)}(\boldsymbol{x})\ \xi_{\text{vp}}^{(l)}(t),$$

with: $\boldsymbol{\rho}_{\text{vp}}^{(k)}(\boldsymbol{x}) = \boldsymbol{L}(\boldsymbol{x}) : \left(\left(\boldsymbol{D} * \boldsymbol{\mu}_{\text{vp}}^{(k)}\right)(\boldsymbol{x}) - \boldsymbol{\mu}_{\text{vp}}^{(k)}(\boldsymbol{x})\right).$

4. NTFA-TSO applied to the 2nd typical example - Implementation & results

- **Implementation** (Labat et al., 2023).

Macroscopic State Law:

$$\frac{\partial \bar{w}}{\partial \bar{\boldsymbol{\varepsilon}}} = \bar{\boldsymbol{\sigma}},\ \bar{\boldsymbol{\sigma}} = \tilde{\boldsymbol{L}} : \bar{\boldsymbol{\varepsilon}} + \sum_{k}^{M_{\text{vp}}} < \boldsymbol{\rho}_{\text{vp}}^{(k)} > \xi_{\text{vp}}^{(l)},$$

$$-\frac{\partial \bar{w}}{\partial \xi_{\text{vp}}^{(k)}} = a_{\text{vp}}^{(k)},\ a_{\text{vp}}^{(k)} = \bar{\boldsymbol{\varepsilon}} : \boldsymbol{a}^{(k)} + \sum_{l} < \boldsymbol{\mu}_{\text{vp}}^{(k)} : \boldsymbol{\rho}_{\text{vp}}^{(l)} > \xi_{\text{vp}}^{(l)},$$

$$-\frac{\partial \bar{w}}{\partial \xi_{\text{p},i}^{(k)}} = a_{\text{p},i}^{(k)},\ a_{\text{p},i}^{(k)} = \begin{cases} -\left(\tau_i^0 < \mu_{\text{p}_i}^{(k)} > + h_i \times \sum_{l}^{M_{\text{p},i}} \xi_{\text{p}_i}^{(l)} < \mu_{\text{p}_i}^{(k)} \mu_{\text{p}_i}^{(l)} > \right) \text{ - [Decomposed]}, \\ -\left(\tau_i^0 + h_i \times \xi_{\text{p}_i}^{(k)}\right) \times c^{(k)} \text{ - [Constant per grain]}, \end{cases}$$

with:

$$\begin{aligned} \boldsymbol{a}^{(k)} &= < \boldsymbol{\mu}_{\text{vp}}^{(k)} : \boldsymbol{L} : \boldsymbol{A} >, \\ \tilde{\boldsymbol{L}} &= < \boldsymbol{L} : \boldsymbol{A} > . \end{aligned}$$

4. NTFA-TSO applied to the 2nd typical example - Implementation & results

- **Implementation** (Labat et al., 2023).

Evolution of the Reduced Thermodynamic Variables:

$$\dot{a}_{\text{vp}}^{(k)}(\bar{\boldsymbol{\varepsilon}}, \xi_{\text{vp}}) = \frac{\partial a_{\text{vp}}^{(k)}}{\partial \bar{\boldsymbol{\varepsilon}}} : \dot{\bar{\boldsymbol{\varepsilon}}} + \sum_{l}^{M_{\text{vp}}} \frac{\partial a_{\text{vp}}^{(k)}}{\partial \xi_{\text{vp}}^{(l)}} \times \dot{\xi}_{\text{vp}}^{(l)}, \text{ with } \dot{\xi}_{\text{vp}}^{(l)} = \frac{\partial \psi_{\text{vp}}^{\text{hom}}}{\partial a_{\text{vp}}^{(l)}} \Longrightarrow \dot{a}_{\text{vp}}^{(k)} = \frac{\partial a_{\text{vp}}^{(k)}}{\partial \bar{\boldsymbol{\varepsilon}}} : \dot{\bar{\boldsymbol{\varepsilon}}} + \frac{\partial \psi_{\text{vp}}^{\text{hom}}}{\partial \xi_{\text{vp}}^{(k)}}$$

$$< \psi_{\text{vp},s}^{\text{TSO}}(\mathcal{A}_{\text{vp},s}, \mathcal{A}_{\text{p},i}) >^{(g)} = \left[\psi_{\text{vp},s}(\bar{\mathcal{A}}_{\text{vp},s}^{(g)}, \bar{\mathcal{A}}_{\text{p},i}^{(g)}) + \frac{\partial^2 \psi_{\text{vp},s}}{\partial \mathcal{A}_{\text{vp},s} \partial \mathcal{A}_{\text{p},i}} \times C^{(g)}\left(\mathcal{A}_{\text{vp},s}^{(g)}, \mathcal{A}_{\text{p},i}^{(g)}\right) \right.$$
$$\left. + \frac{1}{2} \frac{\partial^2 \psi_{\text{vp},s}}{\partial \mathcal{A}_{\text{vp},s}^2} \times C^{(g)}\left(\mathcal{A}_{\text{vp},s}^{(g)}\right) + \frac{1}{2} \frac{\partial^2 \psi_{\text{vp},s}}{\partial \mathcal{A}_{\text{p},i}^2} \times C^{(g)}\left(\mathcal{A}_{\text{p},i}^{(g)}\right) \right] \text{ - [Decomposed]},$$

Tangent Second Order (TSO) linearisation of the effective dissipation potential [**Castañeda**, *JMPS* (1996)] [**Michel and Suquet**, *CM* (2016)].

with:

$$C^{(g)}(X, Y) = < \left(X - \bar{X}^{(g)}\right)\left(Y - \bar{Y}^{(g)}\right) >^{(g)},$$
$$C^{(g)}(X) = < \left(X - \bar{X}^{(g)}\right)^2 >^{(g)}.$$

► Similar work has to be done on $\dot{a}_{\text{p}}^{(k)}$, $\dot{\boldsymbol{a}}_{\text{vp}}^{(k)}$ has to be coupled with $\dot{a}_{\text{p}}^{(k)}$.

4. NTFA-TSO applied to the 2nd typical example - Implementation & results

- **Implementation** (Labat et al., 2023).

Evolution of the Reduced Thermodynamic Variables:

$$\dot{a}_{\mathrm{vp}}^{(k)} = \boldsymbol{a}^{(k)} : \dot{\bar{\varepsilon}} + \sum_g c^{(g)} \sum_s \left[\dot{\gamma}_s^{\mathrm{vp}} \left(\bar{\mathcal{A}}_{\mathrm{vp},s}^{(g)}, \bar{\mathcal{A}}_{\mathrm{p},i}^{(g)} \right) \frac{\partial \bar{\mathcal{A}}_{\mathrm{vp},s}^{(g)}}{\partial \xi_{\mathrm{vp}}^{(k)}} + \frac{1}{2} \frac{\partial \dot{\gamma}_s^{\mathrm{vp}}}{\partial \mathcal{A}_{\mathrm{vp},s}} \frac{\partial C^{(g)}}{\partial \xi_{\mathrm{vp}}^{(k)}} \left(\mathcal{A}_{\mathrm{vp},s}^{(g)} \right) \right.$$
$$+ \frac{1}{2} \frac{\partial^2 \dot{\gamma}_s^{\mathrm{vp}}}{\partial \mathcal{A}_{\mathrm{vp},s}^2} C^{(g)} \left(\mathcal{A}_{\mathrm{vp},s}^{(g)} \right) \frac{\partial \bar{\mathcal{A}}_{\mathrm{vp},s}^{(g)}}{\partial \xi_{\mathrm{vp}}^{(k)}} + \frac{1}{2} \frac{\partial^2 \dot{\gamma}_s^{\mathrm{vp}}}{\partial \mathcal{A}_{\mathrm{p},i}^2} C^{(g)} \left(\mathcal{A}_{\mathrm{p},i}^{(g)} \right) \frac{\partial \bar{\mathcal{A}}_{\mathrm{vp},s}^{(g)}}{\partial \xi_{\mathrm{vp}}^{(k)}}$$
$$\left. + \frac{\partial \dot{\gamma}_s^{\mathrm{vp}}}{\partial \mathcal{A}_{\mathrm{p},i}} \frac{\partial C^{(g)}}{\partial \xi_{\mathrm{vp}}^{(k)}} \left(\mathcal{A}_{\mathrm{vp},s}^{(g)}, \mathcal{A}_{\mathrm{p},i}^{(g)} \right) + \frac{\partial^2 \dot{\gamma}_s^{\mathrm{vp}}}{\partial \mathcal{A}_{\mathrm{vp},s} \partial \mathcal{A}_{\mathrm{p},i}} C^{(g)} \left(\mathcal{A}_{\mathrm{vp},s}^{(g)}, \mathcal{A}_{\mathrm{p},i}^{(g)} \right) \frac{\partial \bar{\mathcal{A}}_{\mathrm{vp},s}^{(g)}}{\partial \xi_{\mathrm{vp}}^{(k)}} \right]$$

$$\dot{a}_{\mathrm{p},i}^{(k)} = \sum_g c^{(g)} \sum_s \left[\dot{\gamma}_s^{\mathrm{p},i} \left(\bar{\mathcal{A}}_{\mathrm{vp},s}^{(g)}, \bar{\mathcal{A}}_{\mathrm{p},i}^{(g)} \right) \frac{\partial \bar{\mathcal{A}}_{\mathrm{p},i}^{(g)}}{\partial \xi_{\mathrm{p},i}^{(k)}} + \frac{1}{2} \frac{\partial^2 \dot{\gamma}_s^{\mathrm{p},i}}{\partial \mathcal{A}_{\mathrm{vp},s}^2} C^{(g)} \left(\mathcal{A}_{\mathrm{vp},s}^{(g)} \right) \frac{\partial \bar{\mathcal{A}}_{\mathrm{p},i}^{(g)}}{\partial \xi_{\mathrm{p},i}^{(k)}} \right.$$
$$+ \frac{1}{2} \frac{\partial \dot{\gamma}_s^{\mathrm{p},i}}{\partial \mathcal{A}_{\mathrm{p},i}} \frac{\partial C^{(g)}}{\partial \xi_{\mathrm{p},i}^{(k)}} \left(\mathcal{A}_{\mathrm{p},i}^{(g)} \right) + \frac{1}{2} \frac{\partial^2 \dot{\gamma}_s^{\mathrm{p},i}}{\partial \mathcal{A}_{\mathrm{p},i}^2} C^{(g)} \left(\mathcal{A}_{\mathrm{p},i}^{(g)} \right) \frac{\partial \bar{\mathcal{A}}_{\mathrm{p},i}^{(g)}}{\partial \xi_{\mathrm{p},i}^{(k)}}$$
$$\left. + \frac{\partial \dot{\gamma}_s^{\mathrm{p},i}}{\partial \mathcal{A}_{\mathrm{vp},s}} \frac{\partial C^{(g)}}{\partial \xi_{\mathrm{p},i}^{(k)}} \left(\mathcal{A}_{\mathrm{vp},s}^{(g)}, \mathcal{A}_{\mathrm{p},i}^{(g)} \right) + \frac{\partial^2 \dot{\gamma}_s^{\mathrm{p},i}}{\partial \mathcal{A}_{\mathrm{vp},s} \partial \mathcal{A}_{\mathrm{p},i}} C^{(g)} \left(\mathcal{A}_{\mathrm{vp},s}^{(g)}, \mathcal{A}_{\mathrm{p},i}^{(g)} \right) \frac{\partial \bar{\mathcal{A}}_{\mathrm{p},i}^{(g)}}{\partial \xi_{\mathrm{p},i}^{(k)}} \right]$$

- **Black:** decomposed strain-hardening
- **Red:** terms deleted for constant strain-hardening per grain

4. NTFA-TSO applied to the 2nd typical example - Implementation & results

- **Implementation** (Labat et al., 2023).

Identification of the modal base – 1st Step:

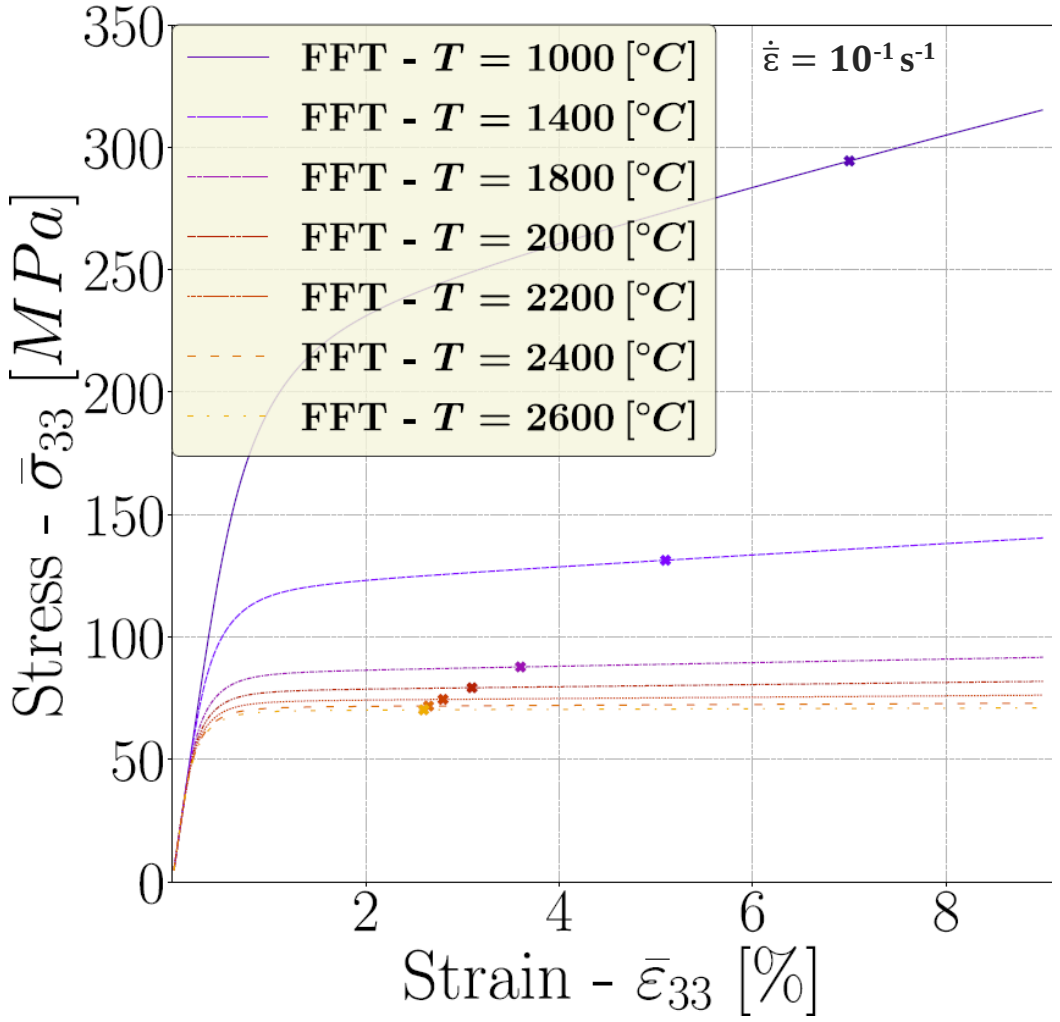

It consists in performing full-field FFT simulations:

- **The snapshots (viscoplastic and strain hardening modes) have been taken from these simulations at different times and for:**

$$T = [1000°C\text{-}2600°C]$$
$$\dot{\bar{\varepsilon}} = [10^{-6}\,s^{-1}\,,\,10^{-1}\,s^{-1}]$$

- **The modal base was made of these types of snapshots:**

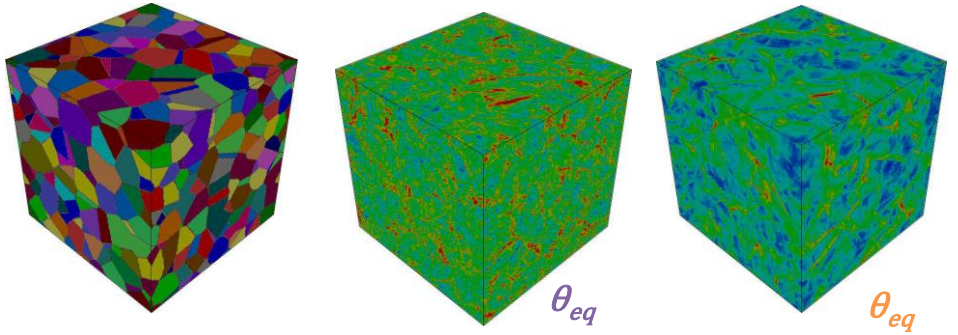

θ (snapshot) – Examples of equivalent viscoplastic strains

4. NTFA-TSO applied to the 2nd typical example - Implementation & results

- **Implementation** (Labat et al., 2023).

Reduction of the modal base – 2nd Step [Rousette et al., CST (2009)]:

$$\theta_{vp}^{(k)}(x) = \varepsilon_{vp}(x, t_{(k)}),\ \theta_{p,i}^{(k)}(x) = p_i(x, t_{(k)}),$$

with: $(\theta_{vp}^{(k)}, \theta_{p,i}^{(k)})$ tensor and scalar associated with the internal time variable t_k ,

$$g_{vp}^{ij} = < \theta_{vp}^{(i)} : \theta_{vp}^{(j)} >,\ g_{p,i}^{ij} = < \theta_{p,i}^{(i)}\ \theta_{p,i}^{(j)} > \ \| \ \textbf{Symmetric matrix.}$$

where: $(g_{vp}, g_{p,i})$ global viscoplastic and strain-hardening correlation matrices.

$$g\ v^{(k)} = \lambda^{(k)}\ v^{(k)},\ \frac{\sum_{k}^{N} \lambda^{(k)}}{\sum_{k}^{N_T} \lambda^{(k)}} > 1 - \alpha,\ \alpha = 10^{-4}\ [-]$$

$$\mu_{vp}^{(k)}(x) = \sum_{l}^{N_T} v_{l,vp}^{(k)}\ \theta_{vp}^{(l)}(x),\ \mu_{p,i}^{(k)}(x) = \sum_{l}^{N_T} v_{l,p}^{(k)}\ \theta_{p,i}^{(l)}(x),$$

$$< \mu_{vp}^{(k)}(x) : \mu_{vp}^{(p)}(x) >= \begin{cases} \lambda^{(k)} & \text{if } k = p, \\ 0 & \text{otherwise,} \end{cases} \ \| \ \textbf{Positive eigenvalues.}$$

$$< \mu_{p,i}^{(k)}(x) \times \mu_{p,i}^{(l)}(x) >= \begin{cases} \lambda^{(k)} & \text{if } k = l, \\ 0 & \text{otherwise.} \end{cases} \ \| \ \textbf{Positive eigenvalues.}$$

After application of this procedure, a total of ~1000 modes were selected for the decomposed strain-hardening model.

4. NTFA-TSO applied to the 2nd typical example - Implementation & results

- **Results** (Labat et al., 2023).

Uniaxial Compressive Strain Test – Macroscopic Comparison between Experimental Results, Full-Field FFT and NTFA-TSO Model:

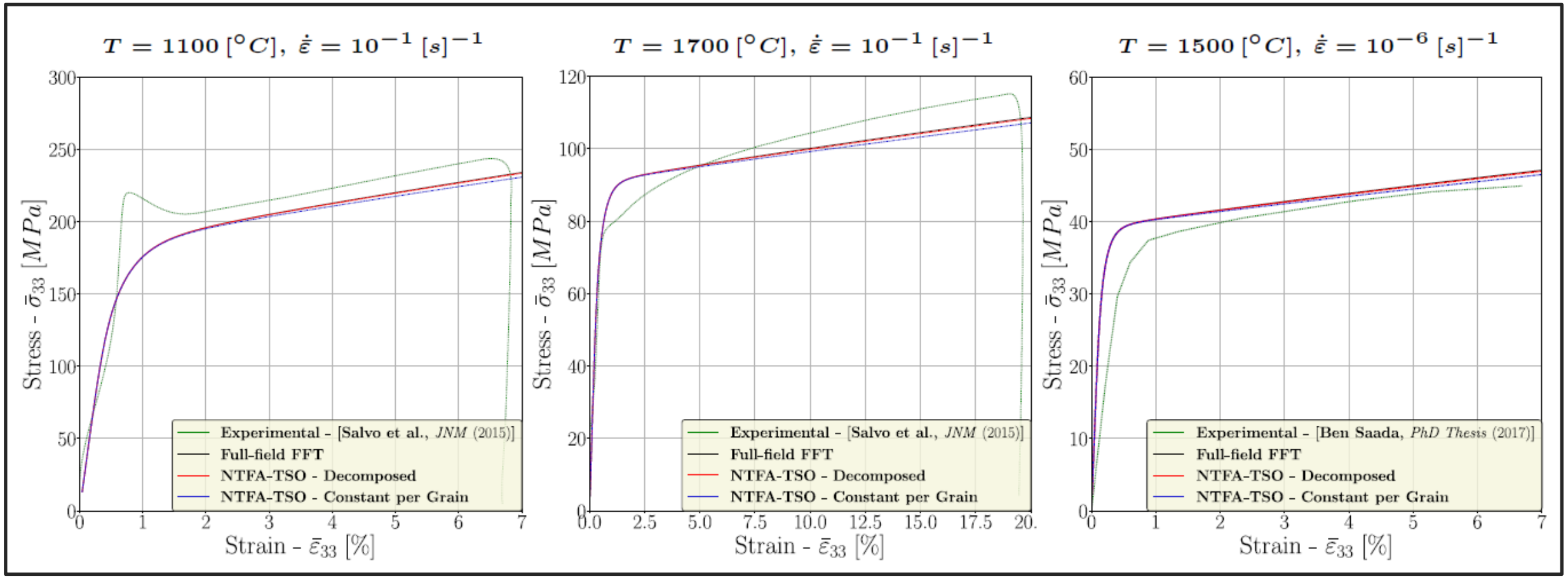

4. NTFA-TSO applied to the 2nd typical example - Implementation & results

- **Results** (Labat et al., 2023).

Uniaxial Compressive Strain Test – Local Comparison between Full-Field FFT and NTFA-TSO Model:

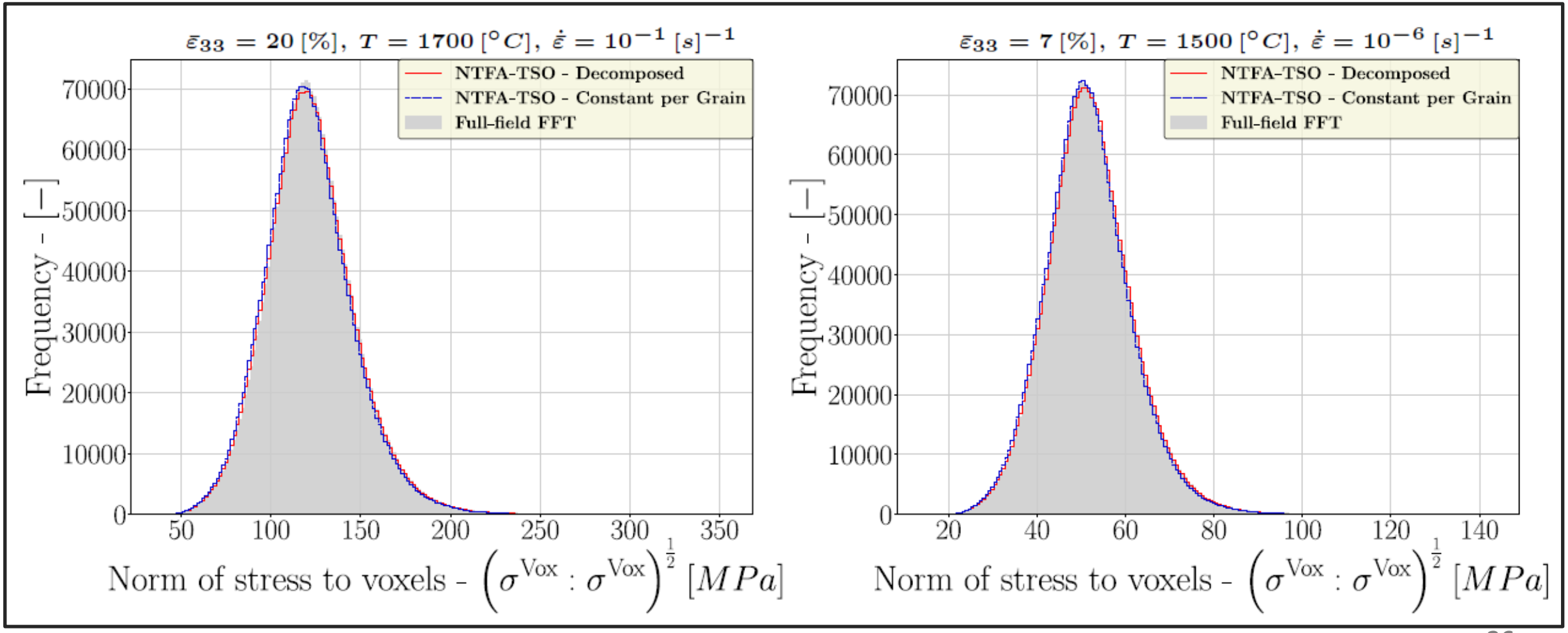

4. NTFA-TSO applied to the 2nd typical example - Implementation & results

- **Results** (Labat et al., 2023).

Triaxial Compressive Strain Test – Macroscopic Comparison between Full-Field FFT and NTFA-TSO Model:

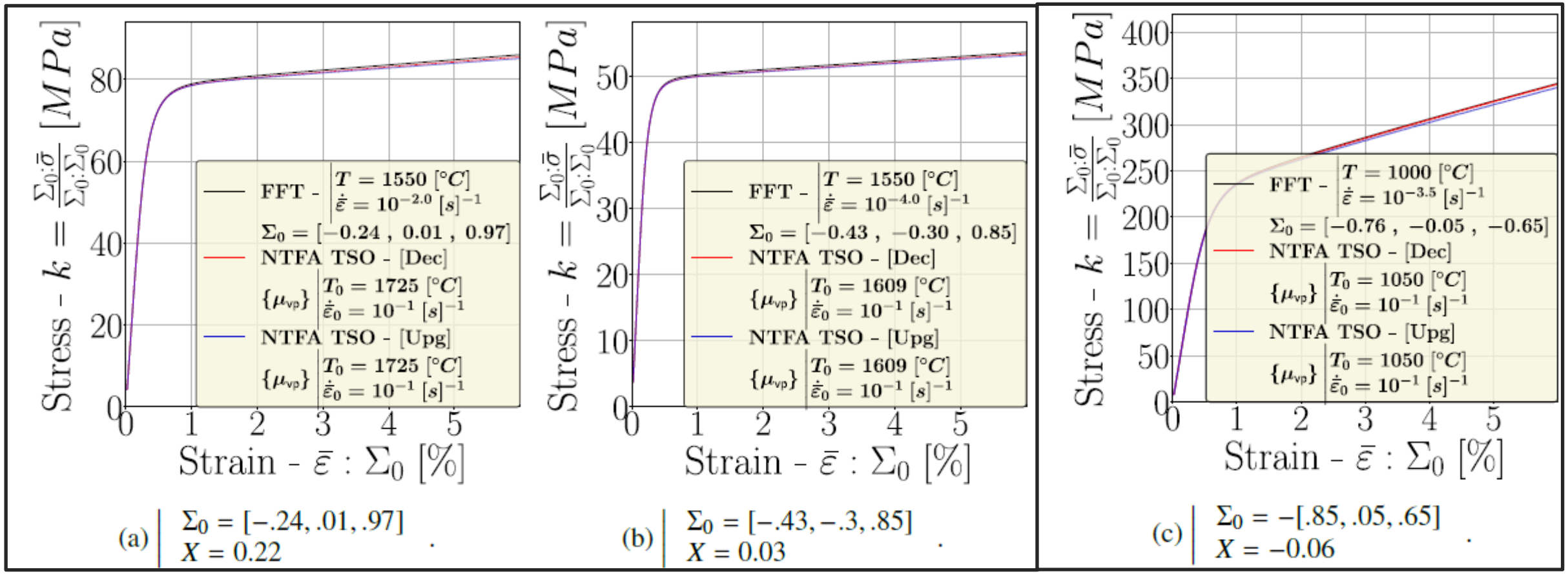

4. NTFA-TSO applied to the 2nd typical example - Implementation & results

- **Results** (Labat et al., 2023).

Triaxial Compressive Strain Test – Local Comparison between Full-Field FFT and NTFA-TSO Model:

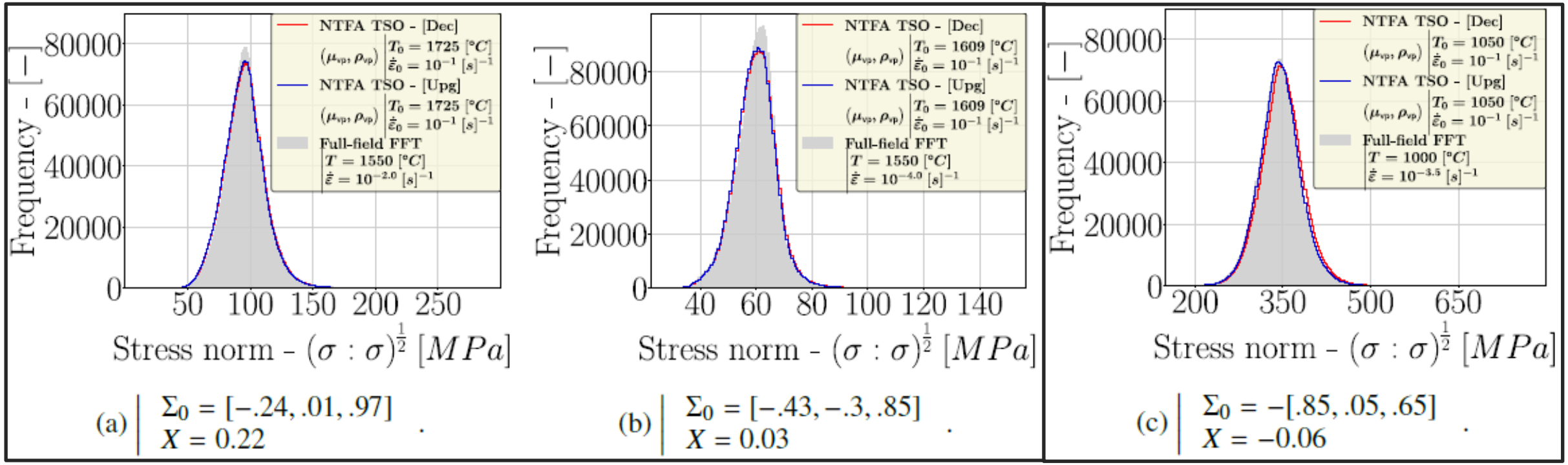

(a) $\Sigma_0 = [-.24, .01, .97]$, $X = 0.22$.

(b) $\Sigma_0 = [-.43, -.3, .85]$, $X = 0.03$.

(c) $\Sigma_0 = -[.85, .05, .65]$, $X = -0.06$.

5. NTFA: Conclusion - Outlook & Reflection

Conclusion:

- In nonlinear composite or polycrystalline materials, intra-phase strain heterogeneity is very important => Elementary patterns or modes of deformation are observed.

- These "modes" are the reduced base for a reduced "homogenized" constitutive model such as NTFA-type models:

  - The modes can be determined numerically by simulating (Full Field approach: FEM, FFT) the response of the r.v.e. along loading paths.

  - There is no universal method for choosing these modes, and you should try to select them according to the loads experienced within the structure (see (Michel and Suquet, 2009) or in appendix 2, see (Leturcq et al., 2022), etc) and/or the microstructure (see this presentation).

  - Reduction of the modal base is achieved by POD.

- The NTFA approach has been applied to many types of materials (composites, polycrystals, porous materials (Michel and Suquet, 2017), etc.) and for different types of linear and non-linear behaviors (aging viscoelastic, viscoplastic, plastic with isotropic and kinematic strain hardening, etc.).

Outlook & Reflection:

- Modal base construction by Artificial Intelligence?

- Probability modes to account for microstructure variability during a manufacturing process?

- Considering damage (see Ju et al., 2025) and crack propagation?

Acknowledgements:

Jean-Claude Michel, Pierre Suquet and the various contributors to the NTFA approach.

Thank You for your attention.

Any questions ?

Dr. Rodrigue Largenton – Senior Expert
EDF R&D - Materials and Mechanics of Components Department
Civil and Fuel Engineering Group
CEA Cadarache Bât. 151 13108 St Paul lez Durance Cedex FRANCE
rodrigue.largenton@edf.fr

REFERENCES

(Largenton et al., 2014) – Largenton R., Michel J.-C., Suquet P. 2014. *Extension of the nonuniform transformation field analysis to linear viscoelastic composites in the presence of aging and swelling.* Mech. Mater. (ISSN 0167-6636) 73 (2014) 76–100, 2014. http://dx.doi.org/10.1016/j.mechmat.2014.02.004.

(Largenton et al., 2019) – Largenton R., Michel J.-C., El Abdi A., Suquet P. 2019. *Extension of the Nonuniform Transformation Field Analysis using Tangent Second-Order expansion to nonlinear viscoelastic composites in the presence of aging and swelling*, Proc. 24ème Congrès Français de Mécanique, France, Brest, 26 au 30 Août 2019.

(Labat et al., 2023) – Labat J., Largenton R., Michel J.-C. 2023. *Multiscale identification and NTFA reduction of the elasto-viscoplastic polycrystalline behaviour of uranium dioxide (UO2) for wide range of loading conditions.* Journal of Nuclear Materials 582, 154471, 2023. https://doi.org/10.1016/j.jnucmat.2023.154471.

[**Knezevic et al**, *IJP* (2013)] **– Knezevic M., McCabe R. J., Tomé C. N., Lebensohn R. A., Chen S. R., Cady C. M., Gray III G. T., Mihaila B. 2013.** Modeling mechanical response and texture evolution of α-uranium as a function of strain rate and temperature using polycrystal plasticity. International Journal of Plasticity 43 (2013) 70–84, http://dx.doi.org/10.1016/j.ijplas.2012.10.011

[Salvo et al., *JNM* (2015)**] – Salvo M., Sercombe J., Helfer T., Sornay P., Desoyer T. 2015.** *Experimental characterization and modelling of UO_2 grain boundary cracking at high temperatures and high strain rates.* J. Nucl. Mater., 2015. https://doi.org/10.1016/j.jnucmat.2015.02.018.

[Ben Saada, *PhD Thesis* (2017)**] – Ben Saada M. 2017.** *Étude du comportement visco-plastique du dioxyde d'uranium: quantification par analyse EBSD et ECCI des effets liés aux conditions de sollicitations et à la microstructure initiale.* PhD Thesis Université de Lorraine, 2017. https://tel .archives -ouvertes .fr /tel -01810127.

(Halphen & Nguyen, 1975) – Halphen B., Nguyen Q. 1975. *Sur les matériaux standard généralisés.* J. Mécanique 14, 39–63.

(Mandel, 1969) – Mandel J. 1969. *Cours de mécanique des milieux continus déformables, Ecole Polyctechnique, Paris, France.*

(Rice 1971) – Rice J. 1971. *Inelastic constitutive relations for solids: an internal variable theory and its application to metal plasticity*. J Mech Phys Solids 19:433–455.

(Suquet, 1982) – Suquet P. 1982. *Thése de doctorat d'état P Suquet Plasticité et homogénéisation.*

(Suquet, 1987) – Suquet P. 1987. *Elements of homogenization for inelastic solid mechanics*, in: E. Sanchez-Palencia, A. Zaoui (Eds.), Homogenization Techniques for Composite Media, Springer-Verlag, 1987, pp. 194–278.

(Dvorak, 1992) – Dvorak G.-J. 1992. *Transformation field analysis of inelastic composite materials.* Proc. R. Soc. Lond. Ser. A, Math. Phys. Sci. 437 (1992) 311–327. https://doi .org /10 .1098/rspa .1992 .0063.

(Michel & Suquet, 2003) – Michel J.-C., Suquet P. 2003. *Nonuniform transformation field analysis*. Int. J. Solids Struct. (ISSN 0020-7683) 40 (25) (2003) 6937–6955. https://doi .org /10 .1016 /S0020 -7683(03)00346 -9.

(Doumalin et al., 2003) – Doumalin P., Bornert M., Crépin J. 2003. *Characterisation of the strain distribution in heterogeneous materials.* Mechanics & Industry, 2003, 4, pp.607-617. 10.1016/j.mecind.2003.09.002. hal-00111395

[Michel and Suquet, *JMPS* (2016)**] – Michel J.-C. , Suquet P. 2016.** *A model-reduction approach in micromechanics of materials preserving the variational structure of constitutive relations*. J. Mech. Phys. Solids 90 (2016) 254–285, 2016. http://dx.doi.org/10.1016/j.jmps.2016.02.005

[Michel and Suquet, *CM* (2016)**] – Michel J.-C., Suquet P. 2016.** *A model-reduction approach to the micromechanical analysis of polycrystalline materials*. Comput. Mech. 57 (3) (2016) 483–508, 2016. https://doi .org /10 .1007 /s00466 -015 -1248 -9.

[Castelnau et al. 2008] – Castelnau O., Duval P., Montagnat M., Brenner R. 2008. *Elastoviscoplastic micromechanical modeling of the transient creep of ice*. J Geophys Res 113:B11203.

[Suquet et al., 2012] – Suquet P., Moulinec H., Castelnau O., Lahellec N., Montagnat M., Grennerat F., Duval P., Brenner R. 2012. *Multi-scale modeling of the mechanical behavior of polycrystalline ice under transient creep.* Proc IUTAM 3:76–90. doi:10.1016/j.piutam.2012.03.006

[Méric and Cailletaud, 1991] – Méric L., Cailletaud G. 1991. *Single crystal modeling for structural calculations. part 2: finite element implementation*. J Eng Mat Technol 113:171–182

[Fritzen and Leuschner, *CMAME* (2013)] **– Fritzen F., Leuschner M. 2013.** *Reduced basis hybrid computational homogenization based on a mixed incremental formulation*. Comput. Methods, Appl. Mech. Eng.260,143–154.

[**Castañeda**, *JMPS* (1996)] – **Ponte Castañeda P. 1996**. *Exact second-order estimates for the effective mechanical properties of nonlinear composite materials*. J.Mech.Phys.Solids 44, 827–862.

[**Rousette et al.**, CST (2009)] – **Roussette S., Michel J.-C., Suquet P. 2009**. *Nonuniform transformation field analysis of elastic–viscoplastic composites*. Compos. Sci. Technol. (ISSN 0266-3538) 69 (1) (2009) 22–27, 2009. https://doi .org /10 .1016 /j .compscitech .2007 .10 .032.

(Michel and Suquet, **2009)** – **Michel J.-C., Suquet P. 2009**. *Nonuniform transformation field analysis: a reduced model for multiscale nonlinear problems in solid mechanics.* In: Aliabadi U., Galvanetto U. (Eds.), Multiscale Modelling in Solid Mechanics — Computational Approaches. Imperial College Press, London, pp. 159–206.(Chapter4).

(Leturcq et al. 2022) – Leturcq B., Le Tallec P., Pascal S., Fandeur O., Lamorte N. 2022. *A new reduced order model to represent the creep induced fuel assembly*

bow in PWR cores. Nuclear Engineering and Design 394 (2022) 111828, https://doi.org/10.1016/j.nucengdes.2022.111828.

(Michel and Suquet, 2017) – **Michel J.-C., Suquet P. 2017**. *Effective potentials in nonlinear polycrystals and quadrature formulae.* Proc. R. Soc. A 473: 20170213. http://dx.doi.org/10.1098/rspa.2017.0213.

(Ju et al., 2025) – Ju X., Zhou C., Xu Y., Linag L. 2025. Reduced order homogenization of composites with strength difference effects in elastoplasticity coupled to damage. Composite Structures 351 (2025) 118564, https://doi.org/10.1016/j.compstruct.2024.118564

[**Levenberg**, *QAM* (1944)] – **Levenberg K. 1944**. *A method for the solution of certain non-linear problems in least squares*. Quarterly of applied mathematics 2.2 pages 164-168.

[**Marquardt**, *JSIAM* (1963)] – **Marquardt D.W. 1963**. *An algorithm for least-squares estimation of nonlinear parameters*. Journal of the society for Industrial and Applied Mathematics 11.2 (1963), pages 431-441.

APPENDIX 1 – TYPICAL EXAMPLE 2

Formalisms of h_i and τ^0_i functions and Identification of parameters

1. Crystal plasticity law for UO_2 fuel

Calibration of $\tau_i^0(T, \dot{\bar{\varepsilon}})$

$$n_{\{100\}} = 4,\ \dot{\gamma}^0_{\{100\}}(\dot{\bar{\varepsilon}}) = 0.7 \times \dot{\bar{\varepsilon}} \text{ and } n_{\{110\}} = 4,\ \dot{\gamma}^0_{\{110\}}(\dot{\bar{\varepsilon}}) = 0.5 \times \dot{\bar{\varepsilon}},$$

with:
- n_i deduced from observations,
- $\dot{\gamma}_i^0(\dot{\bar{\varepsilon}})$ determined using numerical tests at the single crystal scale.

$$\tau_i^0(T, \dot{\bar{\varepsilon}}) = A_i^{\mathsf{f}}(\dot{\bar{\varepsilon}}) \times exp\left(-b_i^{\mathsf{f}} \times T\right) + C_i^{\mathsf{f}}(\dot{\bar{\varepsilon}})$$

$$A_i^{\mathsf{f}}(\dot{\bar{\varepsilon}}) = Max\left[a_i^{\mathsf{f},0} - a_i^{\mathsf{f},1} \times exp\left[-a_i^{\mathsf{f},2} \times log_{10}\left(\dot{\bar{\varepsilon}}\right)\right], 0\right],$$

with:
- $C_i^{\mathsf{f}}(\dot{\bar{\varepsilon}})$ same strain rate dependence as $A_i^{\mathsf{f}}(\dot{\bar{\varepsilon}})$,
- $(A_i^{\mathsf{f}}, b_i^{\mathsf{f}}, C_i^{\mathsf{f}})$ **obtained by minimising error using *LM* algorithm** [**Levenberg**, *QAM* (1944)] [**Marquardt**, *JSIAM* (1963)],
- $\tau_i^0(T, \dot{\bar{\varepsilon}})$ targeted function.

$$\tau_i^{0,(n+1)}(T, \dot{\bar{\varepsilon}}) = \tau_i^{0,(n)}(T, \dot{\bar{\varepsilon}}) + f_s \times {}^{(n)}\Delta\bar{\sigma}^{\mathsf{cr}}_{33}(T, \dot{\bar{\varepsilon}}),\ f_s = 0.5,$$

with:
- $\tau_i^{0,(n+1)}$ input data used in the *LM* algorithm,

$$Er^{(n)} = \frac{1}{N} \times \sum |{}^{(n)}\Delta\bar{\sigma}^{\mathsf{cr}}_{33}(T, \dot{\bar{\varepsilon}})|,\ |Er^{(n)} - Er^{(n-1)}| < \delta \times Er^{(n-1)},$$

with:
- ${}^{(n)}\Delta\bar{\sigma}^{\mathsf{cr}}_{33}(T, \dot{\bar{\varepsilon}})$ error at given loading conditions,
- $(Er^{(n)}, \delta(= 10^{-3}))$ relative error and stopping criterion.

Beginning of the iterative process

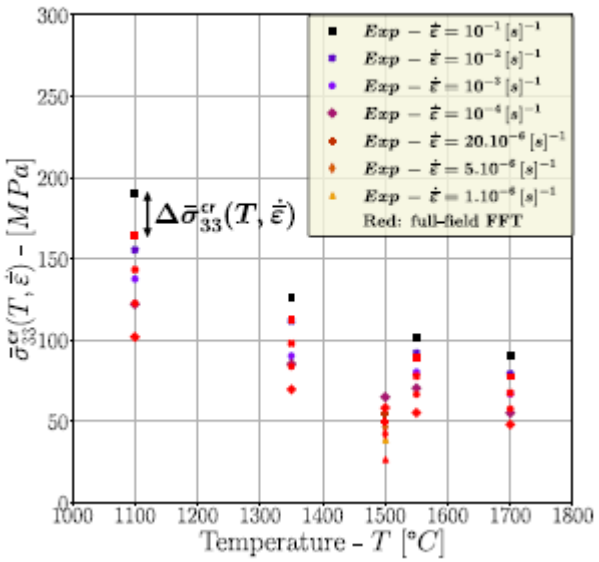

Mechanical tests from [Salvo et al., JNM (2015)] and [Ben Saada, PhD Thesis (2017)]

End of the iterative process

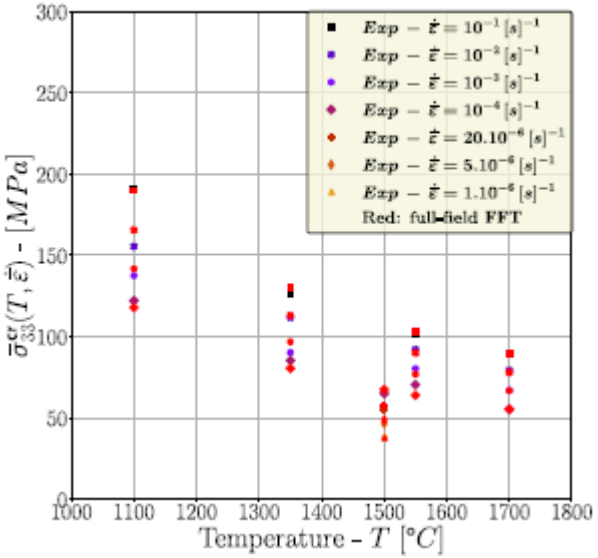

2. Crystal plasticity law for UO_2 fuel

Calibration of $h_i(T, \dot{\bar{\varepsilon}})$

$$h_{\{100\}} = h_{\{110\}} = h$$

$$h^{(n+1)} = \frac{a_{\text{p,exp}} \times h^{(n)}}{a^{(n)}_{\text{p,simu}}}, \; |a^{(n)}_{\text{p,simu}} - a_{\text{p,exp}}| < \delta \times a_{\text{p,exp}},$$

with:

$a_{\text{p,exp}}$	experimental strain hardening slope,
$a^{(n)}_{\text{p,simu}}$	numerical strain hardening slope,
$\delta (= 10^{-4})$	relative stopping criterion.

$$h(T, \dot{\bar{\varepsilon}}) = \frac{a^{\text{h}} \times ln\left(b^{\text{h}} \times \dot{\bar{\varepsilon}} + f^{\text{h}}\right)}{\left(c^{\text{h}} \times T + d^{\text{h}}\right)^{e^{\text{h}}}},$$

with:

$h^{(n)}$	input data used in the LM algorithm,
$(a^{\text{h}}, b^{\text{h}}, c^{\text{h}}, d^{\text{h}}, e^{\text{h}}, f^{\text{h}})$	**coefficients determined by using *LM* algorithm** [**Levenberg**, *QAM* (1944)] [**Marquardt**, *JSIAM* (1963)].

End of the iterative process

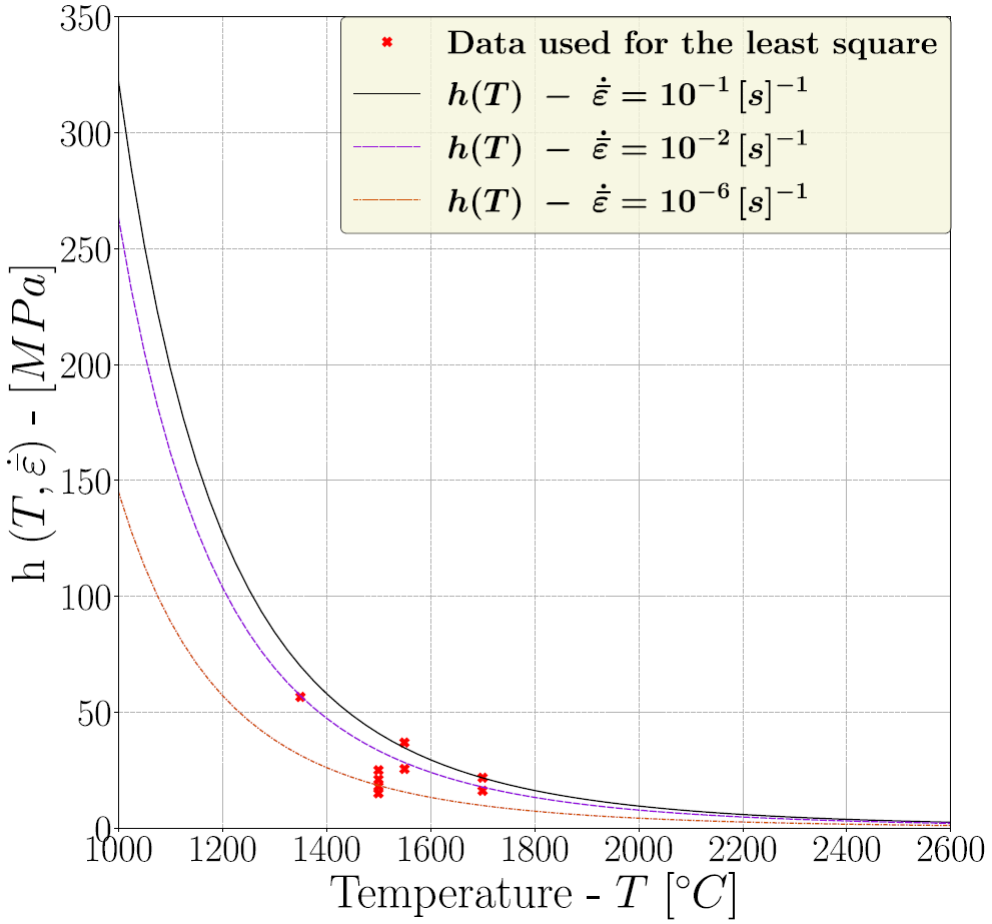

Mechanical tests from [Salvo et al., JNM (2015)] and [Ben Saada, PhD Thesis (2017)]

APPENDIX 2

PLASTIC STRAIN HETEROGENEITY IN COMPOSITE MATERIALS AND THE NONUNIFORM TRANSFORMATION FIELD ANALYSIS

R. Largenton, J.-C. Michel, P. Suquet
suquet@lma.cnrs-mrs.fr

Euromech 537 – Multi-scale Computational Homogenization of Heterogeneous Structures and Materials –
Université Paris-Est, Marne-la-Vallée,
26-28 March 2012

Abstract:

The Nonuniform Transformation Field Analysis is a reduced order model for the effective behavior of nonlinear composite materials. It is based on the decomposition of the plastic strain field on nonuniform plastic modes. It is presented and applied to the modeling of the aging behavior of a nuclear fuel and the life-time prediction of a structure.

Plastic strain heterogeneity in composite materials and the Nonuniform Transformation Field Analysis

R. Largenton[(1)], JC Michel[(2)], P. Suquet[(2)]

[(1)] Dpt MMC EDF R&D, Avenue des Renardières, 77818 Moret Sur Loing, France
[(2)] LMA, CNRS, UPR 7051, 31 Chemin Joseph Aiguier, 13402 Marseille Cedex 20, France

suquet@lma.cnrs-mrs.fr

1. **Motivation**
2. **Classical approach : Transformation Field Analysis**
3. **Reduced model : Nonuniform Transformation Field Analysis**

1. Motivation : two typical examples.

1. Aging of nuclear fuels.

Mixed Oxide (MoX)= Mix UO_2 and U-PuO_2 (recycling fission products).

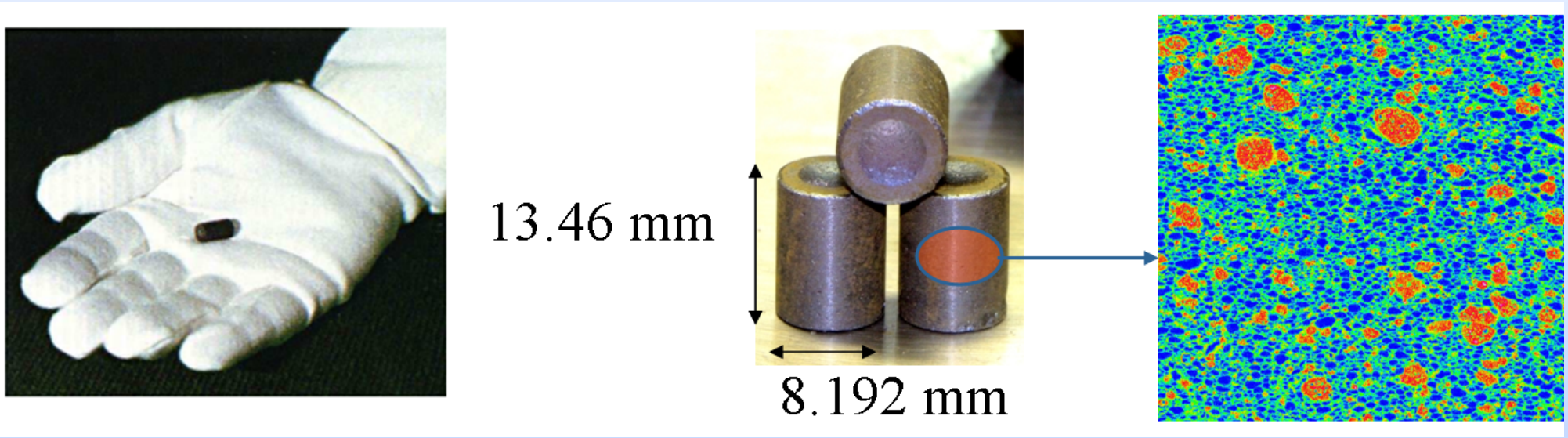

Three-phase composite :

- **composite matrix** where both phases are well mixed (green $\simeq$ 10 % Pu)
- clusters of **UO_2** (blue, 0% Pu), volume fraction $\simeq$ 24%, 10 μm $\leq \phi \leq$ 60 μm,
- clusters of **U-PuO_2** (red, 28% Pu), volume fraction $\simeq$ 15%, 10 μm $\leq \phi \leq$ 150 μm.

Constitutive relations for the individual phases

$$\varepsilon = \varepsilon^{e} + \varepsilon^{an}, \quad \varepsilon^{an} = \varepsilon^{\text{irradiation creep}} + \varepsilon^{\text{solid swelling}}$$

$$\varepsilon^{\text{irradiation creep}} = A\dot{F}(t)e^{-\frac{Q}{RT(t)}}\boldsymbol{M}^{\mathsf{V}} : \boldsymbol{\sigma}, \quad \dot{F} = \text{fission rate},$$

$$\varepsilon^{\text{solid swelling}} = f(t)\boldsymbol{i}, \quad f(t) = aB(t) + b, \quad B = \text{burn-up}.$$

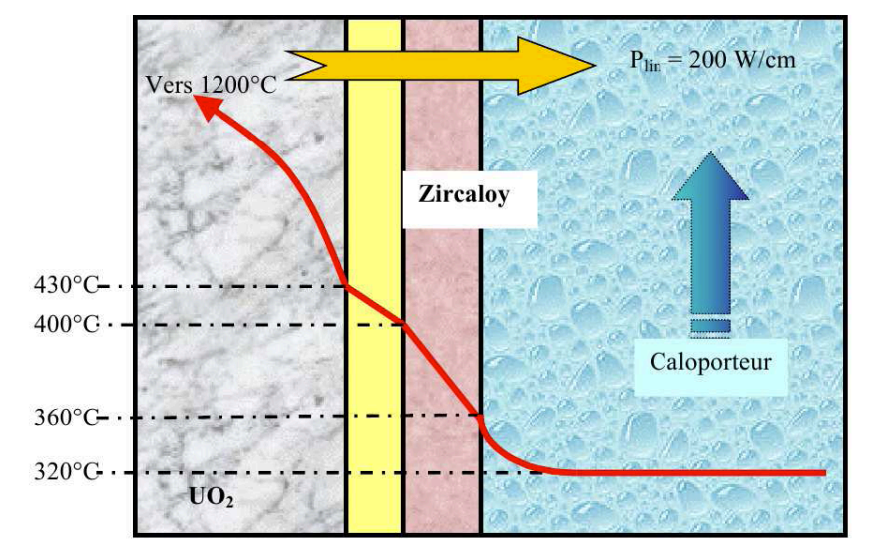

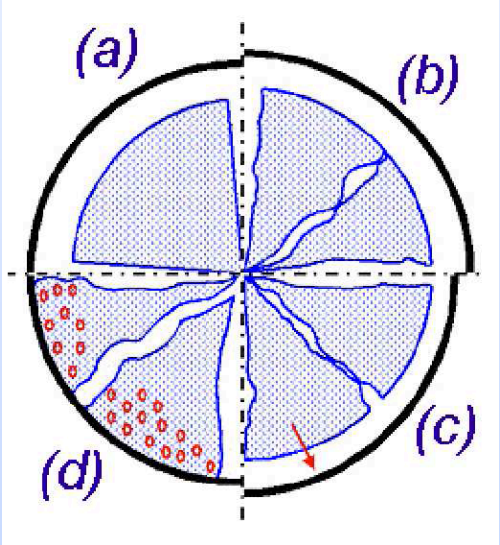

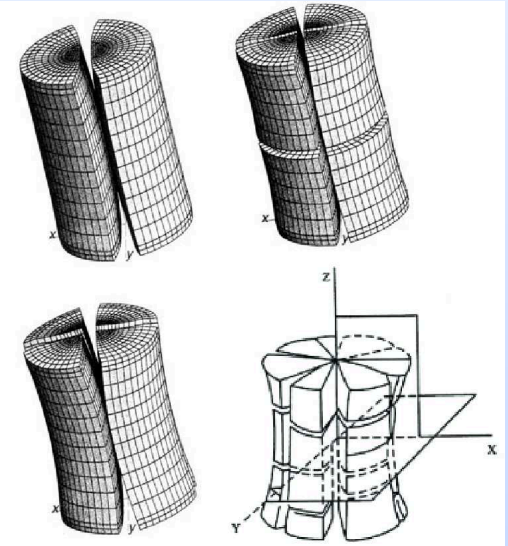

Swelling : fission $\Rightarrow$ diffusion of atoms. **Aging :** time-dependent material properties (function of irradiation which is a function of time).

High temperature gradient $\Rightarrow$ heterogeneous deformation, fracturation, contact with cladding. **PREDICT : overall swelling, effective behavior of MoX ?**

2. Life-time prediction of a structure

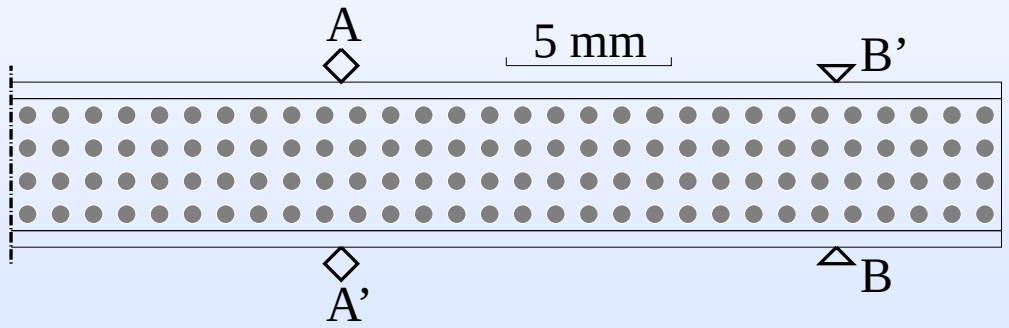

Half-beam (120 fibers).

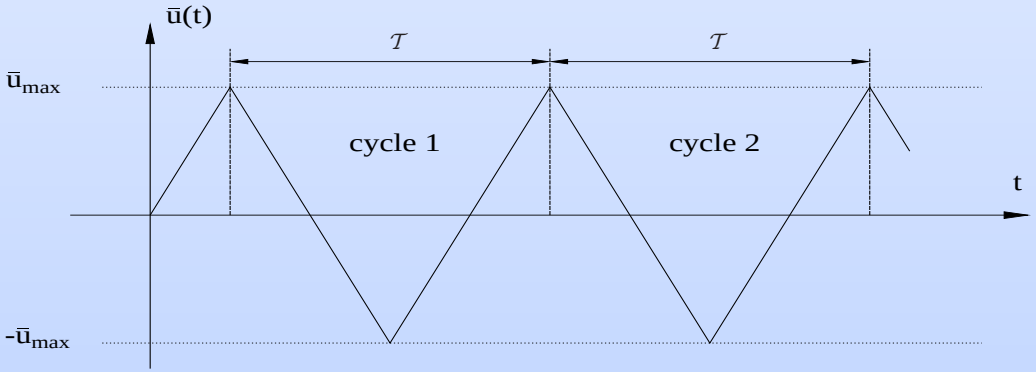

Loading : prescribed vertical displacement at points A and A', frequency 0.1 Hz, 3 different amplitudes

$$\overline{u}_{\max} = 0.15, 0.25, 0.5 \text{ mm}.$$

Fatigue of a composite beam by cyclic 4 point-bending.

Elastic fibers
elasto-viscoplastic matrix with nonlinear kinematic hardening (Chaboche, 1993) :

$$\boldsymbol{\sigma} = \boldsymbol{L} : (\boldsymbol{\varepsilon} - \boldsymbol{\varepsilon}^{\mathsf{p}}), \quad \dot{\boldsymbol{\varepsilon}}^{\mathsf{p}} = \frac{3}{2}\dot{p}\,\frac{\boldsymbol{s} - \boldsymbol{\mathfrak{X}}}{(\sigma - \mathfrak{X})_{\mathsf{eq}}},$$
$$\dot{p} = \dot{\varepsilon}_0 \left[\frac{((\sigma - \mathfrak{X})_{\mathsf{eq}} - \sigma_y)^+}{\sigma_0}\right]^n,$$
$$\dot{\boldsymbol{\mathfrak{X}}} = \frac{2}{3} H\, \dot{\boldsymbol{\varepsilon}}^{\mathsf{p}} - \xi\, \boldsymbol{\mathfrak{X}}\, \dot{p}.$$

Local fatigue criterion (at point X) based on the energy dissipated along the stabilized cycle : $N_{cycl} \# w^{\beta}$ with

$$w(\boldsymbol{X}, \text{cycle}) = \int_{\text{cycle}} \boldsymbol{\sigma}(\boldsymbol{X}, t) : \dot{\boldsymbol{\varepsilon}}^{\mathsf{p}}(\boldsymbol{X}, t)\, dt.$$

Brute force : full-field computation of the composite structure

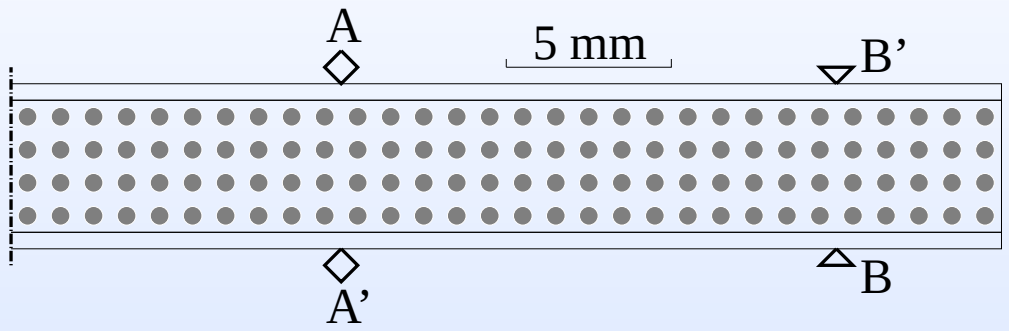

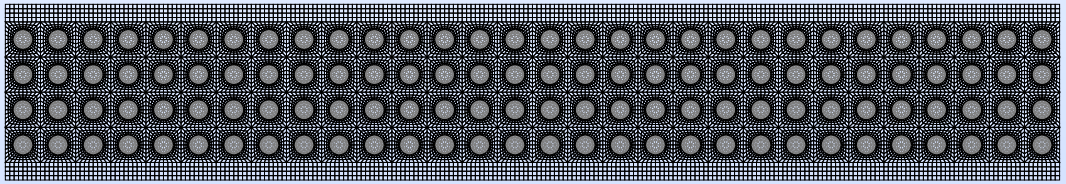

26880 quadratic elements (6 or 8 nodes)

Force/displacement at point A

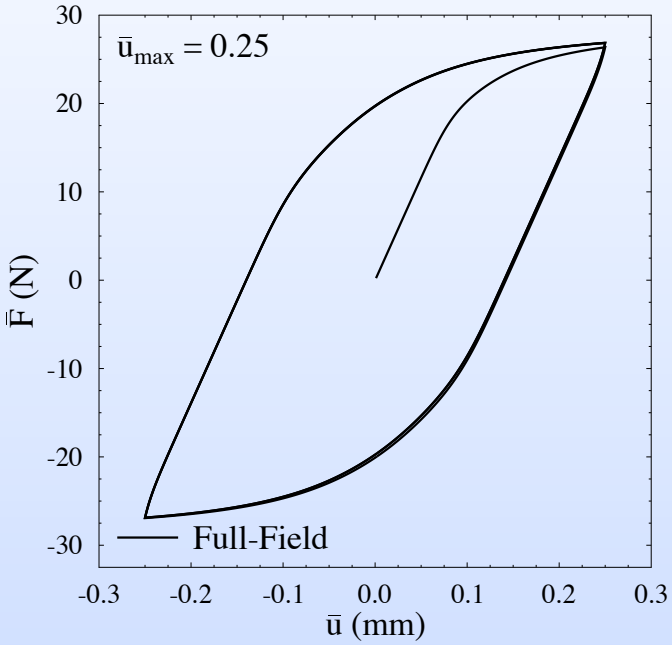

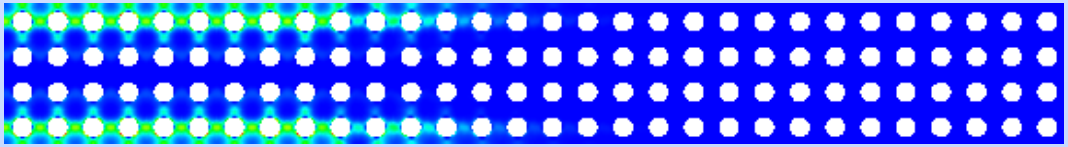

Snapshot of the energy dissipated along the stabilized cycle.

Zoom →

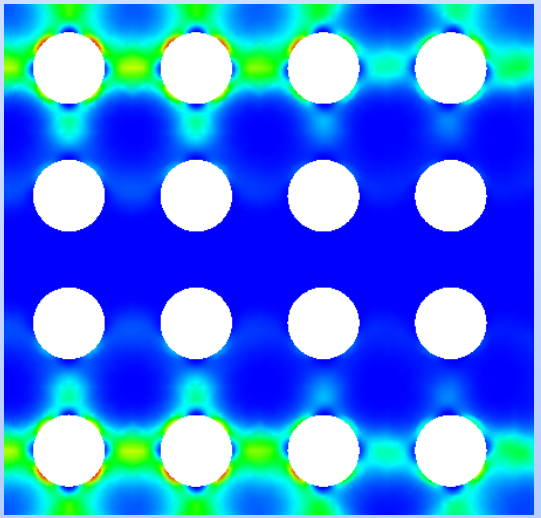

Can the global and the local responses of the beam be predicted by means of an homogenized model ?

Homogenization of highly heterogeneous materials with nonlinear dissipative constituents entering the class of *Generalized Standard Materials* (GSM) (Halphen & Nguyen, 1975) governed by two convex potentials :

At each point x of the (micro)structure :

State of the system (state variables)	:	$\varepsilon, \alpha = \varepsilon^{\mathsf{p}},$
Energy available in the system	:	$w(\varepsilon, \alpha),$
$\Rightarrow$ **Driving forces**	:	$\sigma = \dfrac{\partial w}{\partial \varepsilon}(\varepsilon, \alpha), \quad \mathcal{A} = -\dfrac{\partial w}{\partial \alpha}(\varepsilon, \alpha),$
Evolution of the internal variables	:	$\dot{\alpha} = \dfrac{\partial \psi}{\partial \mathcal{A}}(\mathcal{A}) \quad \Leftrightarrow \quad \mathcal{A} = \dfrac{\partial \varphi}{\partial \dot{\alpha}}(\dot{\alpha}).$

where ψ and φ are dual potentials.

EXACT separation of scales in nonlinear problems is seldomly met : an infinite number of internal variables is required (Mandel 68, Rice 71, PS 82).

State variables	:	$\overline{\varepsilon}, \quad \widetilde{\boldsymbol{\alpha}} = \{\boldsymbol{\varepsilon}^{\mathrm{p}}(\boldsymbol{x})\}_{\boldsymbol{x}\in V},$
Potentials	:	$\widetilde{w}\,(\overline{\varepsilon}, \widetilde{\boldsymbol{\alpha}}) = \left\langle w(\boldsymbol{\varepsilon}, \boldsymbol{\varepsilon}^{\mathrm{p}}) \right\rangle, \quad \widetilde{\varphi}(\dot{\widetilde{\boldsymbol{\alpha}}}) = \left\langle \varphi(\dot{\boldsymbol{\varepsilon}}^{\mathrm{p}}) \right\rangle,$
Driving forces	:	$\overline{\boldsymbol{\sigma}} = \dfrac{\partial \widetilde{w}}{\partial \overline{\varepsilon}}(\overline{\varepsilon}, \widetilde{\boldsymbol{\alpha}}), \quad \widetilde{\boldsymbol{\mathcal{A}}} = -\dfrac{\partial \widetilde{w}}{\partial \widetilde{\boldsymbol{\alpha}}}(\overline{\varepsilon}, \widetilde{\boldsymbol{\alpha}}),$
Evolution of internal variables	:	$\widetilde{\boldsymbol{\mathcal{A}}} = \dfrac{\partial \widetilde{\varphi}}{\partial \dot{\widetilde{\boldsymbol{\alpha}}}}(\dot{\widetilde{\boldsymbol{\alpha}}}).$

$\Rightarrow$ **No scale decoupling : both scales have to be resolved simultaneously.**

Differential Equation in a space of infinite dimension :

$$\dot{\widetilde{\boldsymbol{\alpha}}} = \frac{\partial \widetilde{\psi}}{\partial \widetilde{\boldsymbol{\mathcal{A}}}} \left(-\frac{\partial \widetilde{w}}{\partial \widetilde{\boldsymbol{\alpha}}}(\overline{\varepsilon}, \widetilde{\boldsymbol{\alpha}}) \right).$$

Aim of this work : **derive a reduced model**.

2. Classical approach : Transformation Field Analysis

Objective : approximate homogenized model for the r.v.e. V. Internal variables

$$\tilde{\boldsymbol{\alpha}} = \boldsymbol{\varepsilon}^{\mathsf{p}}(\boldsymbol{x})|_{\boldsymbol{x}\in V},$$

where V = r.v.e. (representative volume element).

Reduction (Dvorak, 1992) of the plastic strain field on the r.v.e to $6 \times N$ internal variables, N= number of phases in the composite :

- **H1. Plastic strain uniform / phase :**

$$\boldsymbol{\varepsilon}^{\mathsf{p}}(\boldsymbol{x}) = \sum_{r=1}^{N} \boldsymbol{\varepsilon}_r^{\mathsf{p}} \chi^{(r)}(\boldsymbol{x}), \quad \boldsymbol{x} \in V$$

  Internal variables : $\boldsymbol{\varepsilon}_r^{\mathsf{p}} | r = 1, ...N$

- **H2. Evolution of $\boldsymbol{\varepsilon}_r^{\mathsf{p}}$ governed by the average stress in phase r :**

$$\boldsymbol{\varepsilon}_r = \boldsymbol{M}^{(r)} : \boldsymbol{\sigma}_r + \boldsymbol{\varepsilon}_r^{\mathsf{p}}, \quad \boldsymbol{\sigma}_r = \langle \boldsymbol{\sigma} \rangle_r, \qquad \dot{\boldsymbol{\varepsilon}}_r^{\mathsf{p}} = \frac{\partial \psi^{(r)}}{\partial \boldsymbol{\sigma}}(\overline{\boldsymbol{\sigma}}_r).$$

Very stiff predictions.....

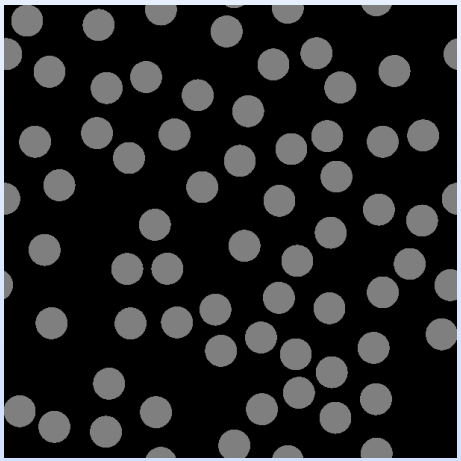

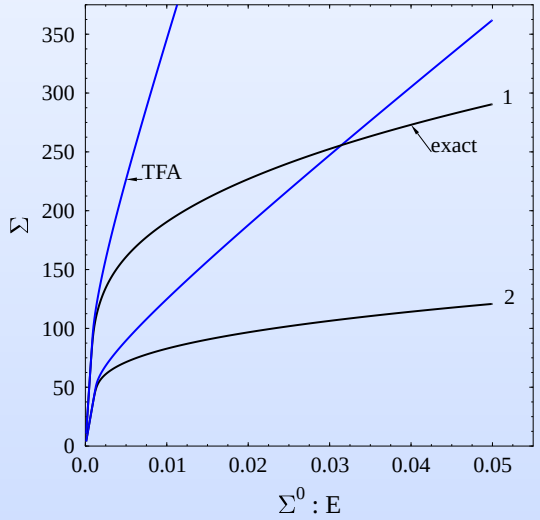

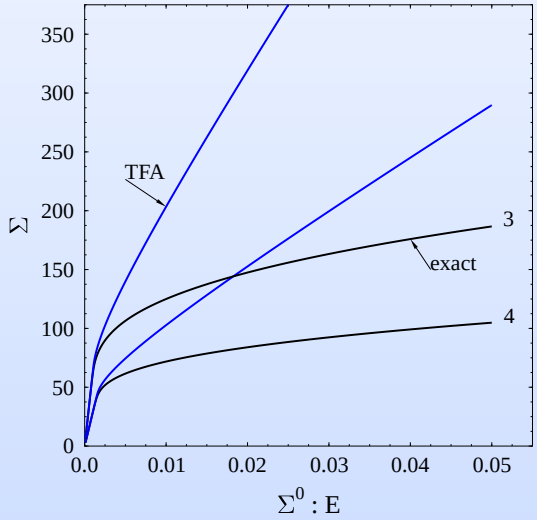

4 loading conditions : $\overline{\boldsymbol{\sigma}} = \overline{\sigma}(t)\boldsymbol{\Sigma}^0$:

$$\boldsymbol{\Sigma}^{(1)} = \boldsymbol{e}_1 \otimes \boldsymbol{e}_1,\ \boldsymbol{\Sigma}^{(2)} = \boldsymbol{e}_1 \otimes \boldsymbol{e}_2 + \boldsymbol{e}_2 \otimes \boldsymbol{e}_1,\ \boldsymbol{\Sigma}^{(3)} = \boldsymbol{\Sigma}^{(1)} + \frac{1}{2}\boldsymbol{\Sigma}^{(2)},\ \boldsymbol{\Sigma}^{(4)} = \boldsymbol{\Sigma}^{(1)} + \boldsymbol{\Sigma}^{(2)}.$$

What's wrong

Nonlinear composite (two−phase)

Actual nonuniform plastic strain field

Uniform plastic strain field (TFA)

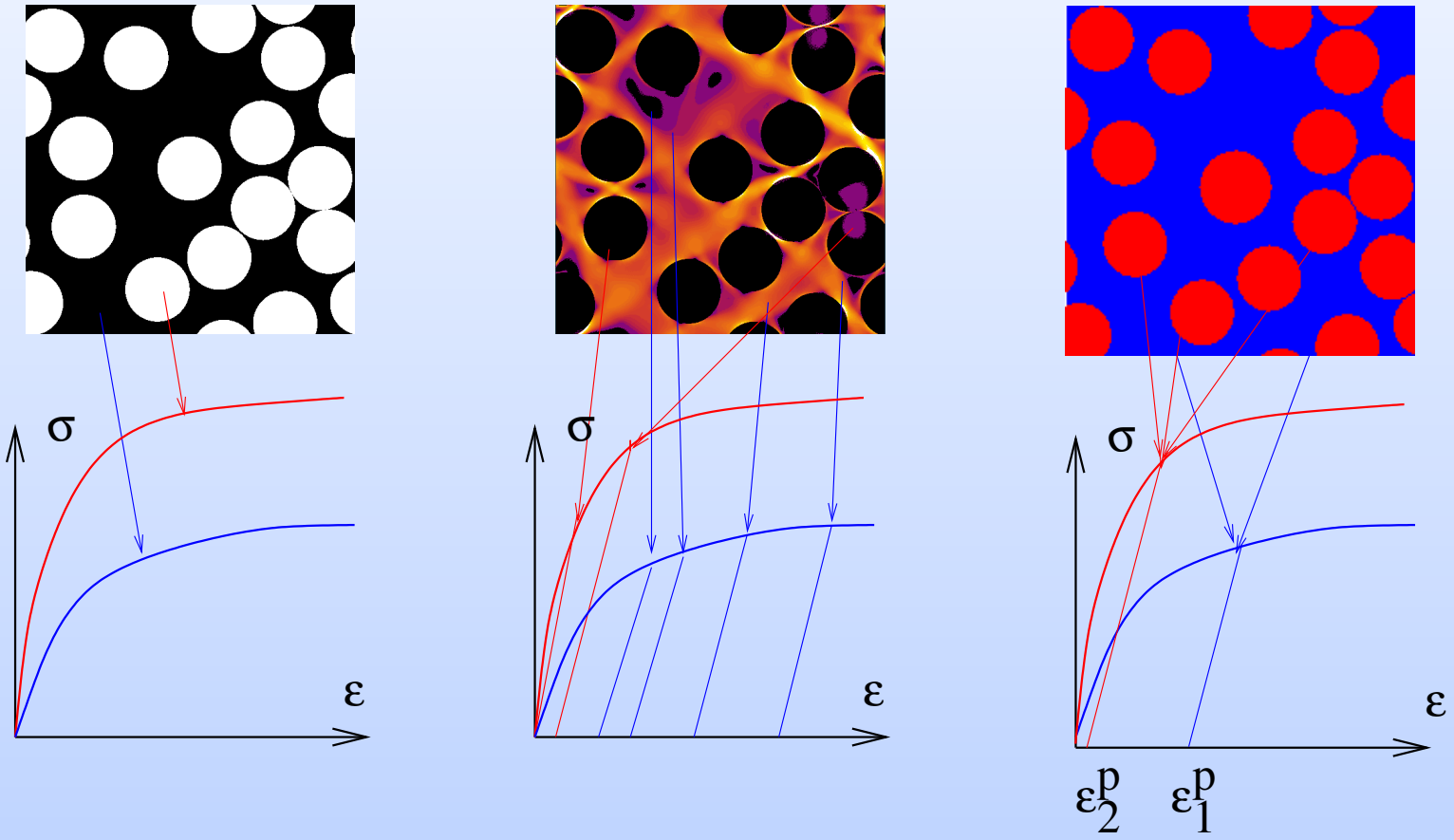

The TFA assumes that the plastic strain field is uniform per phase.

Field fluctuations do exist !

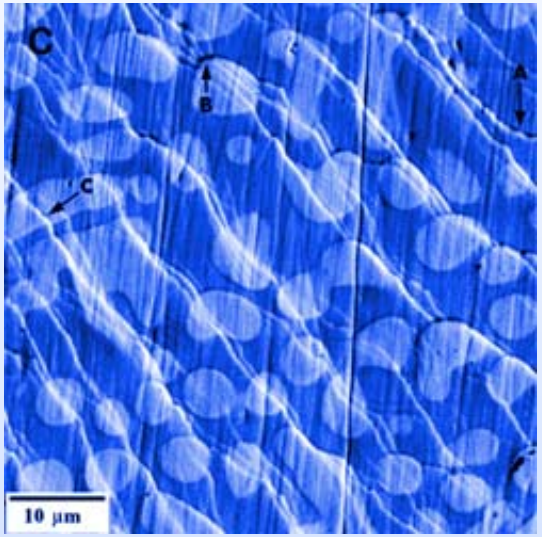

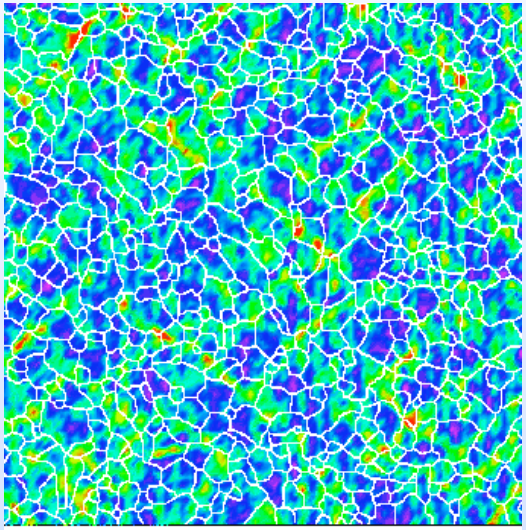

Experiments :

left : metallic glass ©W. Johnson

right : polycrystalline Zirconium. ©Bornert & Doumalin.

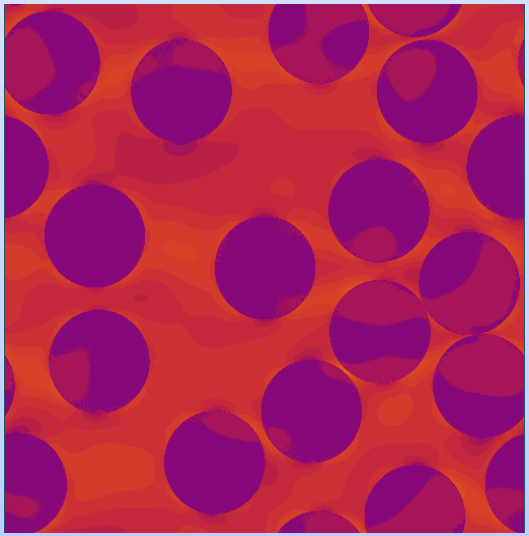

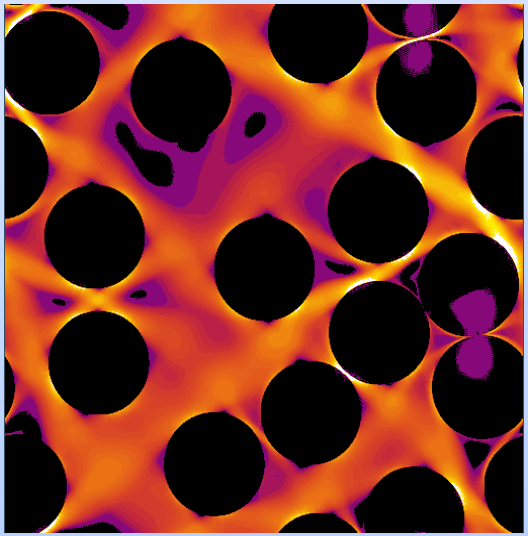

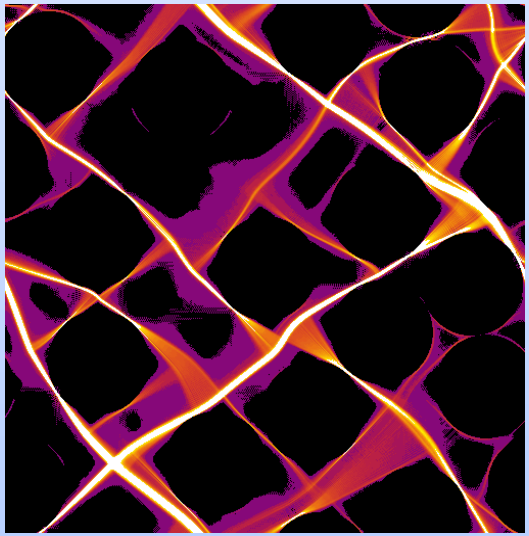

Simulations :

Elastic fibers, matrix :

left : elastic,

center : hardening,

right : ideally plastic.

3. Non Uniform Transformation Field Analysis NTFA

Reduction (*Michel,PS, IJSS 2003*) : reproduce the "dynamics" (evolution) and the observed "patterns" with **just a few variables, but physically motivated.**

1st ingredient : Re-formulation of assumptions H1 : ε^{p} decomposed on nonuniform "plastic modes"

$$\boldsymbol{\varepsilon}^{\mathrm{p}}(\boldsymbol{x},t)=\sum_{k=1}^{M}\varepsilon_k^{\mathrm{p}}(t)\,\boldsymbol{\mu}^{(k)}(\boldsymbol{x}),\quad \boldsymbol{x}=\text{microscopic variable}\in\text{volume element } V.$$

$\boldsymbol{\mu}^{(k)}$ **tensorial field** defined on V only, capturing the pattern of the plastic deformation, $\varepsilon_k^{\mathrm{p}}$ is a **scalar**. The $\varepsilon_k^{\mathrm{p}}$'s are the **internal variables of the model.**

- $\boldsymbol{\mu}^{(k)}$ has its support in a single phase in V.
- $\boldsymbol{\mu}^{(k)}$ are mutually orthogonal : $\left\langle \boldsymbol{\mu}^{(k)} : \boldsymbol{\mu}^{(\ell)} \right\rangle = 0$ when $k\neq\ell$.
- $\mathrm{Tr}\boldsymbol{\mu}^{(k)}=0$ (incompressible plasticity, for simplicity).

State variables : $\overline{\boldsymbol{\varepsilon}},\ (\varepsilon_k^{\mathrm{p}})_{k=1,M}$.

What do these modes look like ? Elastic fibers. Elasto-plastic matrix with isotropic hardening . Fiber volume fraction : 0.25.

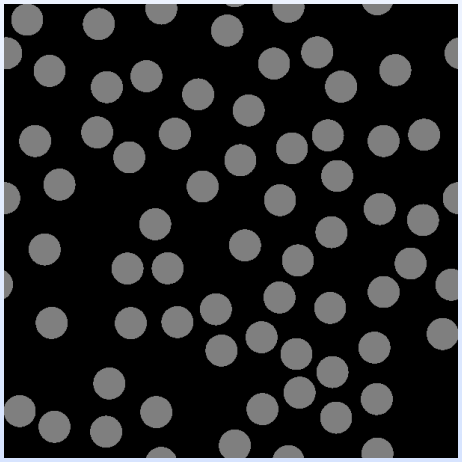

VER (64 fibers).

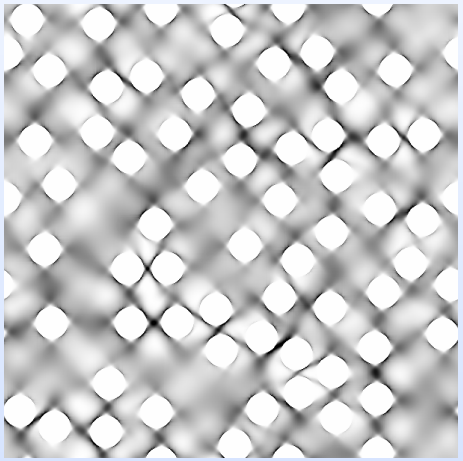

$\mu_{22}^{(1)}$

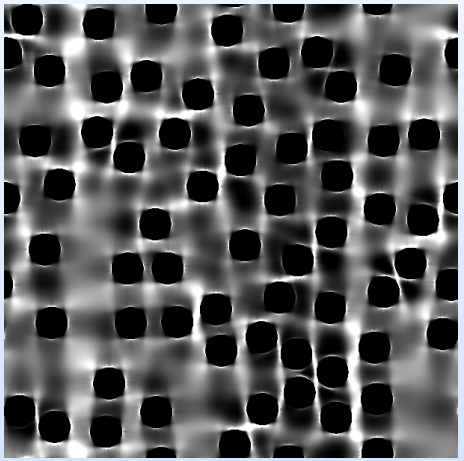

$\mu_{12}^{(2)}$

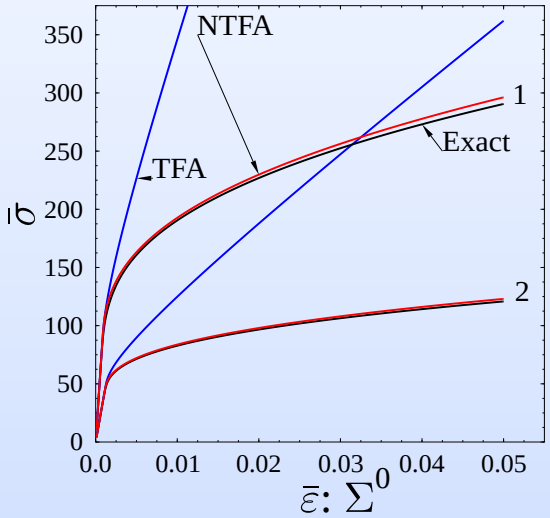

TFA : plastic strain field uniform in the matrix phase (2 internal variables $\varepsilon_{11}^{p}, \varepsilon_{12}^{p}$.)

NTFA : 2 modes $\boldsymbol{\mu}^{(k)}$ = plastic strain field along two loading paths :

$$\overline{\boldsymbol{\sigma}} = \overline{\sigma}(t)\boldsymbol{\Sigma}^{(k)}, \quad \boldsymbol{\Sigma}^{(1)} = \text{simple tension}, \quad \boldsymbol{\Sigma}^{(2)} = \text{pure shear}, \quad \overline{\boldsymbol{\varepsilon}}_t : \boldsymbol{\Sigma}^{(k)} = 5\%.$$

Requires an accurate evolution law for the *amplitudes* ε_k^p *on the modes.*

2nd ingredient : evolution law for the $\varepsilon_k^{\mathsf{p}}$'s

Local fields : Prescribe the macroscopic state variables $\overline{\varepsilon}, (\varepsilon_k^{\mathsf{p}})_{k=1,M}$. Solve :

$$\boldsymbol{\sigma}(x) = \boldsymbol{L}(x) : (\varepsilon(x) - \varepsilon^{\mathsf{p}}(x)), \quad \varepsilon^{\mathsf{p}}(x) = \sum_{k=1}^{M} \varepsilon_k^{\mathsf{p}} \boldsymbol{\mu}^{(k)}(x),$$
$$\operatorname{div}(\boldsymbol{\sigma}(x)) = 0, \quad \langle \varepsilon \rangle = \overline{\varepsilon}, \quad + \text{B.C. (periodicity)}.$$

Linear (thermoelastic) problem $\Rightarrow$ superposition :

$$\begin{aligned} \varepsilon(x,t) &= \boldsymbol{A}(x) : \overline{\varepsilon}(t) + \sum_{k=1}^{M} \boldsymbol{D} * \boldsymbol{\mu}^{(k)}(x) \varepsilon_k^{\mathsf{p}} \\ \boldsymbol{\sigma}(x,t) &= \boldsymbol{L}(x) : \boldsymbol{A}(x) : \overline{\varepsilon}(t) + \sum_{k=1} \boldsymbol{\rho}^{(k)}(x) \varepsilon_k^{\mathsf{p}}(t), \end{aligned}$$

- $\boldsymbol{A}(x)$ **elastic strain-localization tensor**
- $\boldsymbol{D}$ Green's operator, $\boldsymbol{D} * \boldsymbol{\mu}^{(k)}(x)$ **influence tensors**.
- $\boldsymbol{\rho}^{(k)}(x) = \boldsymbol{L}(x) : \left(\boldsymbol{D} * \boldsymbol{\mu}^{(k)}(x) - \boldsymbol{\mu}^{(k)}(x) \right)$.

Local fields σ, ε **depend LINEARLY on** $\overline{\varepsilon}$ **and** $\varepsilon_k^{\mathsf{p}}|_{k=1,\ldots,M}$.

Constitutive relations for the macroscopic state variables $\varepsilon^{\mathsf{p}}_k|_{k=1,M}$'s

More easily expressed in terms of the **reduced variables :**

$$\tau_k = \left\langle \boldsymbol{\mu}^{(k)} : \boldsymbol{\sigma} \right\rangle, \quad e_k = \left\langle \boldsymbol{\mu}^{(k)} : \boldsymbol{\varepsilon} \right\rangle, \quad e^{\mathsf{p}}_k = \left\langle \boldsymbol{\mu}^{(k)} : \boldsymbol{\varepsilon}^{\mathsf{p}} \right\rangle = \left\langle \boldsymbol{\mu}^{(k)} : \boldsymbol{\mu}^{(k)} \right\rangle \varepsilon^{\mathsf{p}}_{k.}$$

$$\dot{\boldsymbol{\sigma}}(\boldsymbol{x}) = \boldsymbol{L}^{(r)} : (\dot{\boldsymbol{\varepsilon}} - \dot{\boldsymbol{\varepsilon}}^{\mathsf{p}}) \quad \Rightarrow \quad \boxed{\dot{\tau}_k = 2G^{(r)}(\dot{e}_k - \dot{e}^{\mathsf{p}}_k)},$$

$$\boldsymbol{\varepsilon}(\boldsymbol{x}) = \boldsymbol{A}(\boldsymbol{x}) : \overline{\boldsymbol{\varepsilon}} + \sum_{k=1}^{M} \boldsymbol{D} * \boldsymbol{\mu}^{(k)}(\boldsymbol{x}) \varepsilon^{\mathsf{p}}_k \quad \Rightarrow \quad \boxed{\dot{e}_k = \boldsymbol{a}_k : \dot{\overline{\boldsymbol{\varepsilon}}} + \sum_{\ell=1}^{M} D_{k\ell}\, \dot{\varepsilon}^{\mathsf{p}}_{\ell},}$$

$$\boldsymbol{a}_k = \left\langle \boldsymbol{\mu}^{(k)} : \boldsymbol{A} \right\rangle, \quad D_{k\ell} = \left\langle \boldsymbol{\mu}^{(k)} : (\boldsymbol{D} * \boldsymbol{\mu}^{(\ell)}) \right\rangle$$

$$\dot{e}^{\mathsf{p}}_k = \left\langle \boldsymbol{\mu}^{(k)} : \dot{\boldsymbol{\varepsilon}}^{\mathsf{p}} \right\rangle = \frac{3}{2} \left\langle \frac{\partial \psi}{\partial \sigma_{\mathsf{eq}}}(\sigma_{\mathsf{eq}}) \frac{\boldsymbol{\mu}^{(k)} : \boldsymbol{\sigma}^{\mathsf{dev}}}{\sigma_{\mathsf{eq}}} \right\rangle \simeq \boxed{\frac{3}{2} \frac{\partial \psi^{(r)}}{\partial \sigma_{\mathsf{eq}}}(\tau^r_{\mathsf{eq}}) \frac{\tau_k}{\tau^r_{\mathsf{eq}}}}$$

Approximation : σ_{eq} approximated by $\tau^r_{\mathsf{eq}} = \left(\sum_{k=1}^{M(r)} (\tau_k)^2 \right)^{1/2} \Rightarrow$

Ordinary differential equations : $\boxed{\dot{\tau}_k = F(\{\tau\}_\ell, \dot{\overline{\boldsymbol{\varepsilon}}})}$ or equivalently $\boxed{\dot{\varepsilon}^{\mathsf{p}}_k = G(\{\varepsilon^{\mathsf{p}}\}_\ell, \dot{\overline{\boldsymbol{\varepsilon}}}).}$

4. Implementation and examples

A. Effective constitutive relations :

1. **Do once for all :**
   - **Select plastic modes $\mu^{(k)}$** on the unit-cell. $\boldsymbol{\mu}^{(k)} \equiv$ extracted **(Karhunen-Loeve)** from computational results for representative loadings on the unit-cell only...
   - **Compute several tensors representing the elastic interactions between modes. Linear elasticity problems** to be solved once for all.

2. **Simulation of the response of a macroscopic material point**

$$\overline{\boldsymbol{\sigma}}(t) = \langle \boldsymbol{\sigma} \rangle = \widetilde{\boldsymbol{L}} : \overline{\boldsymbol{\varepsilon}}(t) + \sum_{k=1}^{M} \left\langle \boldsymbol{\rho}^{(k)} \right\rangle \varepsilon_k^{\mathsf{p}}(t), \quad \dot{\varepsilon}_k^{\mathsf{p}}(t) = G(\{\varepsilon^{\mathsf{p}}\}_\ell(t), \dot{\overline{\boldsymbol{\varepsilon}}}(t)),$$

B. Structural problems :

- **Incorporate the NTFA constitutive equations in a FEM code (internal variables).**
- **fields (post-processing) :**

$$
\begin{aligned}
\boldsymbol{\varepsilon}^{\mathsf{p}}(\boldsymbol{x},t) &= \sum_{k=1}^{M} \varepsilon_k^{\mathsf{p}}(t)\, \boldsymbol{\mu}^{(k)}(\boldsymbol{x}), \\
\boldsymbol{\varepsilon}(\boldsymbol{x},t) &= \boldsymbol{A}(\boldsymbol{x}) : \overline{\boldsymbol{\varepsilon}}(t) + \sum_{k=1}^{M} \boldsymbol{D} * \boldsymbol{\mu}^{(k)}(\boldsymbol{x}) \varepsilon_k^{\mathsf{p}} \\
\boldsymbol{\sigma}(\boldsymbol{x},t) &= \boldsymbol{L}(\boldsymbol{x}) : \boldsymbol{A}(\boldsymbol{x}) : \overline{\boldsymbol{\varepsilon}}(t) + \sum_{k=1}^{M} \boldsymbol{\rho}^{(k)}(\boldsymbol{x}) \varepsilon_k^{\mathsf{p}}(t),
\end{aligned}
$$

where $\boldsymbol{\rho}^{(k)}(\boldsymbol{x}) = \boldsymbol{L}(\boldsymbol{x}) : \left(\boldsymbol{D} * \boldsymbol{\mu}^{(k)}\right)(\boldsymbol{x}) - \boldsymbol{L}(\boldsymbol{x}) : \boldsymbol{\mu}^{(k)}(\boldsymbol{x}).$

LINEAR localization relations !

1. MoX : effective constitutive relations

Full-Field simulations. Monodisperse, polydisperse ? How many phases, 2, 3 ?

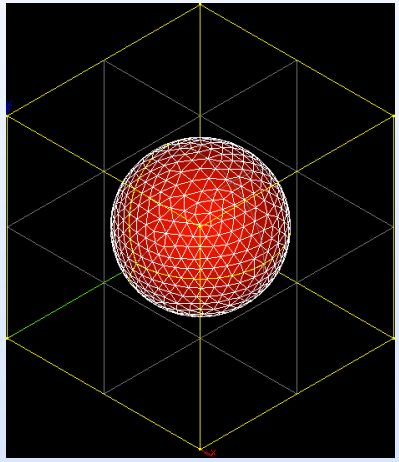
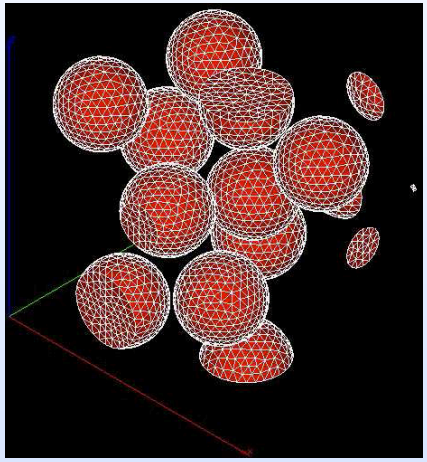
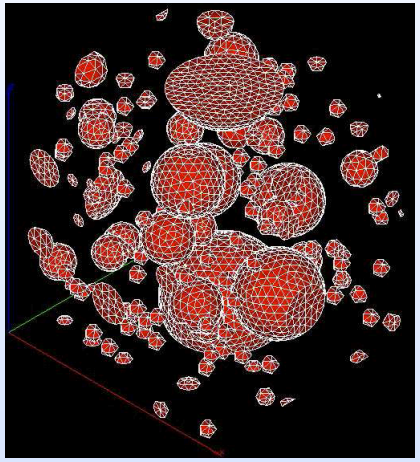
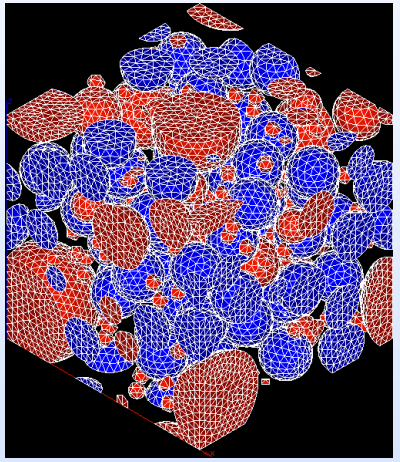

2-phase	E (GPa)	ν (-)	μ (GPa.s)
Pu clusters	200	0.3	21.43
Matrix	200	0.3	64.30

3-phase	E (GPa)	ν (-)	μ (GPa.s)
Pu clusters	200	0.3	21.43
U clusters	200	0.3	158.83
Matrix	200	0.3	52.94

3rd phase does matter !

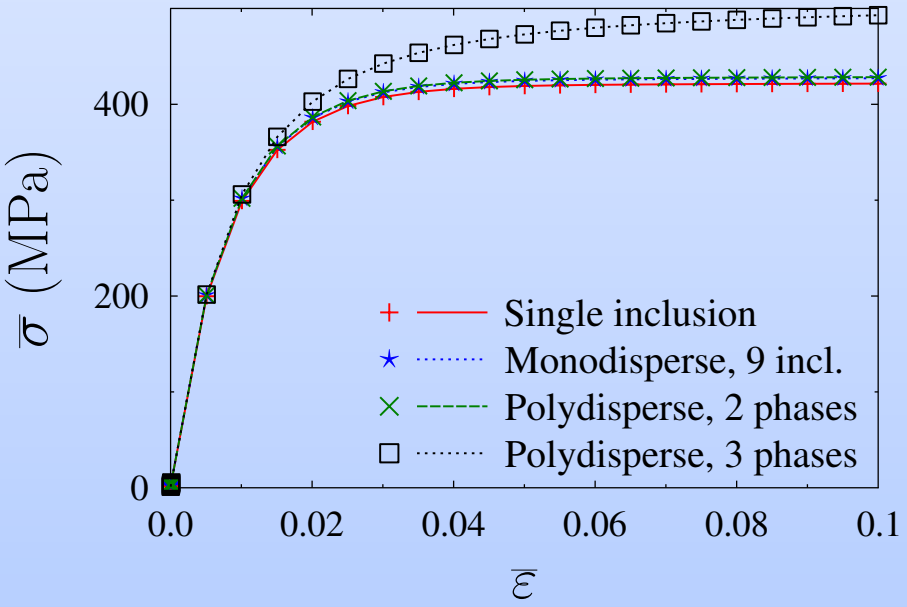

Which polydisperse, 3-phase, microstructure ?

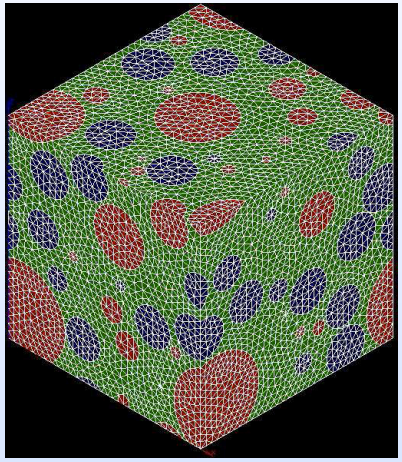

VER

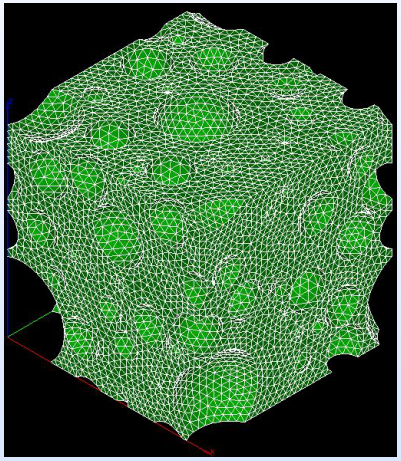

Matrix

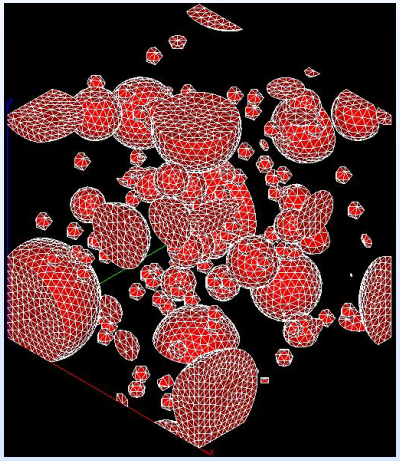

Pu clusters

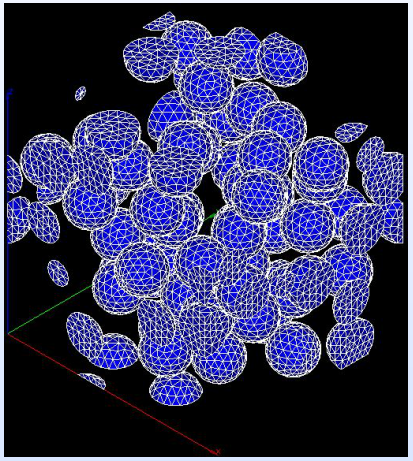

U clusters

8 different configurations

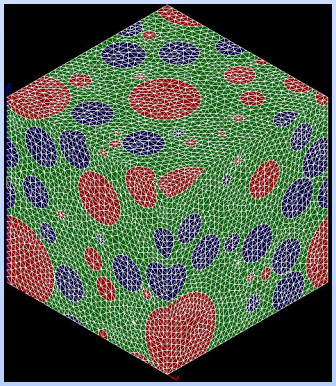

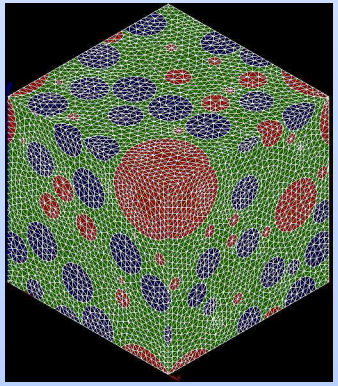

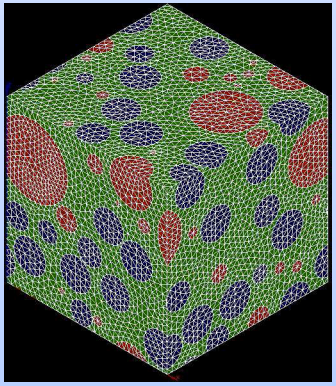

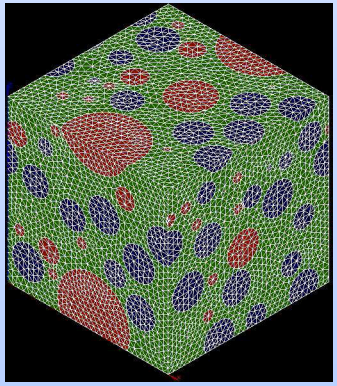

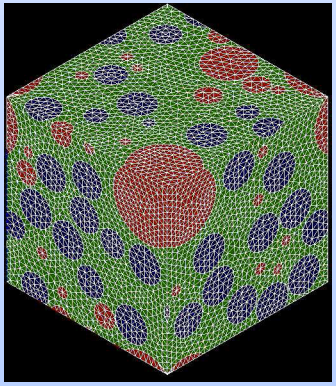

.....

Is the volume element representative ?

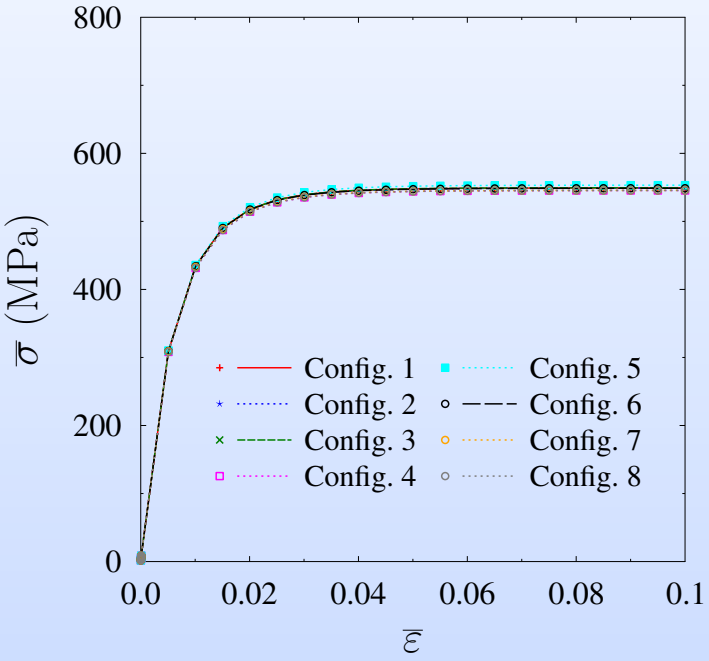

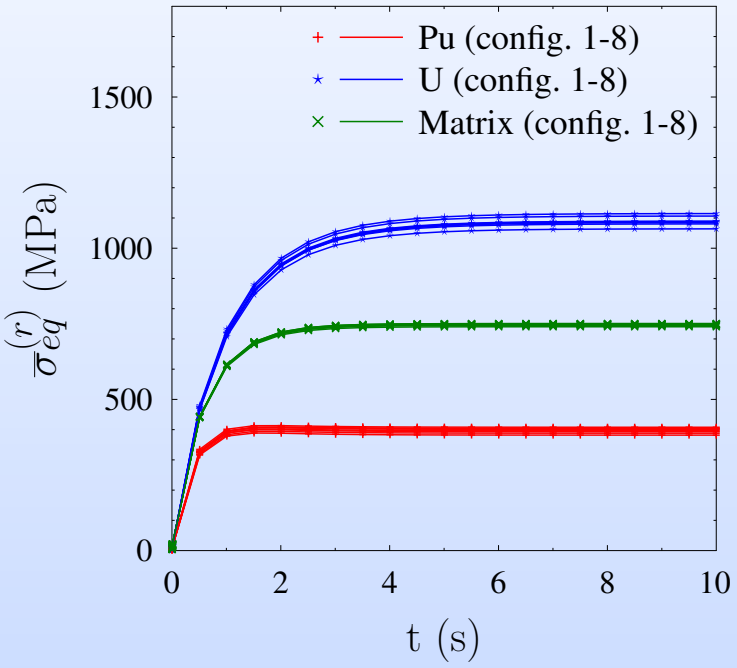

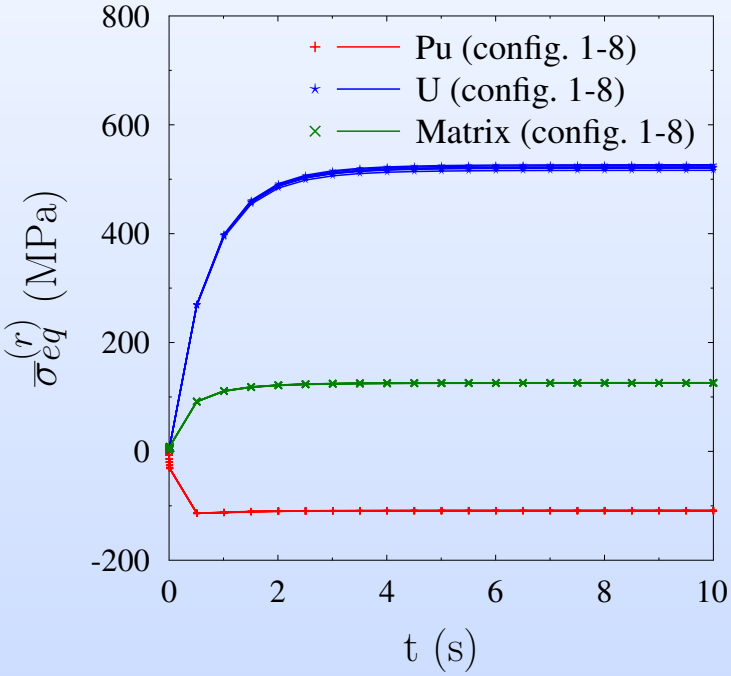

Effective response

$\overline{\sigma}$

Average per phase

$\overline{\sigma}_{\mathrm{eq}}^{(r)}$

Average per phase

$\overline{\sigma}_{\mathrm{m}}^{(r)}$

1 configuration is enough !

NTFA. Mode Selection (Karhunen-Loeve)

Modes $\boldsymbol{\mu}^{(k)}$'s generated from **pre-computed plastic strain-fields along "well-chosen" elementary loading directions (relevant to the problem at hand) on the unit-cell**

- **Numerical simulations** of the response of the RVE along 7 elementary loading paths :

$$\boldsymbol{\Sigma}_0^{(1)} = \boldsymbol{e}_1 \otimes_s \boldsymbol{e}_1 \text{ (uniaxial tension)}, \ \boldsymbol{\Sigma}_0^{(2)} = \boldsymbol{e}_1 \otimes_s \boldsymbol{e}_2 \text{ (pure shear)...}, \boldsymbol{\varepsilon}^{swelling} = \boldsymbol{0},$$

$$\boldsymbol{\Sigma}_0^{(7)} = 0, \quad \boldsymbol{\varepsilon}^{swelling} = f^{(r)}\boldsymbol{i} \quad \text{in phase } r.$$

- **Select snapshots** $\boldsymbol{\theta}^{(i)}$ of the anelastic strain field (25 snapshots for each loading path here).

$$\boldsymbol{\mu}^{(k)}(\boldsymbol{x}) = \sum_{k=1}^{M_T} v_\ell^{(k)} \boldsymbol{\theta}^{(\ell)}(\boldsymbol{x}),$$

- where $v^{(k)}$ **eigenvectors of the correlation matrix :**

$$\sum_{j=1}^{M_T} g_{ij} v_j^{(k)} = \lambda_k v_i^{(k)}, \quad g_{ij} = \left\langle \boldsymbol{\theta}^{(i)} : \boldsymbol{\theta}^{(j)} \right\rangle,$$
$$\left\langle \boldsymbol{\mu}^{(k)} : \boldsymbol{\mu}^{(\ell)} \right\rangle = 0 \quad k \neq \ell, \quad \left\langle \boldsymbol{\mu}^{(k)} : \boldsymbol{\mu}^{(k)} \right\rangle = \lambda_k$$

- **Extract the modes corresponding to a specified information content.** 10^{-4} here.

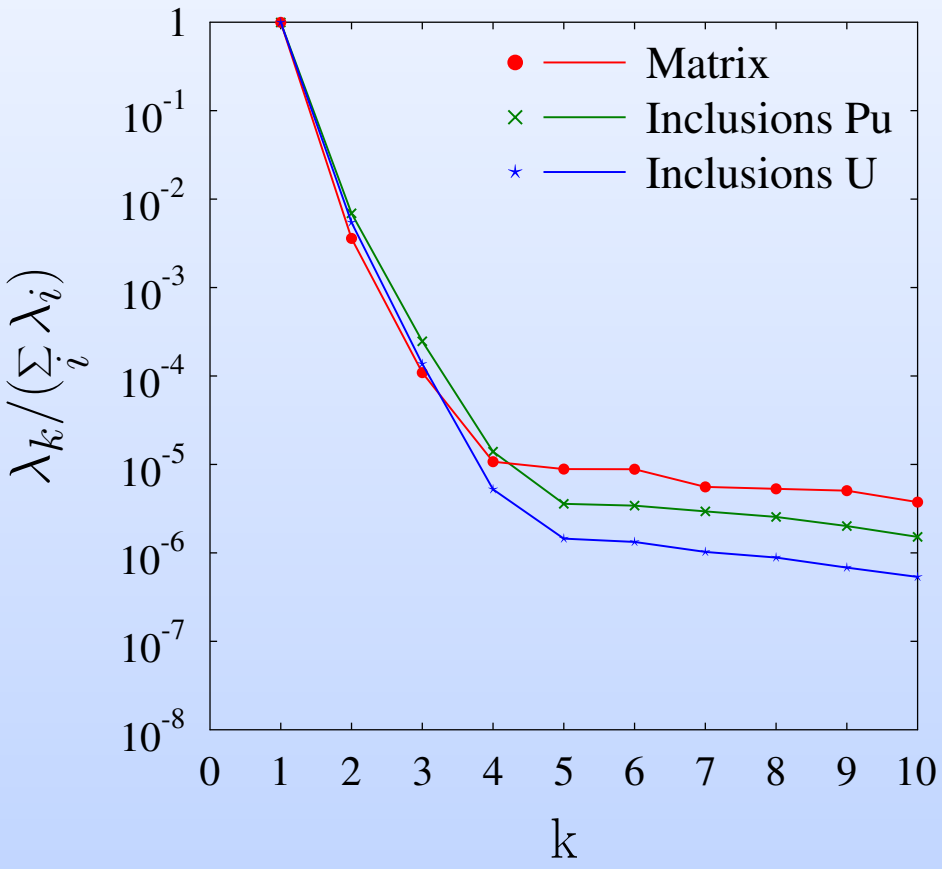

Linear matrix $n = 1$

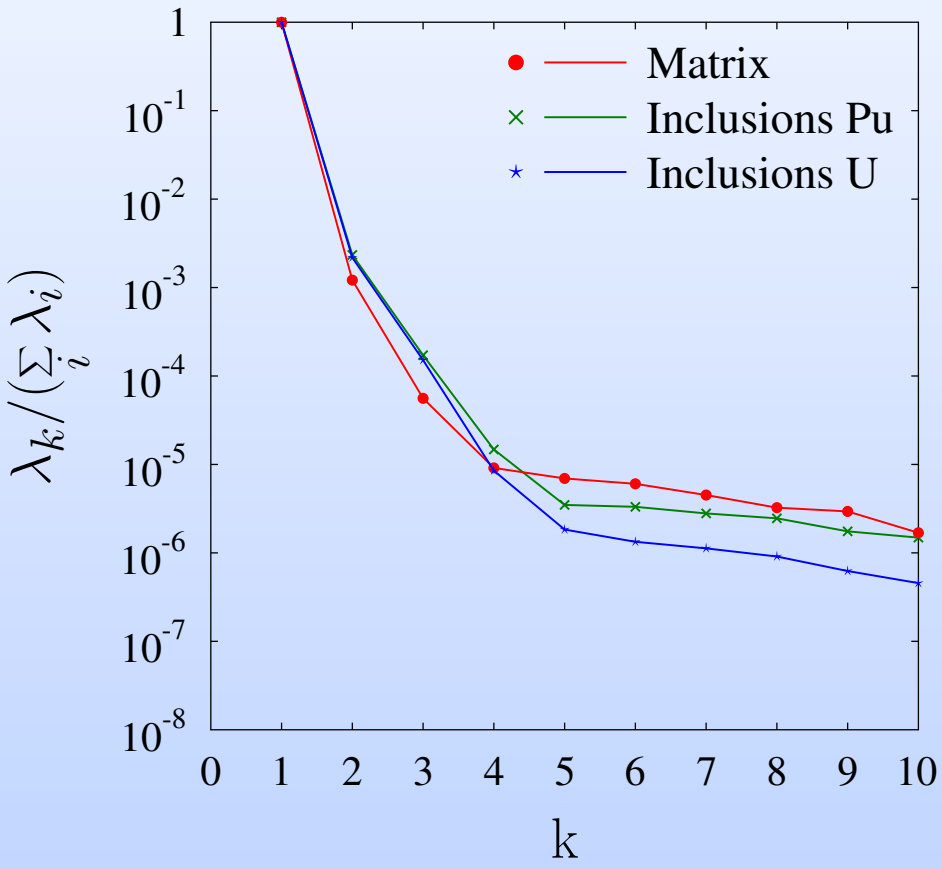

Nonlinear matrix $n = 4$

Modes

Mode 1

Mode 2

Mode 3

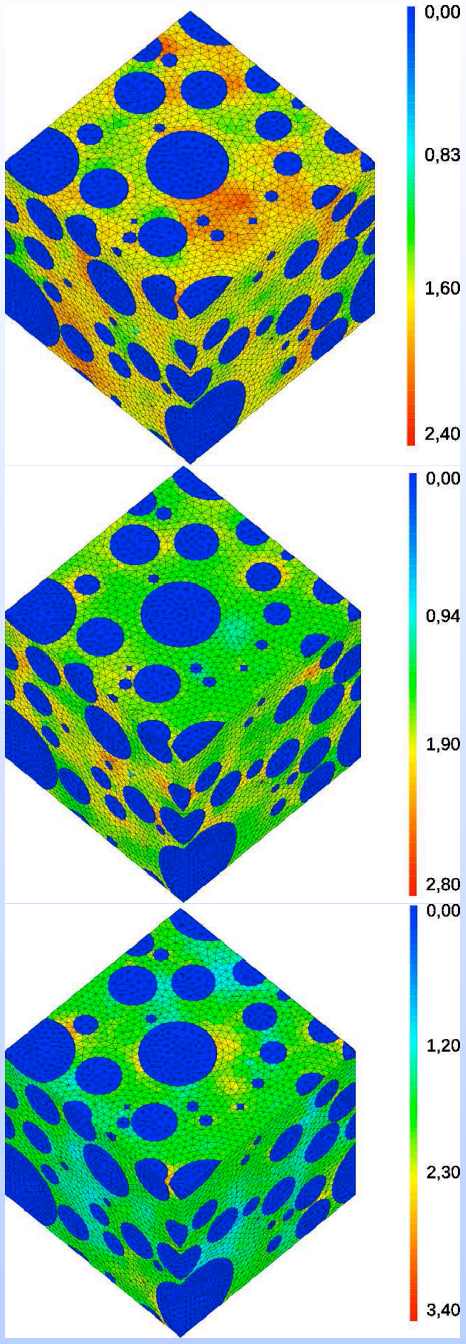

Matrix

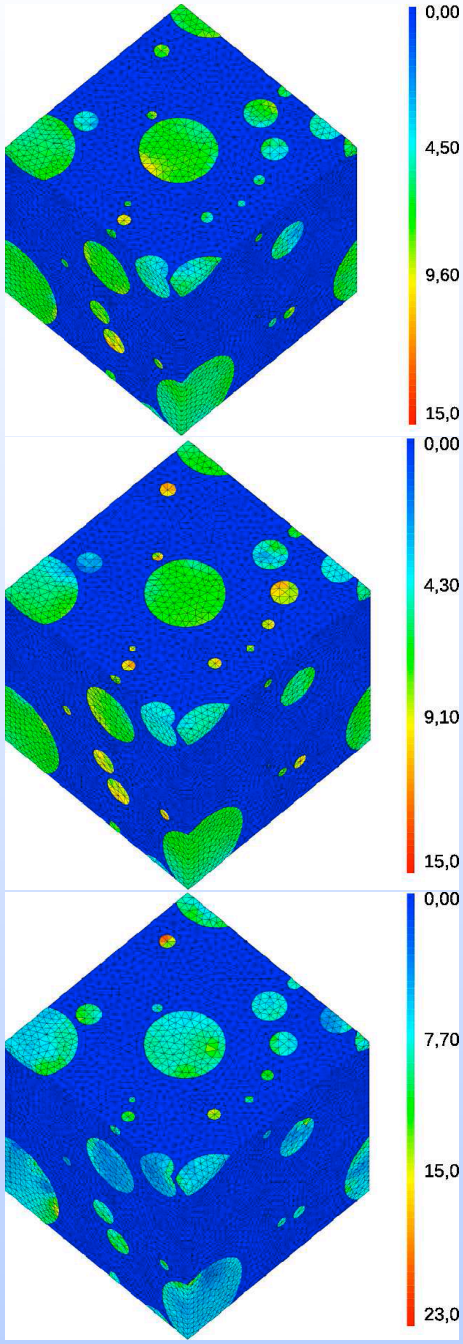

Pu clusters

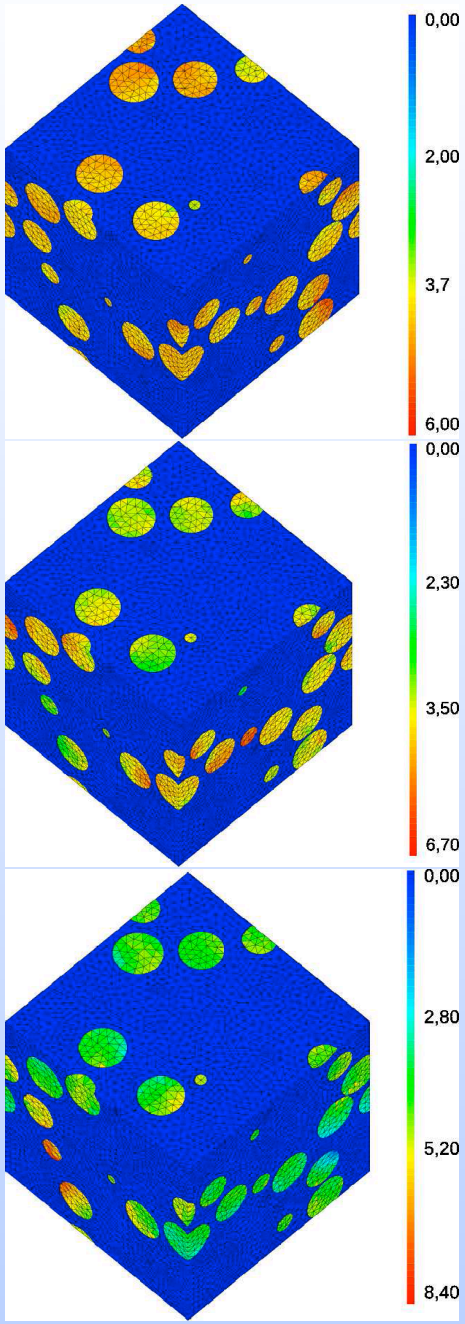

U clusters

Complex loading (tension+shear) with rotation of principal axes

$$\overline{\varepsilon}_{11}(t) = 10^{-1} \sin \omega t,$$

$$\overline{\varepsilon}_{12}(t) = 10^{-1}(1 - \cos \omega t).$$

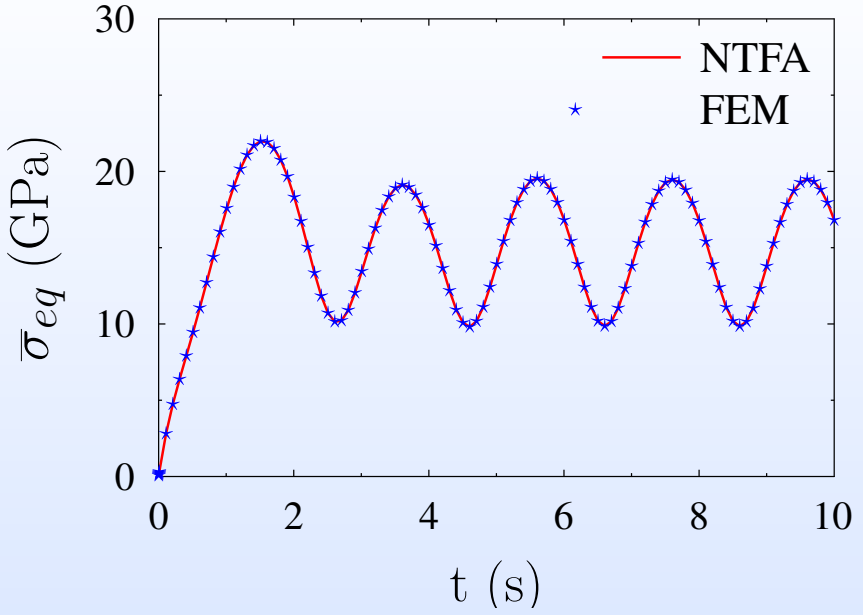

Effective response

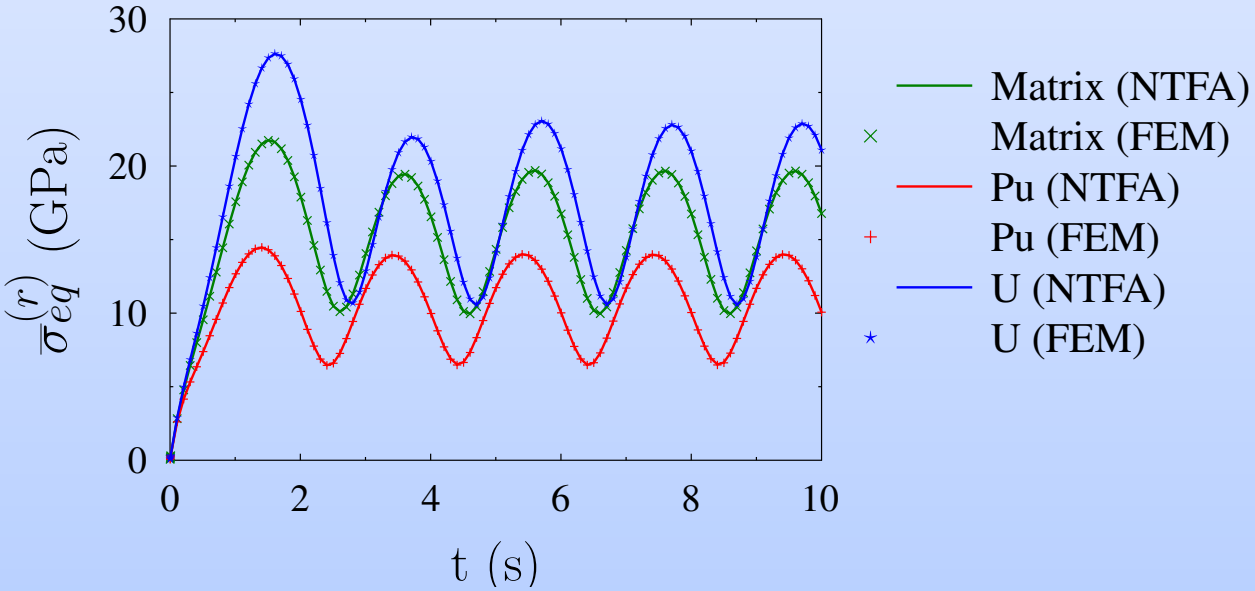

Average per phase $\overline{\sigma}^{(r)}_{\mathrm{eq}}$

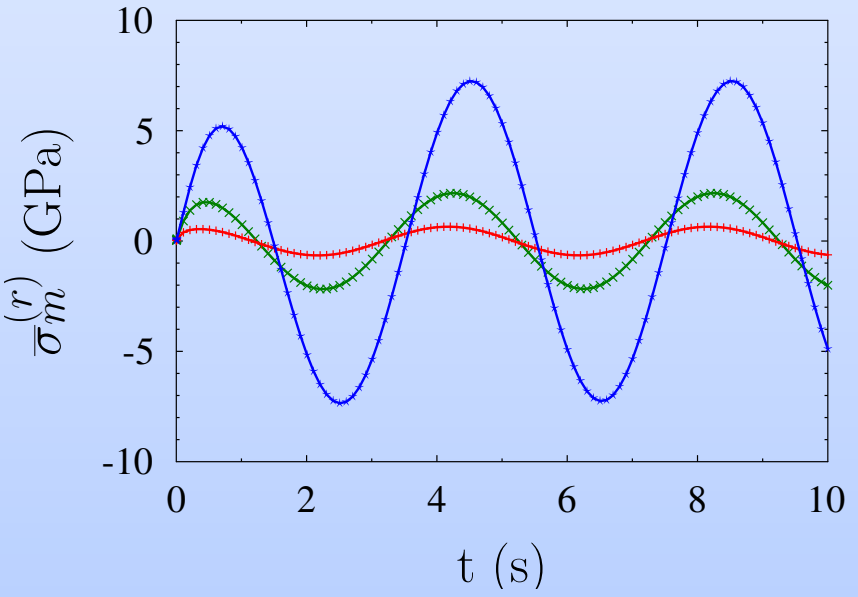

Average per phase $\overline{\sigma}^{(r)}_{\mathrm{m}}$

Aging materials

Time-dependent viscosities (bulk and shear) k_v, μ_v in Pu.

Modes computed once for all.

Loading (tension+shear) at constant strain-rate + swelling.

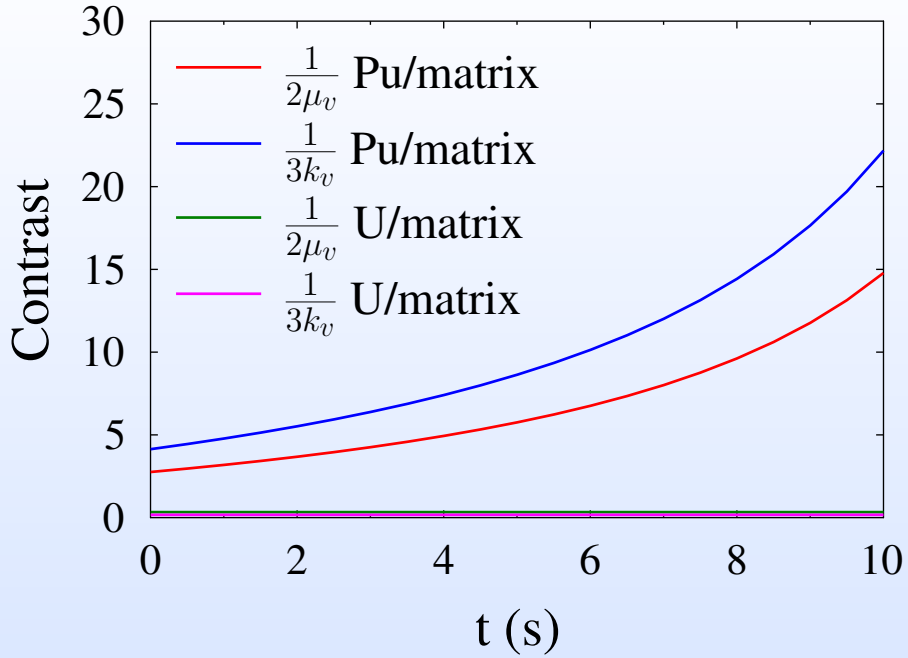

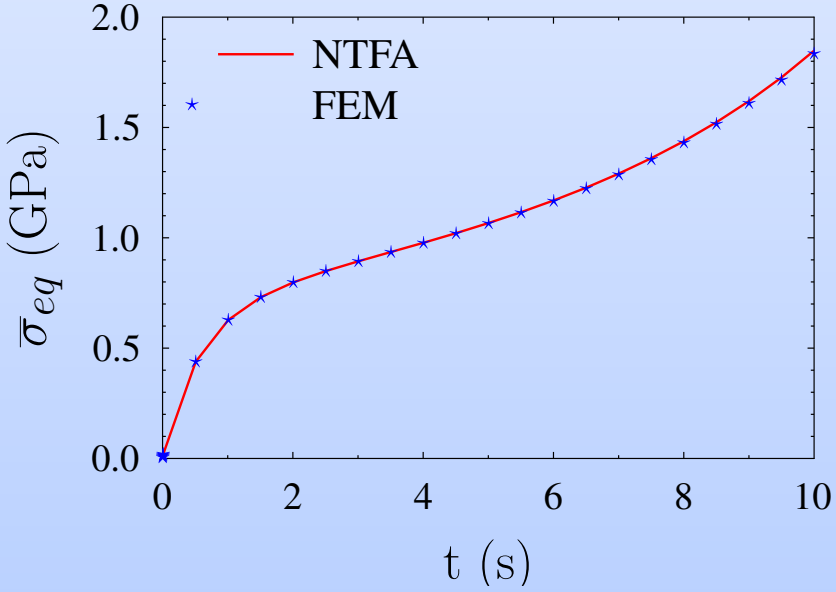

Effective response

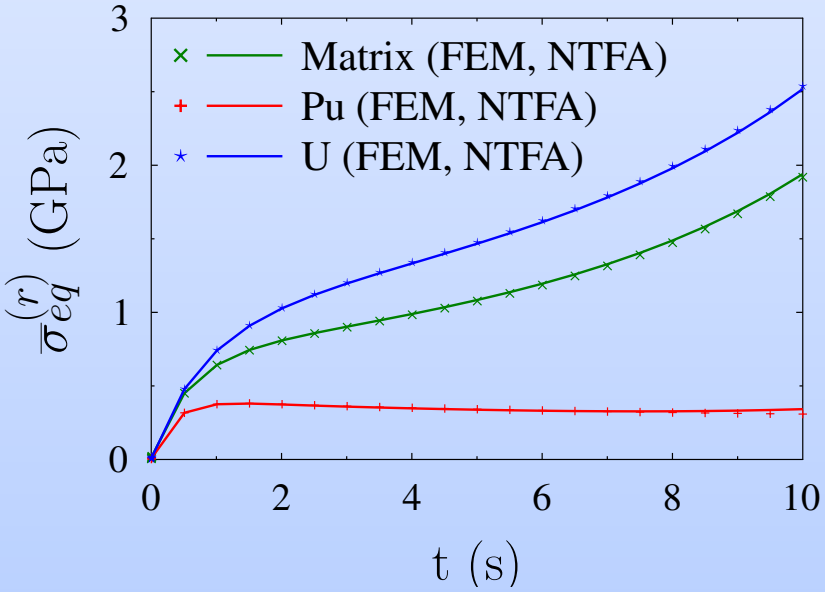

Average per phase

Matrix

Pu

U

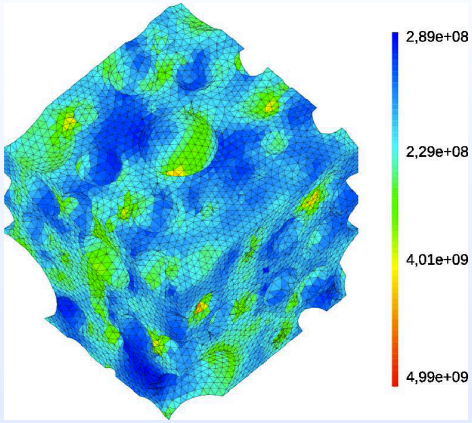

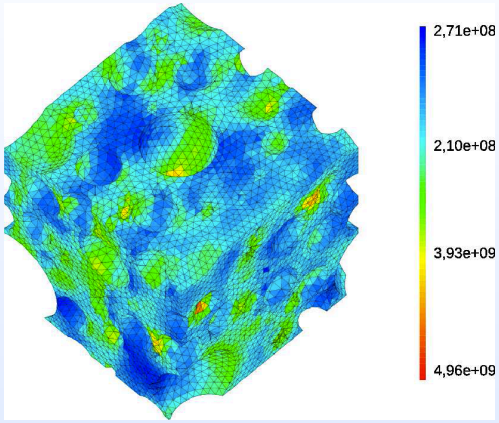

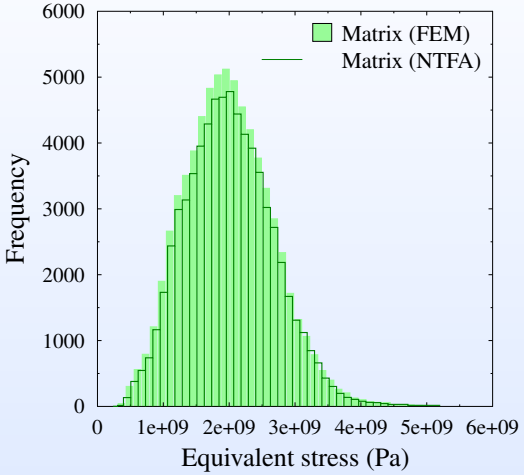

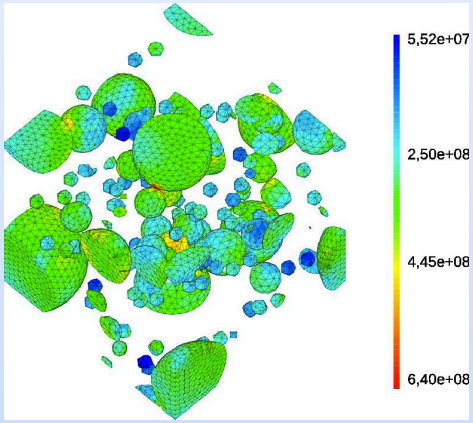

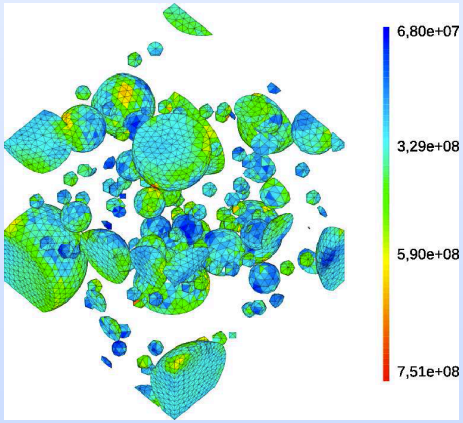

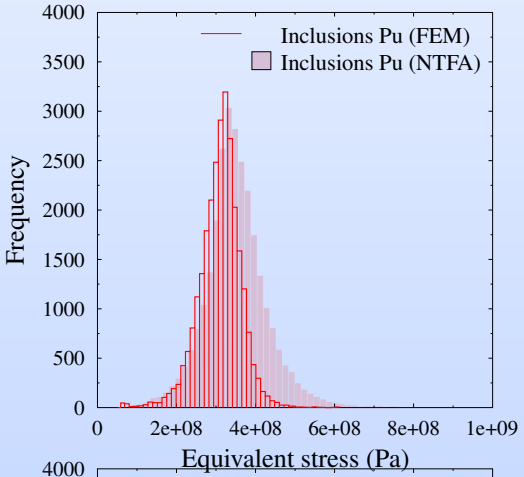

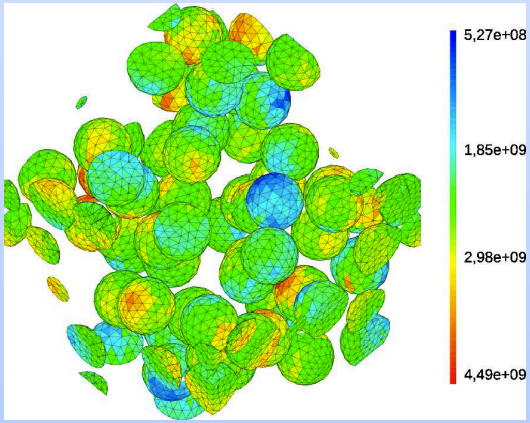

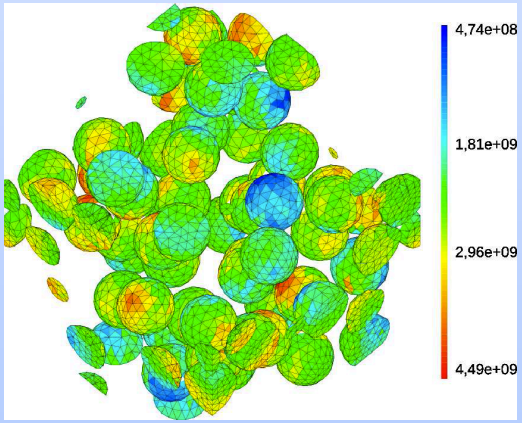

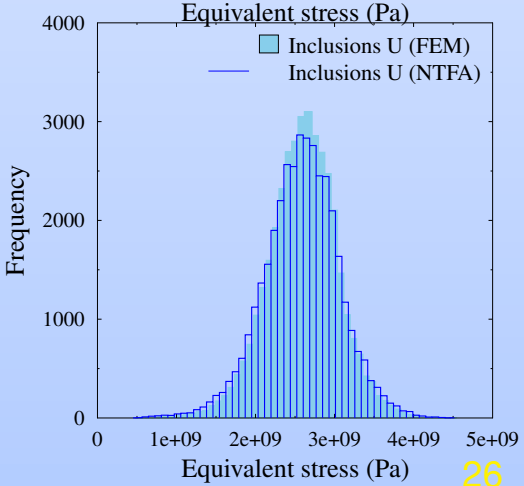

FEM

NTFA

2. Structural problem

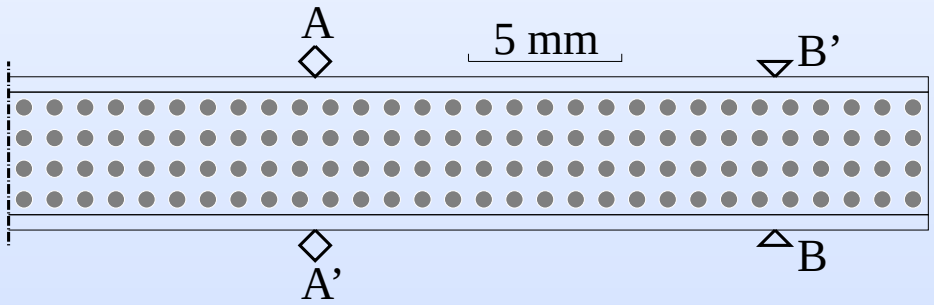

Geometry.

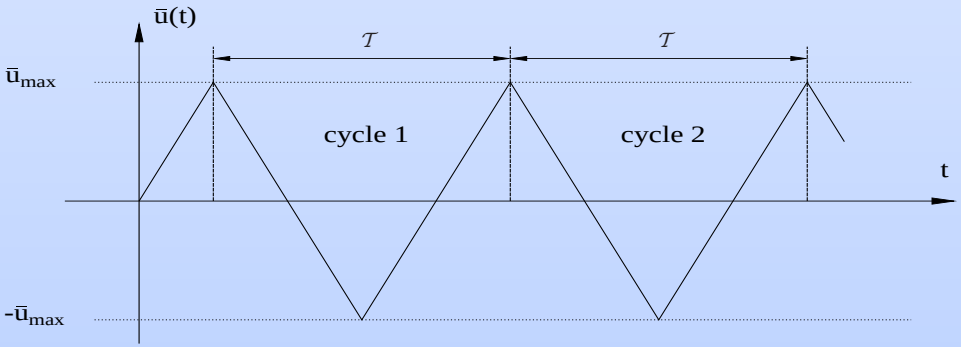

Loading :

Meshes

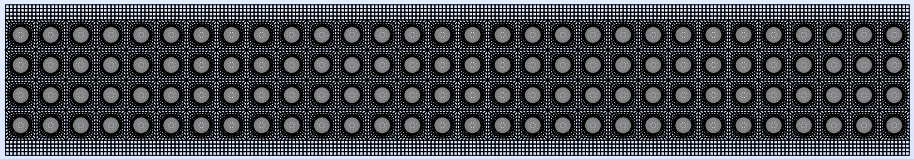

Full-field

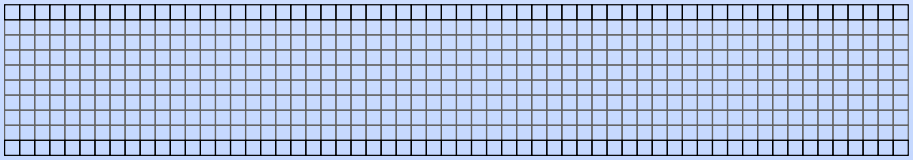

NTFA

Modes

- **Plane problem : 3 directions of macroscopic stress :** horizontal tension, transverse shear, vertical tension.
- **Pre-computations with loading-unloading cycles :**

  For each loading case $\overline{\varepsilon}(t)$ along the applied stress cycled between ± 0.0025,

  $$\dot{\overline{\varepsilon}} = \pm 10^{-3}\ \mathrm{s}^{-1}.$$

  $\theta^{(i)}$: plastic strain field at every quarter of each cycle.
- **5 Karhunen-Loeve modes are generated.**

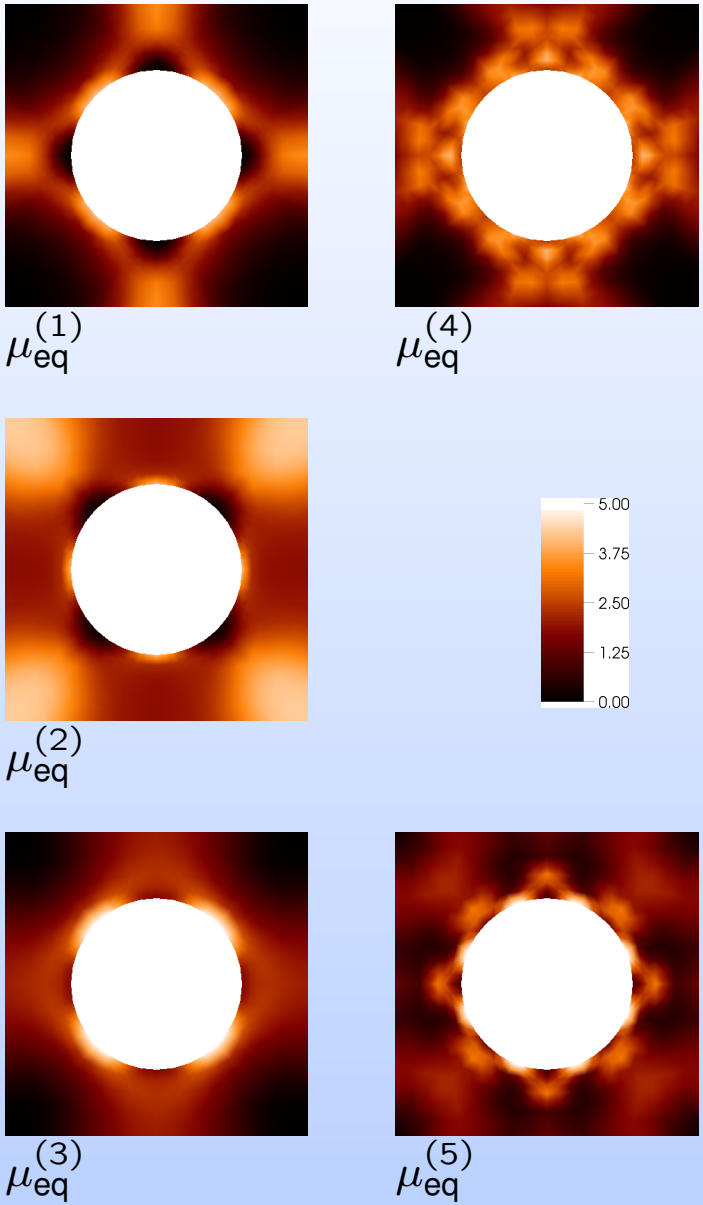

Material response (unit-cell level)

Macroscopic stress-strain response

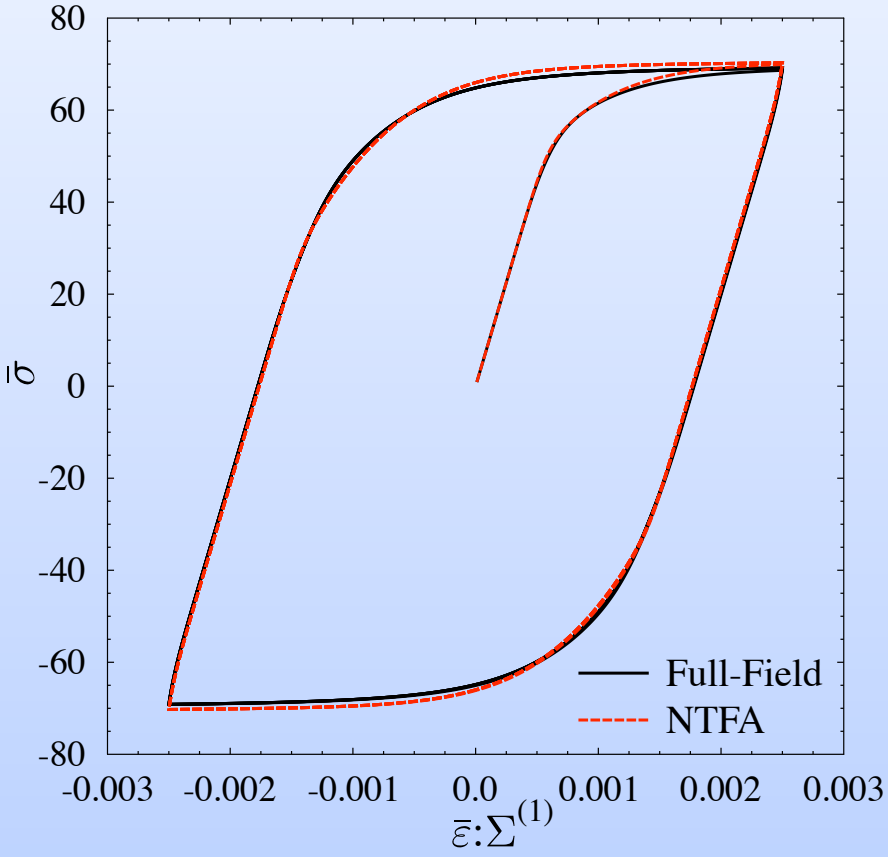

Uniaxial tension

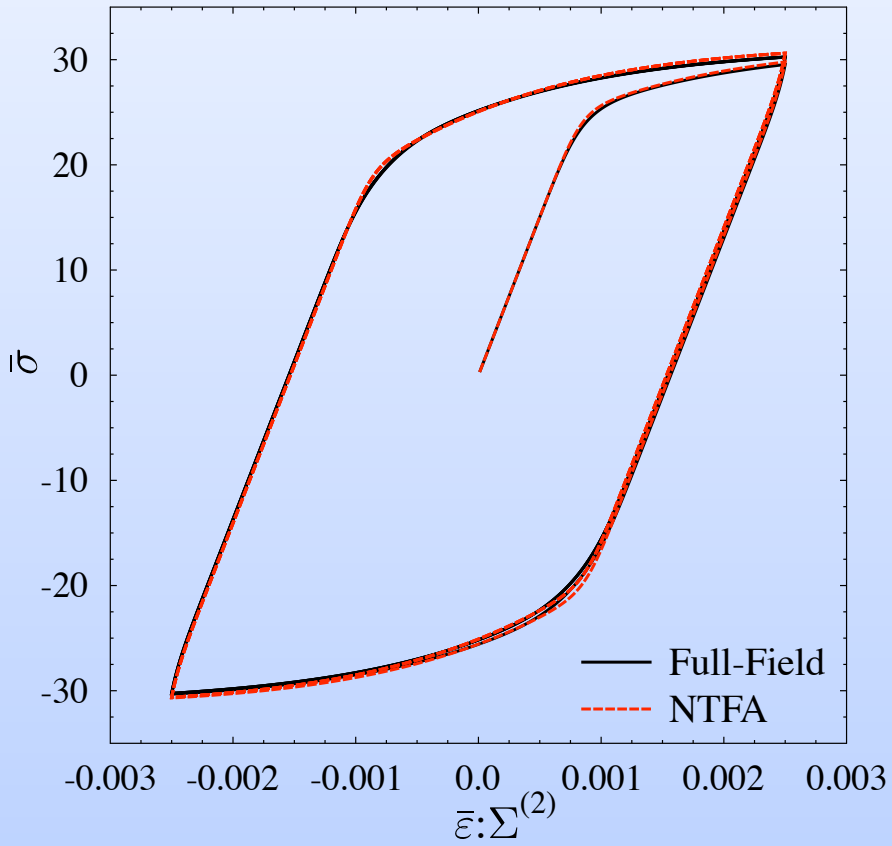

Shear

Snapshot of the energy dissipated along the stabilized cycle (unit-cell)

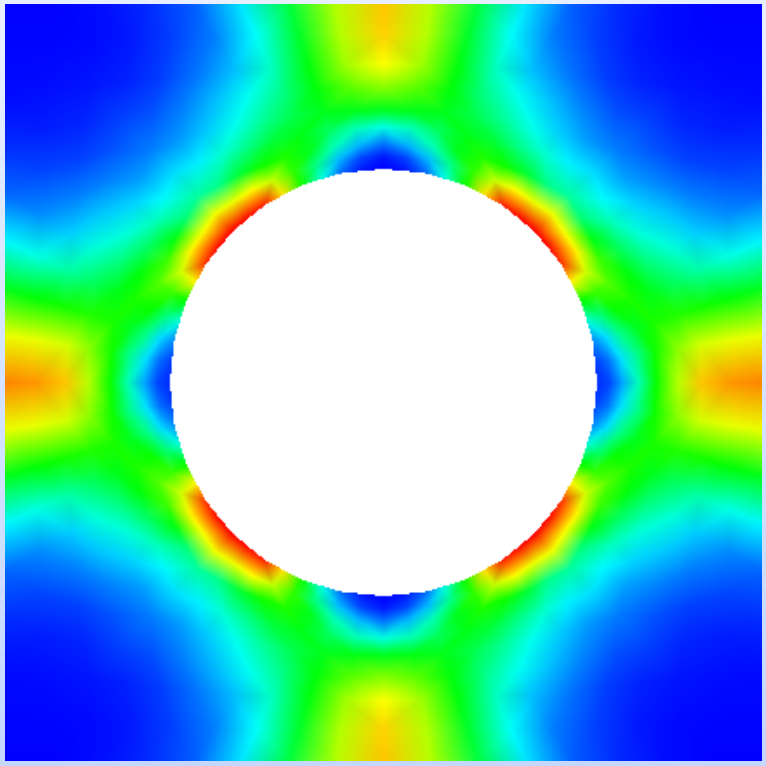

Reference FEM

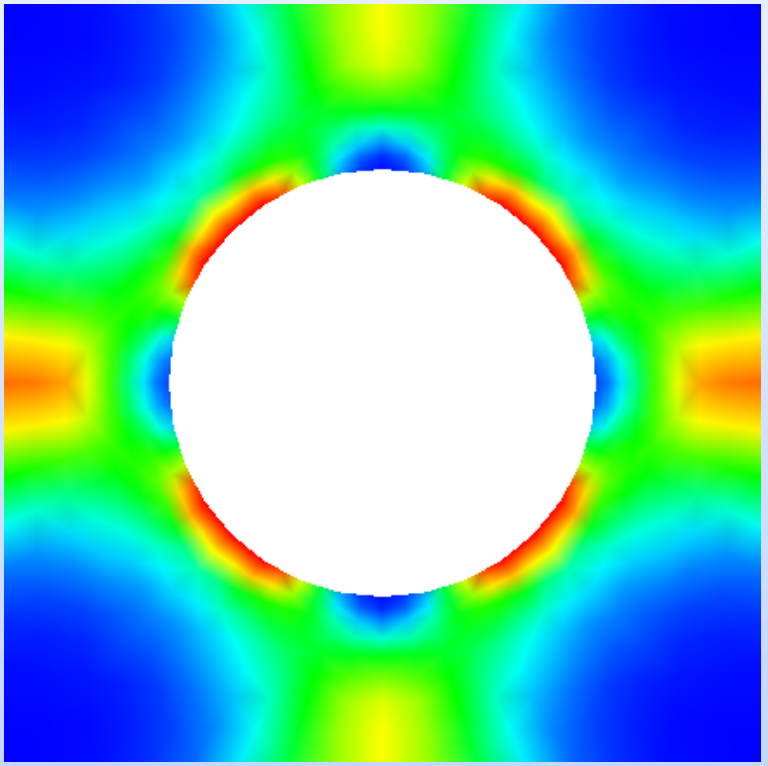

NTFA

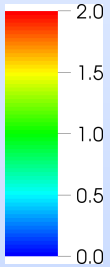

Structural response (entire beam)

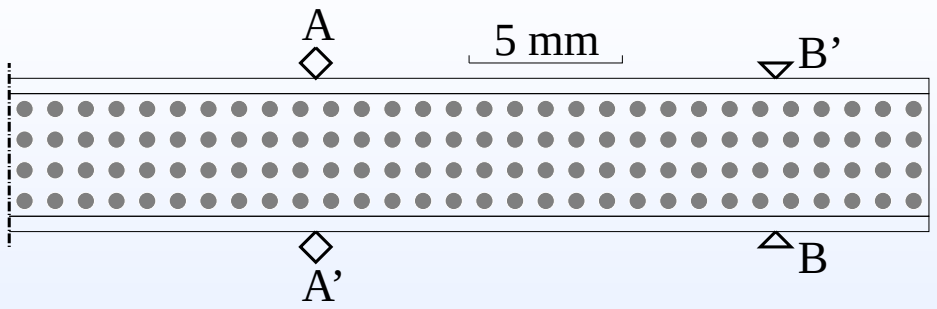

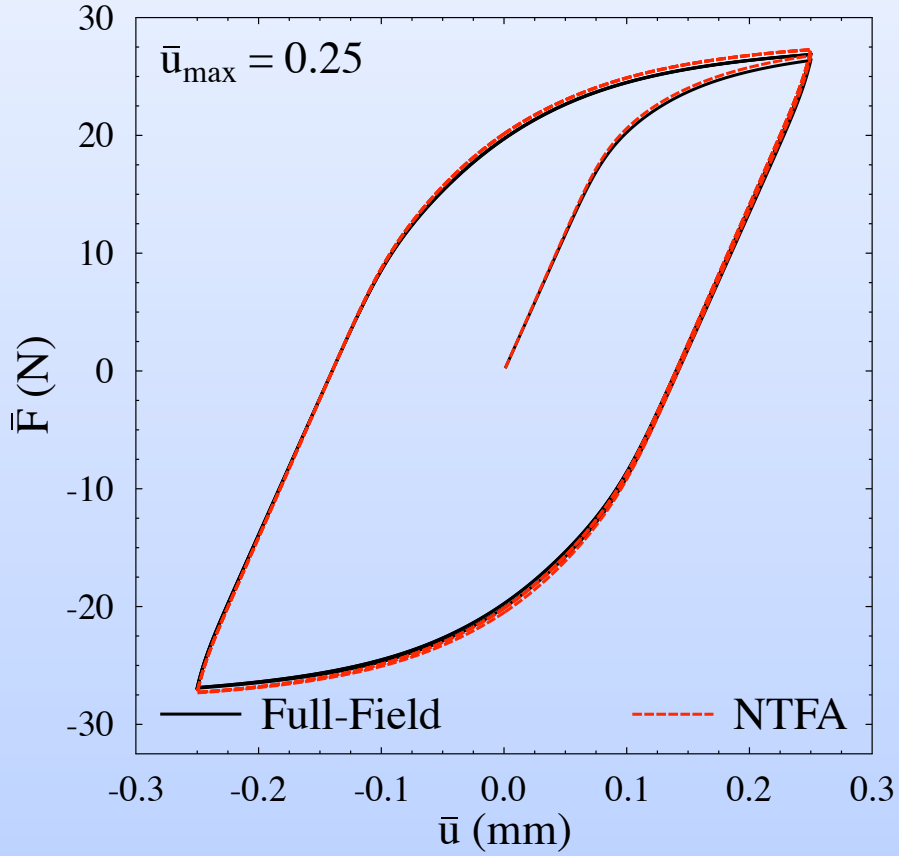

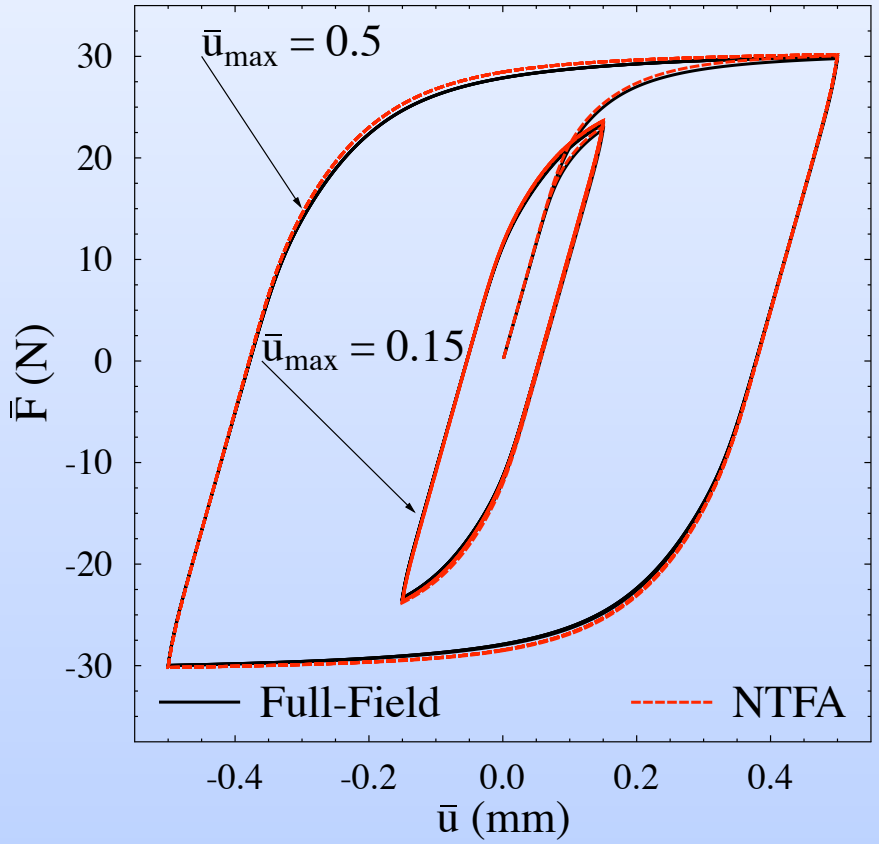

Force/displacement at points A, A'

Local stress fields

$$\boldsymbol{\sigma}(\boldsymbol{X},t) = \boldsymbol{L}(\boldsymbol{x}) : \boldsymbol{A}(\boldsymbol{x}) : \overline{\boldsymbol{\varepsilon}}(\boldsymbol{X},t) + \sum_{k=1}^{M} \boldsymbol{\rho}^{(k)}(\boldsymbol{x}) \varepsilon_k^{\mathrm{p}}(\boldsymbol{X},t), \quad \boldsymbol{x} = \frac{\boldsymbol{X}}{\varepsilon}.$$

$\boldsymbol{X}$ = macroscopic variable (structure), $\boldsymbol{x}$ microscopic variable (unit-cell).

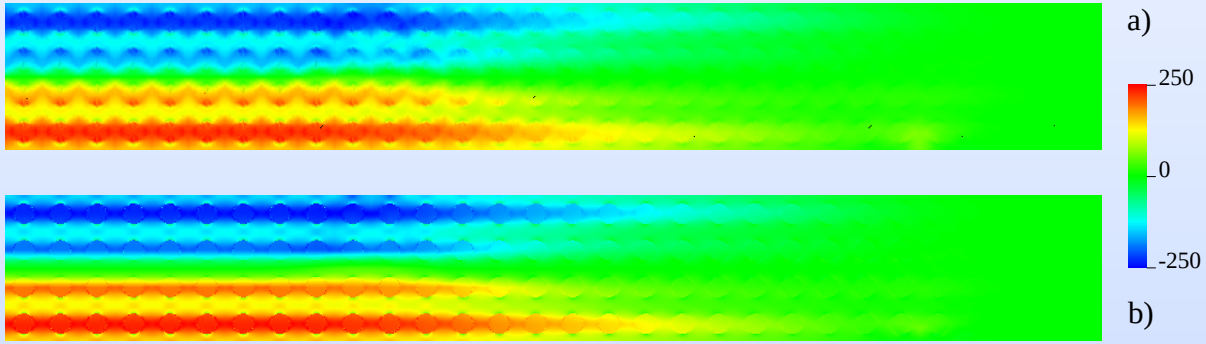

- a) σ_{11} Exact.
- b) σ_{11} Re-localized stress field from the reduced computation.

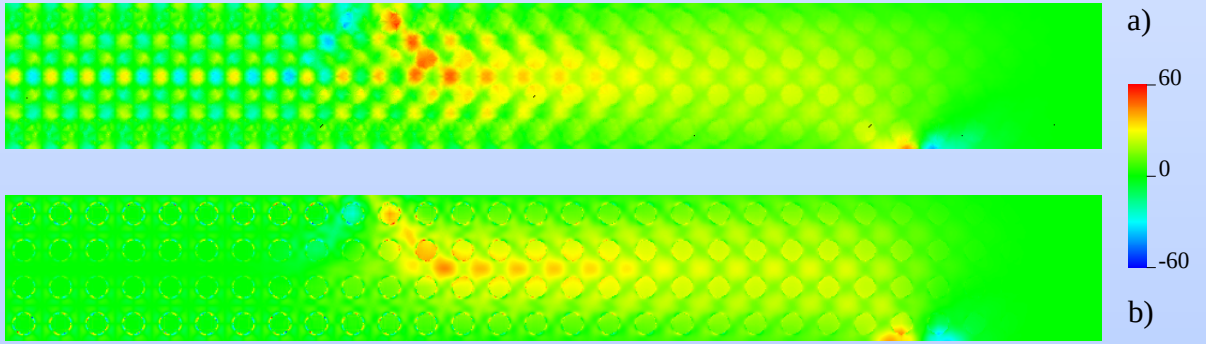

- a) σ_{12} Exact.
- b) σ_{12} Re-localized stress field from the reduced computation.

Post-processing of the computation with homogenized model only !

Snapshot of the energy dissipated along the stabilized cycle

Michel, Suquet, IC Press 2007

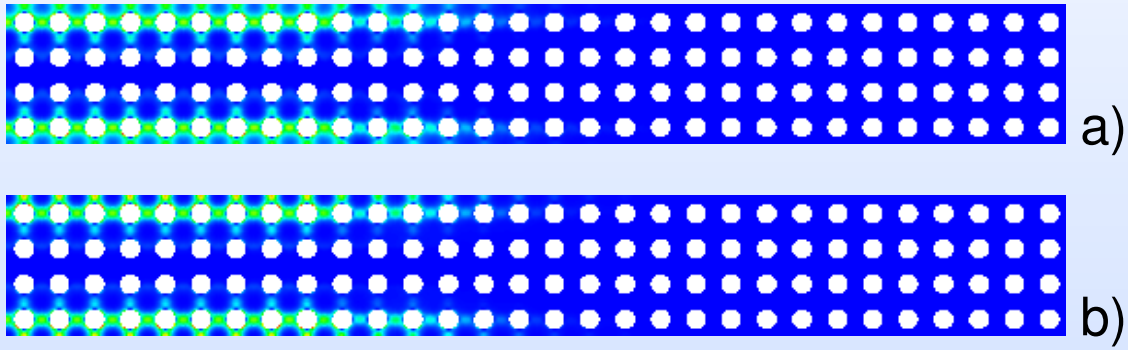

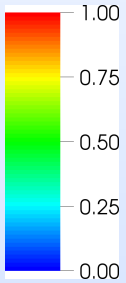

a) Full-Field

b) NTFA + Relocalization

$\overline{u}_{\max}$= 0.25 mm

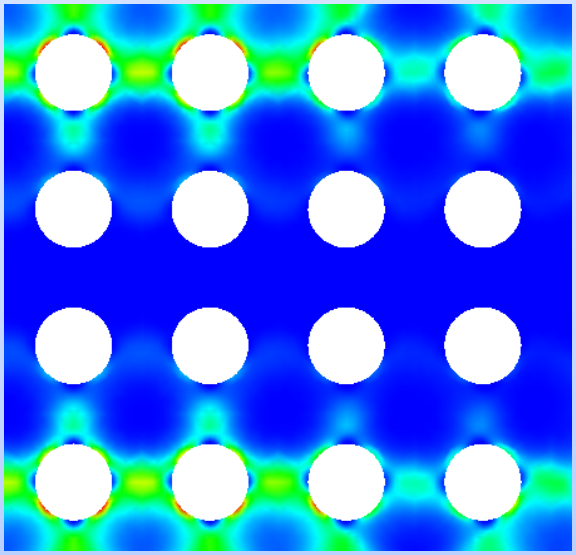
a)

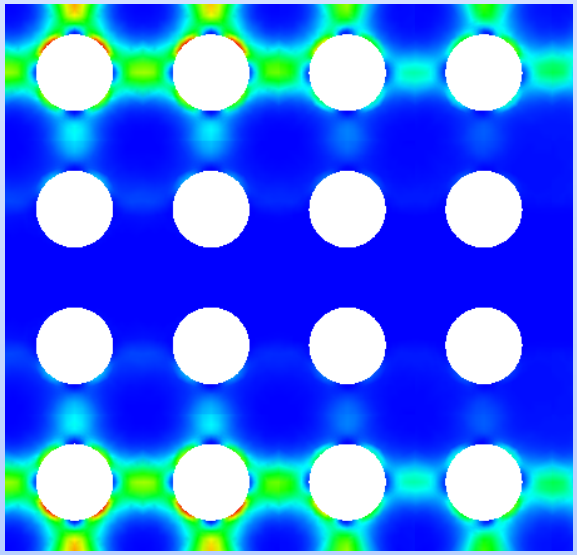
b)

Zoom

$w_{\max}^{\text{NTFA}} \approx 1.2\, w_{\max}^{\text{ref}}$

Conclusion

- **In nonlinear composites** intraphase strain heterogeneity is very important.
- **Elementary patterns or modes of deformation are observed.**
- **These "modes" are the reduced basis for a reduced "homogenized" constitutive model**
- **Localization is a linear operation, even for nonlinear constituents.**